

STUDIES OF ULTRASONIC DISPERSION  
IN GASES BY THE DIFFRACTION OF LIGHT

by

JOSEPH VERGARA MARTINEZ

A THESIS

submitted to


OREGON STATE UNIVERSITY

in partial fulfillment of  
the requirements for the  
degree of


DOCTOR OF PHILOSOPHY


June 1962


APPROVED:

  
\_\_\_\_\_  
Professor of Chemistry

In Charge of Major

  
\_\_\_\_\_  
Chairman of Department of Chemistry

  
\_\_\_\_\_  
Chairman of School Graduate Committee

  
\_\_\_\_\_  
Dean of Graduate School

Date thesis is presented June 9, 1961

Typed by Lilah N. Potter

## ACKNOWLEDGMENT

The author expresses his deep gratitude and sincere appreciation due Dr. J. C. Decius in extending his conscientious guidance, assistance and encouragement in completing this work; to Dr. D. B. Nicodemus, Mr. J. G. Skinner and in particular, Mr. A. R. Tynes, all of the physics department, and Mr. R. R. Michaels of the electrical engineering department for their cooperation in making available essential equipment without which the time for completion of this project would have been extended considerably and for their willingness to participate in thought provoking discussions; to Mr. C. D. Woods who constructed and helped design the high pressure gas cell and the slit elevator; to the local unit of the Naval Reserve for extending the use of the frequency meter.

The author dedicates this work to his wife.

This work was supported in part by the Office of Naval Research under contract No. Nonr-1286(3), Project NR 015-405.

## TABLE OF CONTENTS

	Page
INTRODUCTION. . . . .	1
THEORY. . . . .	16
Equation of Motion and Continuity Equation . .	16
Equation of State. . . . .	19
Relaxation and Velocity Dispersion Equations .	25
SUMMARY OF THEORY FOR DIFFRACTION OF LIGHT BY WEAK ULTRASONIC WAVES . . . . .	37
EXPERIMENTAL APPARATUS. . . . .	55
The Optical System . . . . .	55
The Electrical System. . . . .	59
The Gas Cells. . . . .	66
Quartz Crystals and their Mounts . . . . .	71
The Thermistor and Temperature Measurement . .	75
EXPERIMENTAL RESULTS. . . . .	82
Procedure. . . . .	88
Preliminary Results. . . . .	100
Finals Results . . . . .	109
DISCUSSION OF RESULTS . . . . .	127
BIBLIOGRAPHY. . . . .	149
APPENDIX 1. . . . .	155
APPENDIX 2. . . . .	162



# LIST OF FIGURES

Figure		Page
1a	Experimental Arrangement for Observing Light Diffraction by Ultrasonic Waves. . .	38
1b	Model for the Diffraction Process. . . . .	38
2	Outline of the Optical System. . . . .	56
3	Transmission Characteristics of the Filter Solutions. . . . .	58
4	Crystal Controlled Oscillator Schematic. .	61
5	Hartley Type Oscillator Schematic. . . . .	63
6	Block Diagram of Main Electrical System. .	65
7	Photograph of Low Pressure Gas Cell. . . .	67
8	Photograph of Disassembled High Pressure Cell . . . . .	72
9	Photograph of the Two Crystal Mounts used in This Study. . . . .	76
10	Thermistor Measuring Circuit Schematic . .	77
11	Enlargement of High Pressure Cell in Position in Optical Path . . . . .	80
12	Photograph of Whole System . . . . .	81
13	Light Diffraction by an Ultrasonic Field in Sulfur Dioxide. . . . .	95
14	Light Diffraction by an Ultrasonic Field in Ammonia . . . . .	96
15	Light Diffraction by an Ultrasonic Field in Three Different Gases . . . . .	97
16	Plot of $N_2$ Sound Velocity vs Rf Voltage, $T = 300^\circ K$ . . . . .	105
17	Log Log Plot of $h(U_i)$ vs $(f/p)^2$ for Nitrous Oxide, $T = 300^\circ K$ . . . . .	125

# LIST OF FIGURES - Cont.

Figure		Page
18	Illustration of Refraction Effect on Focal Length. . . . .	165

# LIST OF TABLES

Table		Page
1	Observed Typical Temperature Variations .	94
2	Idealized Sound Velocities Values of Nitrogen at Constant Pressure and Variable rf Voltage. . . . .	104
3	Observed Sound Velocity of Nitrogen at Constant rf Voltage and Variable Pressure	108
4	Experimentally Determined Velocity of Argon . . . . .	111
5	Observed Velocity of N <sub>2</sub> O using Low Pressure Cell . . . . .	112
6	Observed Velocity of Nitrogen using the High Pressure Cell. . . . .	114
7	Observed Velocity of Nitrous Oxide; 1 to 10 Atmospheres. . . . .	116
8	Idealized Nitrogen Velocities . . . . .	119
9	Corrected Sound Velocities of Nitrous Oxide. T = 300°K . . . . .	120
10	Values of $h(U_i)$ for Nitrous Oxide from Optical Data . . . . .	122
11	Values of $h(U_i)$ for Nitrous Oxide (Walker <u>et al.</u> ) . . . . .	123
12	Values of $h(U_i)$ for Nitrous Oxide (Holmes <u>et al.</u> ) . . . . .	124

LIST OF TABLES - Cont.

Table		Page
13	Correlation of First Order Diffraction as Predicted by David's Theory . . . . .	129
14	Summary of G Values for $N_2O$ . . . . .	160

# ADVANCE BOND

## STUDIES OF ULTRASONIC DISPERSION IN GASES BY THE DIFFRACTION OF LIGHT

### INTRODUCTION

Investigations dealing with the structure of relatively simple molecules have now become sufficiently fruitful as to make accessible an opportunity to examine the nature of energy exchange among the various modes of molecular motion. Such examinations should contribute to the understanding of the ordinary transformation of matter and to the dynamical behavior of molecules.

For molecules in which the electronic contribution may be deferred, these molecular motions are translational, vibrational and rotational in character. Presently, it seems difficult to conceive that exchange of energy among these motions could occur except through collisions of the molecules. Thus, the study of vibrational relaxation times, where special emphasis is focused on the energy exchange, has the goal of elucidating the nature of the collision mechanism by which energy is transferred and distributed within the various molecular degrees of freedom.

Studies of dispersion and absorption of sound waves in gases has been but one means by which such phenomena have been investigated. Up to now this has



been the most active method. The activity of this method may be due to the fact that the experimental requirements are less complex than those of other methods, but it remains true that with this method only the lowest energy levels of the quantized vibrational and rotational energy are involved in the energy transfer. This condition restrains the problem to a minimum in complexity.

Propagation of sound through a fluid medium was first treated by Newton (8, p. 378) and later refined by Laplace (38, p. 297). Laplace related the velocity of sound in a gas to the ratio of its heat capacities by considering the propagation as an adiabatic process. Experimental results from studies in air supported Laplace's concept. This concept was built on the idea that when a gas is suddenly compressed, the pressure increases since the density increases and the work done on the gas increases its temperature. Even for sound of low frequencies, the accompanying alterations due to the pressure wave are sufficiently rapid that the flow of heat from one element to another is compensated by the immediate rarefaction. The gas element then behaves as though the element had neither gained nor lost heat. To this extent the process is adiabatic. However, Newton's formulation is appropriate when the changes are so slow that the temperature remains constant because the added



heat is lost through radiation and heat conduction.

The total energy possessed by a molecule is considered to be a sum of energies associated with each type of molecular motion. This is just the interpretation of the principle of equipartition of energy (50, p. 86). Likewise, the total heat capacity of a molecule is a sum of the individual heat capacities. Moreover, the magnitude of thermal energy transferred to each type of motion depends upon its individual heat capacity. The velocity of sound may then be examined in terms of the variance in these individual heat capacities.

Herzfeld and Rice (22) were the first to develop a tangible explanation for the dispersion of sound velocity in gases based upon an energy transfer during the collision process. They pointed out that if the statistical equilibrium of a gas is suddenly disturbed, as occurs in the transmission of sound, a finite lag occurs for reestablishment of thermal equilibrium between the external and internal energies of the gas molecules. The classification of external and internal degrees of freedom associated with these energies is a relative one depending on which of the three types of molecular motion(s) is responsible for the lag. Such motion(s) causing the lag is considered as an internal degree(s) of freedom with the other(s), which attains

WILL BROWN Paper

equilibrium rapidly, is considered as an external degree(s) of freedom.

According to their interpretation, as the rate of compressions and rarefactions in a gas is increased, that is, as the frequency of the sound wave is increased, the establishment of equilibrium becomes increasingly more difficult because of the finite time involved in the transfer of energy from the translational to the internal degrees of freedom. The result is that the internal energy is prevented from reaching its full equilibrium value. The gas then displays an effective heat capacity which is smaller than its static value. In the region of very high sound frequencies, the effective heat capacity of the gas takes on values between the static heat capacity and that due to the translational energy alone. The velocity of the sound propagation is related to the heat capacities in such a manner that it increases with decreasing effective heat capacity of the gas.

Such phenomena were mathematically formulated by Herzfeld and Rice into a relaxation equation containing the important parameter  $\tau$ , called the relaxation time. This time is that required for the energy departure from thermal equilibrium to decay to  $1/e$  of its initial value.

In order to specialize the study to vibrational relaxation times it is only necessary to state that the

rotational energy reaches its equilibrium value much sooner than the vibrational energy by a factor of about one hundred. The translational energy reaches its equilibrium value even faster. Hence, it is the equilibrium energy value of the vibrational motion which first lags the equilibrium adjustment process and in many situations is well enough separated from the rotational counterpart that it is possible to consider only the phenomena associated with the vibrational motion.

Most experimental results obtained thus far of dispersion and absorption of ultrasound have been obtained through use of the interferometer. The interferometer used in this method was first proposed by Pierce (44, p. 271-302) and later improved by Hubbard (26, p. 523-535) in 1931.

In its simplest form the instrument consists essentially of a movable reflector parallel and coaxial to an x-cut quartz crystal which by virtue of the piezoelectric effect may be made to emit nearly planar ultrasonic waves upon activation by a transmitter. The distance between reflector and transducer may be varied at will and is determined and controlled with a micrometer whose shaft is adhered to the reflector. Whenever the reflector is positioned at a distance from the quartz equal to an integral number of half-wavelengths of the



ultrasound, a standing wave pattern is formed in the space between them. At positions of resonance, when the distance between the transducer and the reflector is an integral number of half-wavelengths, the damping on the transducer is a maximum. Such a condition is accompanied with an observed maximum in the anode current of the transmitter. As the distance between the transducer and the reflector is increased, a series of decreasing maxima corresponding to the increasing value of the integral half-wavelengths is observed. The ultrasonic absorption is found from the rate of decrease of the envelope of the maxima in an anode current versus reflector-transducer distance plot. The ultrasonic wavelength is determined from the interval between maxima and when this interval is multiplied by the frequency of ultrasound yields its velocity.

As an example of results obtained from the interferometric method, it is sufficient to note that Klose (32) has reported the velocity of n-hexane to an accuracy of one part in a thousand. He used ultrasonic frequencies of approximately 700 and 1000 kilocycles per second and obtained as many as eighteen peaks in an anode current versus reflector-transducer distance plot.

In contrast to the well established interferometric method is an optical method. In this effect the

nearly planar ultrasonic waves are used as a pseudo-grating in as much that the ultrasonic field will diffract a parallel beam of light upon passing through the field. An inspection of the resulting image shows diffracted lines on each side of the zero order. Actually the modulation of the light is achieved by virtue of the fact that a sinusoidal variation in the index of refraction is produced by the resulting compressions and rarefactions accompanying the ultrasonic waves. It is possible to associate with the effect a pseudo-grating constant  $\Lambda$  which is nothing more than the sound wavelength. Application of the grating formula to the observed diffraction yields the ultrasound wavelength which when multiplied by the frequency yields the ultrasonic velocity. The intensity of the image in this effect for gases is not as spectacular as the diffraction by a grating since the change in the index of refraction is rather small to even approximate the construction of the grating. However, it has been used in conjunction with liquids with considerable success (2, p. 280-302).

The first optical investigations of ultrasonic fields in gases were taken by Tawil (57) and by Pohlmann (45). These workers were not making use of the sound field as a pseudo-grating but rather made successful attempts to obtain patterns of a standing



ultrasonic field. The results of Pohlmann led him to comment that on account of the small change in the index of refraction the diffraction by ultrasound could not be observed in gases. Bar(1) in 1936 extended the study of Tawil and Pohlmann using an ultrasonic frequency of 935 kilocycles per second. Although Bar indicates that he observed a diffraction effect with air to the extent of seeing the first order clearly and a very weak second order diffraction, he does not present any photographs of the phenomenon.

The first acceptable theory regarding the intensity distribution of the various orders as observed in liquids was given by Raman and Nath (46, 47, 48, 49). Later David (9) presented a similar theory to account for the intensity distribution of the first and second orders associated with the diffraction of light by ultrasound in gases. Up to this time only these orders had been observed in gases by Bar and by Korff (33, p. 708-720).

Korff undertook the task of verifying the acceptability of David's theory for the intensity distribution in the first orders and is the first work to examine in detail the diffraction of light by ultrasonic waves in gases. Korff worked with an ultrasonic frequency of 4.28 megacycles per second in air presumably at

atmospheric pressure.

Petersen (42) pursued the problem of obtaining values of absorption of sound by studying the diffraction of light by ultrasonic waves in gases. He discussed a refinement of the method used by Korff and suggested that the technique reaches a limit in accuracy at pressures below one atmosphere. The refinement consists essentially in integrating the intensity of the first order. This total intensity is then to be correlated with the distance of the incoming light beam from the sound emitting surface.

David has given a theoretical account of the method proposed by Petersen and Keller (31) has applied the technique to obtain absorption coefficients for argon, nitrogen, ammonia, carbon dioxide and a mixture of carbon dioxide with 8% hydrogen. The deviation of the measured absorption from theory as shown by nitrogen and ammonia was explained by Keller as due to the rotational energy relaxation effect. The analogous deviation shown by carbon dioxide and its hydrogen mixture was also discussed by Keller in terms of relaxation effects for which account was made to obtain better agreement to the classical theory of absorption.

What appears to be the most outstanding account from the standpoint of the number of diffracted orders

occurring in gases has been given by Gollmick (17, p. 1-44). In his work the main objectives are to determine the optimum conditions under which an ultrasonic field of sufficient intensity may be produced to yield several orders of diffraction and to compare the measured intensities to those predicted by the theory of Raman and Nath. Although Gollmick was aware of the use of the method to determine ultrasonic velocities in gases, this was not his primary concern. With his most favorable arrangement, Gollmick was able to photograph as many as fifteen diffracted orders on each side of the zero order, again presumably at one atmosphere pressure. To achieve this result, Gollmick used a rectangular x-cut quartz crystal having a fundamental frequency of 593.8 kilocycles per second. He placed a reflector above the quartz crystal in order to set up a standing sound field and thus increasing the intensity of the ultrasonic field. Gollmick found that it was necessary to consider in great detail the manner of mounting the quartz crystal such that it will have the minimum damping contribution by the holder. He found that the best mounting arrangement was a freely suspended crystal. The rectangular crystal was grooved about its perimeter such that four points supported the crystal in its median plane. The points were the tapered ends of four thin

Meerscham rods. These rods were placed in hollowed out sections of four screws. The screws were secured in a Pertinax ring and permitted the adjustment of the pressure of the points against the crystal.

With this basic arrangement Gollmick made intensity distribution measurements and compared the results with the theory of Raman and Nath. He concluded that the theory was not adequate to explain the results. However, Hayess and Winde (19, p. 195-209) have pointed out that Gollmick was working in a region not covered by the theory, which requires that  $\frac{n_1}{n_0} \left( \frac{d}{\Lambda} \right)^2 \ll 1$ . In this relation  $n_0$  is the index of refraction,  $n_1$  is the amplitude of the change in the index of refraction due to the pressure wave,  $d$  is the length of path of the light through the ultrasound field and  $\Lambda$  is the sound wavelength.

Bömmel's (3, p. 3-20) work of 1945 was the first to examine the value of the diffraction of light by ultrasonic waves in gases for the determination of the velocity and absorption of ultrasound for observing relaxation effects. Because of the objection that the ultrasonic field is not ideally planar, Bömmel made relative measurements to detect relaxation effects. In his experiment, the crystal having a fundamental frequency of 951 kilocycles was simultaneously activated



in its fundamental and third overtone or in its fundamental and fifth overtone. Thus if no dispersion was present in the gas under study, the distance ratio between the two first orders corresponding to the crystal's fundamental and overtone frequencies should be in the same ratio as the frequencies. Bömmel made velocity measurements in argon, carbon dioxide, oxygen, nitrogen, and air each at a pressure of 720 mm and then only by making use of the first order diffraction. From his results, of which no photographs are presented, Bömmel concluded that in the gases studied no dispersion effects were observable over the frequency range of about one to five megacycles. Velocity values are reported to an accuracy of 0.3%.

However, Bömmel noted that the observed velocity value for carbon dioxide was 3.8% higher than that reported at audio frequencies. In order to determine the velocity at the inflection point of the dispersion curve for pure carbon dioxide, Bömmel used a 10% hydrogen-carbon dioxide mixture. This was done to place the velocity at the inflection point within his experimental reach. In doing so, Bömmel found the ratio of first order diffraction interval to be  $2.9445 \pm 0.0067$  while the frequency ratio was 3.0095. This was interpreted as convincing evidence for detection of dispersion.



Of the literature cited thus far, with the exception of the works by Petersen and Keller, the works that have attributed more to the feasibility of using the diffraction of light by ultrasonic waves for determining ultrasonic velocities in gases have been performed with pressures in the neighborhood of one atmosphere. It is to be noted that the diffraction effect should be more pronounced with gases at higher pressures. The reason being that as the density of the gas is increased by the higher pressure, the change in index of refraction is greater and the ultrasonic absorption is due to viscosity and thermal conduction effects is less. Also the transfer of ultrasonic energy by the quartz crystal to the gas is more efficient since the acoustic impedance match is better. With respect to observation of the diffraction of light by ultrasonic waves in gases under pressure, Lacam and Noury (34; 35; 36; 37, p. 217-259) have worked with several gases at pressures ranging from 10 to 1150 atmospheres using a crystal fundamental frequency of 900 kilocycles per second. In addition, what seems to be the latest work on the examination of the applicability of the diffraction of light by ultrasonic waves in gases for the determination of ultrasonic absorption and velocity dispersion is that of Hayess and Winde. They have attempted an absolute measurement in

nitrogen at pressures from 10 to 85 atmospheres and used frequencies of 0.804, 2.01 and 9.86 megacycles per second. They seem to have incorporated all the features which can yield the optimum experimental conditions for observation of the diffraction effect. Besides using higher pressures, they used a quartz mount similar to the one used by Gollmick, a reflector for increasing the ultrasound intensity and a higher pressure mercury lamp. With the reflector in place and using a pressure of 80 atmospheres, they observed up to 26 orders on one side of the zero order. This was accomplished with the 2.01 megacycle crystal. They reported an accuracy in velocity measurements of 0.3% and suggest means by which the error may be reduced to 0.05%.

In regard to the intensity distribution for nitrogen at higher pressures, Hayess and Winde found suitable agreement with the theory of Raman and Nath. The observed absorption has been discussed by Hayess (18) in which he found that the theory available to him could not adequately explain the observed results. He was led to postulate the occurrence of triple collisions and the appearance of a superposition of different processes in order to account for the observed results.

From the foregoing it appears fruitful to examine more directly the usefulness of the diffraction of light

by ultrasonic waves in following a complete region of velocity dispersion for some gas. In doing so, it will be possible to determine the vibrational relaxation time of that gas and interpret the result from the standpoint of the collision mechanism. In working with atmospheric pressure and below, it should be possible to examine the limitations and accuracy of the method. Any positive contributions with this method should give confidence in its use and serve to introduce another means by which vibrational relaxation times may be determined. These are the goals of the present work and will require the construction of an adequate optical system and transmitter to properly activate the quartz transducer. Moreover, it will become of great significance to consider the temperature variation of the gas during the production of the ultrasonic field. This item has certainly lacked detailed consideration in the previous works.

## THEORY

In order to develop the velocity dispersion equation for a single relaxation time, it is necessary to state three basic equations. These are the continuity equation, the equation of motion, and an equation of state. These are then combined with a relaxation equation to obtain the velocity dispersion equation. The development follows closely that given by Herzfeld and Litovitz (21, p. 25-170).

Equation of Motion and the Continuity Equation

The general treatment for the adiabatic propagation of a periodic wave through a fluid medium may be simplified considerably by specializing the problem to the propagation of plane ultrasonic waves of moderately weak intensity. This restriction permits the density variation caused by the wave being propagated through a gas to be written as the linear function

$$\rho = \rho_0(1+s) \quad (1)$$

Here  $\rho_0$  is the equilibrium density,  $\rho$  the actual density and  $s$  is called the condensation and is the ratio of the excess pressure to the equilibrium pressure. For the adiabatic process the linearization condition



requires that the experimental conditions correspond to the linear portion of a  $p$  versus  $(1/V)^\gamma$  plot where  $p$  is the pressure,  $V$  the volume and  $\gamma$  the ratio of the static heat capacities,  $C_p/C_v$  for the gas.

In such a case, the continuity equation is

$$\frac{\partial s}{\partial t} + \frac{\partial u}{\partial z} = 0, \quad (2)$$

and the equation of motion is

$$\frac{\partial u}{\partial t} + \frac{1}{\rho_0} \frac{\partial p}{\partial z} = 0. \quad (3)$$

Besides the previously defined quantities,  $u$  is the  $z$ -component of the mass flow velocity,  $t$  is the time and  $z$  is the normal of the propagated plane waves.

The plane waves are described by the relation

$$\exp \left\{ i\omega \left( t - \frac{z}{U} \left[ 1 - \frac{i\alpha U}{\omega} \right] \right) \right\}. \quad (4)$$

Here  $\omega$  is the angular frequency,  $2\pi f$ , of the ultrasonic waves,  $U$  is their velocity and  $\alpha$  is the absorption coefficient for the amplitude of the waves. It is to be assumed that  $s$  and  $u$  are also proportional to the exponential expression (4).

Equation (3) is written as



$$\frac{\partial u}{\partial t} = - \frac{1}{\rho_0} \frac{\partial p}{\partial s} \frac{\partial s}{\partial z}. \quad (5)$$

It is also true that

$$\frac{\partial s}{\partial z} = - \frac{i\omega}{U} \left(1 - \frac{i\alpha U}{\omega}\right) s, \quad (6)$$

and

$$\frac{\partial u}{\partial t} = i\omega u. \quad (7)$$

Substitution of equations (6) and (7) into (5) yields

$$u = \frac{1}{\rho_0} \frac{dp}{ds} \frac{1}{U} \left(1 - \frac{i\alpha U}{\omega}\right) s. \quad (8)$$

A relation between  $s$  and  $u$  is obtained by substituting their forms in terms of the exponential equation into the continuity equation (2). Thus,

$$\frac{\partial s}{\partial t} = - \frac{\partial u}{\partial z}$$

becomes

$$i\omega s = \frac{i\omega}{U} \left(1 - \frac{i\alpha U}{\omega}\right) u; \quad (9)$$

so

$$\frac{s}{u} = \left(1 - \frac{i\alpha U}{\omega}\right) / U. \quad (10)$$

The useful result needed here is obtained by substituting equation (10) into (8) to eliminate  $u$  and  $s$ . This yields

$$1 = \frac{1}{\rho_0} \frac{dp}{ds} \frac{1}{U} - \frac{i\alpha}{Uw}^2. \quad (11)$$

### Equation of State

The heat capacities are introduced by an equation of state which depends only on the translational temperature which is denoted by  $T_{tr}$ .

The enthalpy relation for the isentropic variation is separated into a sum of two terms. One is defined in terms of the translational temperature and includes the work term. The other term is defined in terms of the temperature  $T'$  of the internal degrees of freedom. Thus, the enthalpy,  $H$ , is expressed as

$$H = H_{T_{tr}} + E'. \quad (12)$$

Two heat capacities are defined by

$$\left( \frac{\partial H_{T_{tr}}}{\partial T_{tr}} \right)_p = \tilde{C}_p \text{ and } \frac{dE'}{dT'} = C', \quad (13)$$

where

$$\tilde{C}_p + C' = C_p, \quad (14)$$

$C_p$  being the static heat capacity at constant pressure.

Applying the first law of thermodynamics to the adiabatic process and acknowledging that any work done on an element of volume goes toward increasing the internal energy yields

$$dE = -pdV$$

or

$$d(E + pV) = Vdp.$$

Now

$$H = E + pV$$

and from

$$H = H(T, p)$$

one writes

$$\left(\frac{\partial H}{\partial T}\right)_p dT + \left(\frac{\partial H}{\partial p}\right)_T dp = Vdp. \quad (15)$$

It is noted that

$$C_p = \left(\frac{\partial H}{\partial T}\right)_p \quad (16)$$

also

$$dH = Tds + Vdp$$

and

$$dE = Tds - pdV;$$

therefore,

$$dH = TdS + Vdp$$

or

$$\left(\frac{\partial H}{\partial p}\right)_T = T\left(\frac{\partial S}{\partial p}\right)_T + V. \quad (17)$$

Using the Maxwell relation

$$\left(\frac{\partial S}{\partial p}\right)_T = -\left(\frac{\partial V}{\partial T}\right)_p$$

equation (17) becomes

$$\left(\frac{\partial H}{\partial p}\right)_T = V - T\left(\frac{\partial V}{\partial T}\right)_p. \quad (18)$$

Substitution of equations (16) and (18) into equation (15) gives

$$C_p dT = T\left(\frac{\partial V}{\partial T}\right)_p dp. \quad (19)$$

In terms of the separation of the enthalpy as shown in equation (12),

$$C_p dT_{tr} + C'dT' = T_{tr}\left(\frac{\partial V}{\partial T}\right)_p dp. \quad (20)$$

The assumption has been used that  $E'$  does not depend upon pressure at constant temperature.

Using the definition for the coefficient of thermal expansion  $\beta$ ,



$$\beta = \frac{1}{V} \left( \frac{\partial V}{\partial T} \right)_p, \quad (21)$$

equation (20) may be expressed as

$$\tilde{C}_p dT_{tr} + C' dT' = [C_p]_{eff} dT_{tr} = T_{tr} V \beta dp, \quad (22)$$

where  $[C_p]_{eff}$  is the effective heat capacity.

Considering the volume as a function of pressure and temperature, it is possible to write

$$dV = \left( \frac{\partial V}{\partial p} \right)_T dp + \left( \frac{\partial V}{\partial T} \right)_p dT. \quad (23)$$

Using equation (21) and the definition of compressibility,  $K_T$ , namely,

$$K_T = - \frac{1}{V} \left( \frac{\partial V}{\partial p} \right)_T, \quad (24)$$

equation (23) may be written as

$$dV = V( - K_T dp + \beta dT ). \quad (25)$$

Under the condition previously stated, this latter equation is written as

$$dV = V( - K_T dp + \beta dT_{tr} ). \quad (26)$$

By the linearization condition stated in equation (1), it is possible to write

$$ds = - dV/V,$$

and introducing this into equation (26) yields

$$ds = K_T dp - \beta dT_{tr}, \quad (27)$$

or

$$\frac{ds}{dp} = K_T \left( 1 - \frac{\beta}{K_T} \frac{dT_{tr}}{dp} \right). \quad (28)$$

Using expression (22) in the form

$$\frac{\partial T_{tr}}{\partial p} = T_{tr} \frac{V\beta}{(C_p)_{eff}}$$

and substituting into equation (28), it is seen that

$$\frac{ds}{dp} = K_T \left\{ 1 - T_{tr} V \beta^2 / K_T (C_p)_{eff} \right\}. \quad (29)$$

Use is now made of the equation giving the dependence of the difference of the heat capacity at constant pressure and of the heat capacity at constant volume on the coefficients of compressibility and of expansion. Herzfeld and Litovitz write this as

$$C_p - C_v = TV\beta^2/K_T. \quad (30)$$

Assuming that the temperature in this latter equation may be represented by  $T_{tr}$  and substituting in equation (29)

$$\frac{ds}{dp} = K_T \left\{ 1 - \frac{(C_p - C_v)}{(C_p)_{\text{eff}}} \right\}. \quad (31)$$

Equation (22) is written as

$$(C_p)_{\text{eff}} = C_p + C' \left( \frac{dT'}{dT_{\text{tr}}} - 1 \right), \quad (32)$$

and similarly

$$(C_v)_{\text{eff}} = C_v + C' \left( \frac{dT'}{dT_{\text{tr}}} - 1 \right). \quad (33)$$

Hence it follows that

$$(C_p)_{\text{eff}} = (C_v)_{\text{eff}} + C_p - C_v. \quad (34)$$

An effective specific heat ratio,  $\gamma_{\text{eff}}$ , may be defined through equation (34) as

$$(\gamma)_{\text{eff}} = 1 + \frac{C_p - C_v}{(C_v)_{\text{eff}}}, \quad (35)$$

or

$$\frac{1}{(\gamma)_{\text{eff}}} = 1 - \frac{C_p - C_v}{(C_p)_{\text{eff}}}. \quad (36)$$

Using equations (11), (31) and (36) it is possible to write

$$\left( \frac{1}{U} - \frac{i\alpha}{w} \right)^2 = \rho_o / \left( \frac{dp}{ds} \right) = \rho_o K_T / \gamma_{\text{eff}}. \quad (37)$$

Denoting the quasi-static values by the index

zero and multiplying equation (37) by  $U_o^2$ , one has

$$\left( \frac{U_o}{U} - \frac{i\alpha U_o}{w} \right)^2 = U_o^2 \rho_o K_T / \gamma_{\text{eff}} \quad (38)$$

From the expression for the ideal gas velocity,  $U_o$ , given by

$$U_o^2 = \gamma_o \frac{RT}{M}$$

it is possible to write

$$\gamma_o = U_o^2 \rho_o K_T \quad (39)$$

This relation is used to simplify equation (38) to read

$$\left( \frac{U_o}{U} - \frac{i\alpha U_o}{w} \right)^2 = \gamma_o / \gamma_{\text{eff}} \quad (40)$$

Equation (40) shows the velocity dependence on the heat capacity ratios and illustrates the effect of the absorption of the sound waves. At this stage it is necessary to introduce a relaxation equation.

### Relaxation and Velocity Dispersion Equations

The relaxation equation dealing with the internal degrees of freedom has been given by Herzfeld and Rice and adopted by Herzfeld and Litovitz in the form



$$-\frac{dE'}{dt} = \frac{1}{\tau} \{E' - E'(T_{tr})\}, \quad (41)$$

where  $E'$  denotes the momentary value of the internal energy. The term  $E'(T_{tr})$  represents the value of the internal energy which would be present if the internal degrees of freedom were in thermal equilibrium with the external degrees which are at the temperature  $T_{tr}$ . The constant  $\tau$  denotes the relaxation time.

Equation (41) may be written as

$$-\frac{dT'}{dt} = \frac{1}{\tau} (T' - T_{tr}). \quad (42)$$

The validity of this equation is based upon the assumption that if the specific heat  $C'$  is independent of the temperature or if the temperature never deviates far from a value  $T_0$ , it is possible to write

$$E' - E'_0 = C'(T' - T_0). \quad (43)$$

Equation (42) may be written as

$$-\tau \frac{dT'}{dt} = T' - T_0 - (T_{tr} - T_0), \quad (44)$$

or

$$T' - T_0 + \tau \frac{d}{dt}(T' - T_0) = T_{tr} - T_0. \quad (45)$$

Since the quantity  $(T_{tr} - T_0)$  is proportional to  $\exp(i\omega t)$ , the quantity  $(T' - T_0)$  varies accordingly.

Substitution of this proportionality condition into equation (45) takes the following form for the steady state condition:

$$T' - T_o = \frac{T_{tr} - T_o}{1 + iw\tau}. \quad (47)$$

Substituting equation (47) into equation (32) it is possible to deduce that

$$(C_p)_{\text{eff}} = \tilde{C}_p - \frac{C'}{1 + iw\tau} = C_p - C' \frac{iw\tau}{1 + iw\tau}. \quad (48)$$

Thus, it is possible to write equation (40) as

$$\left( \frac{U_o}{U} - \frac{i\alpha U_o}{w} \right)^2 = \frac{C_p}{C_v} \left( \tilde{C}_v + \frac{C'}{1 + iw\tau} \right) / \left( \tilde{C}_p + \frac{C'}{1 + iw\tau} \right), \quad (49)$$

where

$$\chi_{\text{eff}} = \frac{(\tilde{C}_p + C' / 1 + iw\tau)}{(C_v + C' / 1 + iw\tau)}.$$

Equation (49) is then simplified to read

$$\left( \frac{U_o}{U} - \frac{i\alpha U_o}{w} \right)^2 = (1 + \frac{\tilde{C}_v}{C_v} iw\tau) / (1 + \frac{\tilde{C}_p}{C_p} iw\tau). \quad (50)$$

Using the relation

$$\tau' = \frac{C_p - C'}{C_p} \tau$$

the right hand side of equation (50) becomes equal to

$$1 - \frac{C'(C_p - C_v)}{C_v(C_p - C')} \frac{i w \tau'}{1 + i w \tau'} . \quad (51)$$

Separating equation (50), in terms of equation (51), into its real and imaginary parts it is seen that

$$\left(\frac{U_o}{U}\right)^2 - \left(\frac{\alpha U_o}{w}\right)^2 = 1 - \frac{C'(C_p - C_v)}{C_v(C_p - C')} \frac{w^2 \tau'^2}{1 + w^2 \tau'^2} , \quad (52)$$

and

$$\frac{\alpha U_o^2}{2 w U} = \frac{C'(C_p - C_v)}{C_v(C_p - C')} \frac{w \tau'}{1 + w^2 \tau'^2} . \quad (53)$$

For dispersion measurements, use is made of equation (52); however, the term in this equation containing the absorption coefficient  $\alpha$  is neglected. According to Herzfeld and Litovitz, the error introduced by neglecting this term is still beyond present experimental error. Thus, the dispersion equation is written as

$$\left(\frac{U_o}{U}\right)^2 = 1 - \frac{C'(C_p - C_v)}{C_v(C_p - C')} \frac{w^2 \tau'^2}{1 + w^2 \tau'^2} . \quad (54)$$

In order to obtain expressions for the limiting velocities, equation (54) may be represented by:

$$\left(\frac{U_o}{U}\right)^2 = 1 \quad (55)$$

for low frequency, and for high frequency it becomes

$$\left(\frac{U_o}{U_\infty}\right)^2 = 1 - \frac{C'(C_p - C_v)}{C_v(C_p - C')} = \frac{C_p(C_v - C')}{C_v(C_p - C')}. \quad (56)$$

When the symbol  $\infty$  is used as a subscript or superscript, the value of the quantity involved is that value at "infinite" frequency.

To evaluate the dispersion equation at intermediate frequencies, it becomes easier to consider the reciprocal of equation (50). Defining  $\tau''$  by

$$\tau'' = \frac{\tilde{C}_v}{C_v} \tau = \frac{C_v - C'}{C_v} \tau = \frac{C_v^\infty}{C_v^0} \tau, \quad (57)$$

the simplification as before yields

$$\left(\frac{U}{U_o}\right)^2 = 1 + \frac{w^2 \tau''^2}{1 + w^2 \tau''^2} \frac{C'(C_p - C_v)}{C_p(C_v - C')}. \quad (58)$$

For purposes of plotting the experimental values, one notes that equation (56) may be written as

$$\frac{U_\infty^2 - U_o^2}{U_\infty^2} = \frac{C'(C_p - C_v)}{C_v(C_p - C')}. \quad (59)$$

Dividing equation (59) by equation (56), one has



$$\frac{U_{\infty}^2 - U_0^2}{U_0^2} = \frac{C'(C_p - C_v)}{C_p(C_v - C')} \quad (60)$$

Use of this relation in conjunction with equation (58) yields

$$\left(\frac{U}{U_0}\right)^2 = 1 + \frac{w^2 \tau''^2}{1 + w^2 \tau''^2} \left(\frac{U_{\infty}^2 - U_0^2}{U_0^2}\right)$$

or

$$\frac{U^2 - U_0^2}{U_{\infty}^2 - U_0^2} = \frac{w^2 \tau''^2}{1 + w^2 \tau''^2} \quad (61)$$

In principle the limiting velocities  $U_0$  and  $U_{\infty}$  may be calculated a priori and by an examination of the dependence of the velocities expression on the product term  $w \tau''$ , the relaxation time may be evaluated for the case of an ideal gas.

To inspect the variation of the velocity  $U$  upon the product term  $w \tau''$ , equation (61) is rewritten as,

$$g(U) = \frac{1}{2} \left( 1 - \frac{1 - w^2 \tau''^2}{1 + w^2 \tau''^2} \right)$$

or

$$g(U) = \frac{1}{2} - \frac{1}{2} \left( \frac{1/w \tau'' - w \tau''}{1/w \tau'' + w \tau''} \right), \quad (62)$$

where  $g(U)$  denotes the left hand side of equation (61).  
Making the substitution

$$x = \ln w \tau'' \quad (63)$$

into equation (62), it is found that

$$g(U) = \frac{1}{2} + \frac{1}{2} \left( \frac{e^x - e^{-x}}{e^x + e^{-x}} \right), \quad (64)$$

or

$$g(U) = \frac{1}{2} + \frac{1}{2} \tanh x. \quad (65)$$

Since the theoretical limits set on  $w$  are zero and infinity, the limits of  $x$  as determined by equation (63) are minus and plus infinity. Noting that the hyperbolic tangent for a negative argument is the negative hyperbolic tangent of that argument, but positive, the variation of  $\tanh x$  is such that for  $w = 0$ ,  $\tanh \infty = -1$ ; goes through zero at  $x = 0$  or what is equivalent,  $w \tau'' = 1$ ; finally for  $w = \infty$ ,  $x = \infty$  and  $\tanh \infty = +1$ . Thus the curve envisaged for  $\tanh x$  is such that it is "S" shaped, occupying the first and third quadrants and having a point of inversion at the origin, (0,0).

Then these properties of the hyperbolic function are applied to the function  $g(U)$  as expressed in

equation (65), it is seen that  $g(U)$ , as plotted against  $\ln w\tau''$ , varies between 0 and 1 with an inflection point corresponding to  $g(U) = \frac{1}{2}$  where  $w\tau'' = 1$ . The use of Briggs logarithms will result in the same behavior. Thus, a plot of  $g(U)$  against  $\log w\tau''$  should yield an "S" shaped for a single vibrational relaxation time mechanism, with a point of inflection at  $g(U) = \frac{1}{2}$  where  $w\tau'' = 1$  and knowing the value of  $w$ ,  $\tau''$  and  $\tau$  may be evaluated.

As was shown earlier in equation (57),  $\tau''$  is directly proportional to the true relaxation time  $\tau$ . If the energy transfer process is assumed to occur through double collisions, then  $\tau$  must be proportional to the number of collisions  $Z$  and the time between collisions  $\tau_c$ . Now the time between collisions is inversely proportional to the pressure. Consequently, the relaxation time  $\tau$ , as well as  $\tau''$ , is inversely proportional to the pressure. Thus, with the assumption of a double collision energy transfer process,  $w\tau''$  may be replaced by

$$w\tau''_0/p$$

where  $\tau''_0$  is the time constant for a standard pressure, usually one atmosphere. Moreover, the same variation of  $g(U)$  should appear if the frequency  $f$  is increased

or if the pressure  $p$  is decreased in the same ratio. It then is possible to rewrite equation (61) in the following form:

$$g(U) = \frac{U^2 - U_\infty^2}{U_\infty^2 - U_0} = \frac{(2\pi f \tau_0''/p)^2}{1 + (2\pi f \tau_0''/p)^2} . \quad (66)$$

From a plot of  $g(U)$  against  $\log(f/p)$ , the point of inflection is given by

$$2\pi(f/p)_{\text{infl}} \tau_0'' = 1$$

or

$$\tau_0'' = 1 / [2\pi(f/p)_{\text{infl}}] . \quad (67)$$

From this, one has

$$\tau_0 = \frac{C_v^0}{C_v^\infty} \tau_0'' = \frac{C_v^0}{C_v^\infty} \frac{1}{2\pi(f/p)_{\text{infl}}} \quad (68)$$

where  $\text{infl}$  means the value of that quantity at the point of inflection of the curve of  $g(U)$  versus  $\log(f/p)$ .

To obtain the value of a single occurring vibrational relaxation time for experimental data, it seems sufficient to plot the velocity function  $g(U)$  against  $\log(f/p)$  and to superimpose on the plot an "S" shape curve plotted previously from considerations of the behavior of the hyperbolic tangent. A curve



may then be drawn to accomodate the best fit consistent with the experimental data and a relaxation time evaluated from the value of the coordinates corresponding to the point of inflection.

On the other hand, it is possible to rearrange equation (66) into a form which may be used to obtain a linear plot. Such a plot seems to be preferable over the curve fitting method described in the last paragraph. In this case equation (66) is written as

$$h(U) = \frac{U^2 - U_0^2}{U_\infty^2 - U^2} = (w/p)^2 \tau_0''^2, \quad (69)$$

or

$$\log (f/p)^2 = \log h(U) - \log (2\pi\tau_0'')^2. \quad (70)$$

The interesting fact about this equation for a straight line is that it insists on a slope of 45 degrees when  $\log (f/p)^2$  is plotted against  $\log h(U)$ . This condition of restraint is equivalent to the insistence of an "S" shape curve in the curve fitting procedure described previously.

Thus having drawn the straight line through the data at a 45 degree slope, the value of  $h(U)$  corresponding to the value of  $(f/p)^2$  equal to  $1 \text{ mc}^2 \text{ atm}^{-2}$  is equated to  $(2\pi\tau_0'')^2$  since then

$$\log h(U) = \log (2 \pi \tau_0'')^2$$

or

$$\tau_0'' = \frac{1}{2\pi} \sqrt{h(U)} \quad (\mu \text{ sec atm}) \quad (71)$$

and  $\tau_0$  is determined from use of equation (68).

The selection of that value of  $h(U)$  for which the quantity  $f/p$  is equal to  $1 \text{ mc atm}^{-1}$  is equivalent to obtaining the relaxation time at the point of inflection from the plot yielding the "S" shaped curve.

According to the author's knowledge, the rearrangement of the involved quantities to obtain expression (70) and its application as discussed here for determining a value for the vibrational relaxation time has not hitherto been made. Subsequently, it is necessary to emphasize that the subjection of the experimental results with reference to a straight line as required by expression (70) imposes a more severe condition on the results than interpreting the results in terms of expression (66) with reference to an "S" shaped curve. Nonetheless, it is equally true that insertion of experimental values of velocity approaching the value of either  $U_0$  or  $U_\infty$  in equation (70) are to be discouraged since the exactness imposed by this equation for these values produces too large a deviation.

However, use of equation (70) in conjunction with velocity values sufficiently removed from the limiting values is an excellent and convenient test for evaluating the relaxation time associated with a single vibrational relaxation process.

This theoretical treatment has served to explain most observed results obtained thus far. This model for a single vibrational relaxation time is further substantiated by the statistical mechanical treatment of the harmonic oscillator as outlined by Herzfeld and Litovitz and which was first treated by Landau and Teller (37).

The simple selection rules for energy transitions in the simple harmonic oscillator and the fact that the energy levels are equally spaced have made the treatment possible. For the relaxation process involving rotational energies the theoretical treatment becomes more formidable. Also the existence of more than one vibrational relaxation time increases the complexity of the problem but presents a relatively more favorable case. The interpretation of the occurrence of more than one vibrational relaxation time may be made with good success by extension of this simple treatment; however, most observed results may be interpreted in terms of a single vibrational relaxation time.

SUMMARY OF THEORY FOR DIFFRACTION OF LIGHT  
BY WEAK ULTRASONIC WAVES

In 1922 Brillouin (6, p. 88-122) presented theoretical arguments regarding the scattering of light and x-rays by thermal density fluctuations which, according to him, had their origin from a superposition of sound waves in a body. This has been recognized as the suggestion which led to the experiment in which a plane ultrasonic wave field acts as a grating insofar that if a parallel beam of light passes through the sound field it would be diffracted. Through use of appropriate optics, this light would result in a diffraction spectrum when focused on a screen.

The first such experiment has been credited to two groups of workers, Lucas and Biquard (40) in France and Debye and Sears (10) in America. Both groups reported observing the phenomenon in conjunction with liquids in 1932.

The qualitative interpretation of the effect, as presented by Born and Wolf (4, p. 590-607), is illustrated in Figures 1A and 1B. Figure 1A outlines the typical experimental setup. In this figure S is a slit source of monochromatic radiation of wavelength which is made parallel by the collimator lens  $L_1$ . The light beam then traverses the sound wave field through



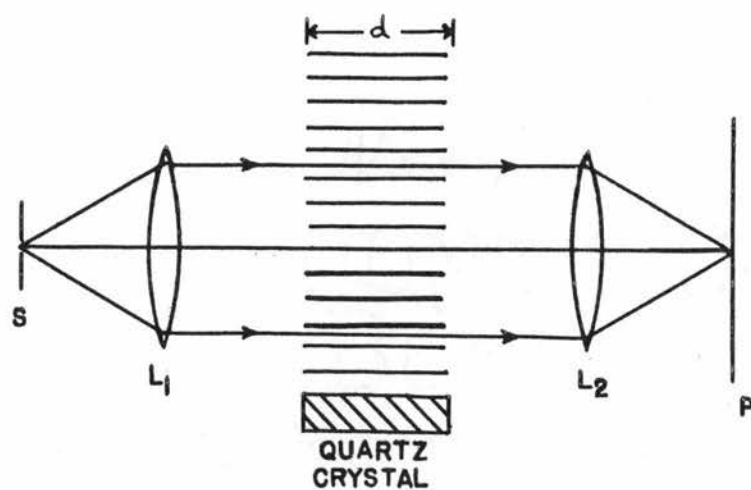


FIGURE 1A EXPERIMENTAL ARRANGEMENT FOR OBSERVING LIGHT DIFFRACTION BY ULTRASONIC WAVES

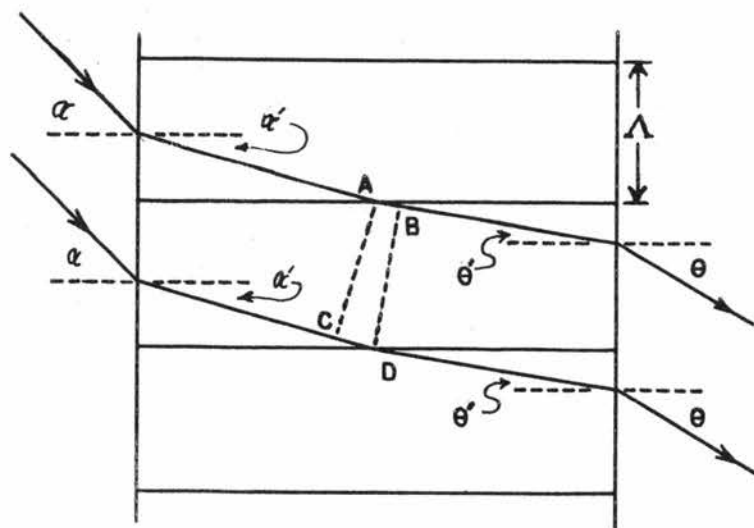


FIGURE 1B MODEL FOR THE DIFFRACTION PROCESS

the effective width  $d$ . The sound field is produced by the proper activation of an x-cut piece of quartz. The emergent light rays are made to focus on the photographic plate  $P$  by the condensing lens  $L_2$ .

Figure 1B shows the manner in which the light rays are diffracted in the ultrasonic plane wave field. For purposes of illustration the regions of compression are shown as lines. The light rays are diffracted by these regions because of the relatively greater index of refraction. The constant value of the distance between two adjacent compressions is designated by  $\Lambda$  and is equivalent to the sound wavelength.

In general the medium under study does not have the same index of refraction as that of the external surroundings. Hence, because of the difference in the indices of refraction under static conditions, the angles are shown as primed and unprimed.

The necessary condition that the two rays emerge in phase to give rise to constructive interference is that expressed by the equation

$$AB - CD = (\sin \theta - \sin \alpha') = k \frac{\lambda'}{\Lambda},$$

$$k = (0, \pm 1, \pm 2, \dots),$$

where  $\lambda'$  is the wavelength of light inside the medium. By Snell's law, it is also true that

$$\frac{\sin \alpha'}{\sin \alpha} = \frac{\sin \theta'}{\sin \theta} = \frac{\lambda'}{\lambda}.$$

With this relation it is possible to write

$$\Lambda(\sin \theta_k - \sin \alpha) = k\lambda,$$

$$k = (0, \pm 1, \pm 2, \dots).$$

Thus for two consecutive values of  $k$ ,

$$\sin \theta_{k+1} - \sin \theta \cong \theta_{k+1} - \theta_k = \lambda/\Lambda,$$

which indicates that as the wavelength of sound increases, i.e., frequency of sound decreases, the angular separation between rays becomes indistinguishable. This equation is usually written as a grating equation with the grating constant being identical to the sound wavelength,  $\Lambda$ . Thus,

$$\Lambda \sin \theta_k = k\lambda, \quad k = (0, \pm 1, \pm 2, \dots).$$

The spacing between the  $k^{\text{th}}$  order line and the zero order,  $\delta_k$ , is related to the focal length of the objective lens,  $F$ , and the angle  $\theta$  by

$$\delta_k/F \cong \sin \theta_k.$$

(This approximation is discussed in Appendix 2.)

Substituting this last relation into the grating

form of the equation and solving for the wavelength, it is found that

$$\Delta \cong k \lambda F / \delta_k;$$

hence, knowing the separation between the  $k^{\text{th}}$  order and the zero order or some such related distance it becomes possible to determine the wavelength. Knowing the frequency of the ultrasonic wave, the velocity is easily determined from the product of the sound wavelength and frequency.

As stated in a previous section, the first acceptable theoretical description of the intensity distribution involving several diffraction orders produced by a plane ultrasonic wave field was given by Raman and Nath (46, 47, 48, 49). A similar treatment was carried out by David (9) but whereas the former work was directed to account for the phenomena involving the appearance of several orders in the spectrum, David's approach was confined to describe the intensity distribution for a spectrum comprised of at most the first and second orders. Both works use the wave equation as the starting point in their derivation; however, whereas David chooses to use the expression for the variation of the index of refraction as



$$n = n_0 + n_1 \cos (2\pi z/\Lambda)$$

Raman and Nath, in treating the problem for a progressive ultrasonic field, choose the expression

$$n = n_0 + n_1 \sin [2\pi(ft - z/\Lambda)] .$$

In these expressions,  $n$  signifies the instantaneous index of refraction,  $n_0$  the index of refraction in the medium in the absence of ultrasonic energy,  $n_1$  the amplitude of the change in the index of refraction due to the pressure wave,  $z$  the perpendicular distance between the source of ultrasound and a point in the ultrasonic field,  $f$  signifies the frequency of the ultrasound having a wavelength  $\Lambda$ , and  $t$  represents the time.

The inclusion of the time dependence in the instantaneous refraction in the treatment by Raman and Nath, establishes the presence of a Doppler shift and coherence phenomena in the diffracted light. Such a result should not detract from the comparison of intensity expressions given by David and by Raman and Nath, but is nonetheless an interesting result.

The validity of the result given by Raman and Nath -- that the relative intensity for the  $k$ th order varies as the square of a Bessel function,  $J_k^2(2\pi n_1 d/\lambda)$ , where in the argument of the Bessel function  $d$  is the

length of path of the light through the ultrasonic field -- is based on the magnitude of the expression

$$k^2 \lambda^2 / n_0 n_1 \Lambda^2$$

where  $k$  is the order number and  $\lambda$  the light wavelength, the other quantities having been defined previously. For their derivation, Raman and Nath require that this quantity be small, but actually this quantity is to vanish for an exact solution. Certainly the quantity cannot vanish but the formulation implies that the closer this quantity is to zero the better will be the correlation between theory and experiment.

The validity of the expressions derived by David depends upon the restriction that the intensity of the zero order is not affected by the intensities of the diffracted orders. David points out that for the general case, the intensity of the  $k^{\text{th}}$  order is proportional to  $\epsilon^{2k}$  where  $\epsilon = n_1 \lambda^2 / n_0 \Lambda^2$  which for a gas takes the form  $\epsilon = n_1 \lambda^2 / \Lambda^2$ . In view of this David mentions that if  $\epsilon \sim 1$  or  $\epsilon > 1$ , the theory predicts the appearance of several orders in the diffraction spectrum related with a complicated distribution in intensities.

David's expression for the intensity of the first diffracted order is

$$I_1 = \left[ \frac{e \sin(\bar{\alpha} + \frac{1}{2}) \bar{x}_0}{\bar{\alpha} + \frac{1}{2}} \right]^2 ,$$

where  $\bar{\alpha} = \frac{\Lambda}{\lambda} \alpha$ ,  $\bar{x}_0 = \pi \lambda d / \Lambda^2$ , and of the yet undefined quantities,  $\alpha$  is the angle between the parallel light beam and the sound wave fronts of the ultrasound.

For a comparison of the theories of David and of Raman and Nath, it is necessary to obtain the intensity expression found from David's treatment for which  $\alpha = 0$ , a condition under which the intensities of the plus and minus first orders are equal. In this case

$$I_1 = \left[ \frac{e \sin(\bar{x}_0/2)}{\frac{1}{2}} \right]^2 .$$

Moreover, the restrictions characteristics of the treatments must be recognized. One such restriction imposed by the solution of Raman and Nath requires that the quantity  $\lambda^2/n_1\Lambda^2$  be small. This is satisfied by the condition  $n_1 > (\lambda/\Lambda)^2$ . Now it is true (29, p. 128) that if  $|\xi| \ll 1$ ,

$$J_k(\xi) \cong \xi^k / k! 2^k .$$

This means that if for the expression of Raman and Nath

$$J_k^2(2\pi n_1 d / \lambda) \cong (2\pi n_1 d / \lambda)^{2k} / (k!)^2 2^{2k}$$

it must be true that  $n_1 d / \lambda \ll 1$ . In particular if  $k = 1$ ,

$$J_1^2(2\pi n_1 d / \lambda) \quad (\pi n_1 d / \lambda)^2.$$

This then means that if the intensity of the first diffracted order is given by  $(\pi n_1 d / \lambda)^2$ , then in the theory of Raman and Nath, it is necessary and sufficient that

$$\frac{\lambda}{d} \gg n_1 > \left( \frac{\lambda}{\Lambda} \right)^2.$$

The equality can also read

$$\frac{\lambda}{d} \gg \left( \frac{\lambda}{\Lambda} \right)^2 \quad \text{or} \quad \frac{\lambda d}{\Lambda^2} \ll 1.$$

It is to be noted that David's expression for the first order intensity

$$I_1 = \left[ \frac{\epsilon \bar{x}_0 \sin(\bar{x}_0/2)}{(\bar{x}_0/2)} \right]^2$$

becomes

$$I_1 \cong (\epsilon \bar{x}_0)^2 \quad \text{if} \quad \bar{x}_0/2 \ll 1.$$

On substituting for the quantities as previously defined, this latter equation reads

$$I_1 \cong (n_1 \Lambda^2 \pi \lambda d / \lambda^2 \Lambda^2)^2$$



$$I_1 \cong (n_1 \pi d / \lambda)^2 \quad \text{if} \quad (\pi \lambda d / 2 \Lambda^2) \ll 1.$$

Also to be noted is that the condition  $\bar{x}_0 \ll 1$ , follows from the two conditions imposed in the reduction of the expression given by Raman and Nath and that the condition

$$\frac{\lambda}{d} \gg n_1 > \left( \frac{\lambda}{\Lambda} \right)^2$$

is necessary and sufficient for both theoretical expressions to become identical.

The inequality which is necessary for reduction of both theoretical treatments, but which is a sufficient condition only for David's theory,

$$(\pi \lambda d / 2 \Lambda^2) \ll 1$$

or

$$d \ll (2 \Lambda^2 / \lambda \pi)$$

is easily evaluated. For example, assuming  $\lambda = 5000 \text{ \AA}$  and  $U = 350$  meters per second, for the reduction to be possible

$$d \ll 15.6 \text{ cm} / f_{\text{mc}}$$

where  $f$  is in megacycles per second.

In the present work, a crystal of circular shape was used, with a diameter of 4.45 cm. Although no treatment of the case of an ultrasonic field of circular cross-section appears to have been considered in the literature, it would appear reasonable to state that the average  $d$  for the present work was appreciably less than 4 cm.; thus, the inequality  $d < (2\Lambda^2/\pi\lambda)$  is satisfied for frequencies of one megacycle per second or less.

On the other hand, the additional condition peculiar to the theory of Raman and Nath

$$n_1 > (\lambda/\Lambda)^2$$

requires an evaluation of the experimental quantity  $n_1$  but can, in principle, be satisfied.

Reference is now made to the results obtained by Korff (33, p. 708-720) in an experiment undertaken to examine the validity of David's theory. In his work, Korff used a quartz crystal having a fundamental frequency of  $4.28 \text{ mc sec}^{-1}$  as the source of ultrasound. The medium was air at one atmosphere pressure.

The expression for the first order intensity obtained by David is conveniently written by Korff as

$$\frac{I_1}{I_0} = \frac{2\pi^2(n_0 - 1)^2}{\rho U^2} E \frac{d^2}{\lambda^2} \frac{\sin^2 \beta}{\beta^2}$$

where, summarizing,

$$\beta = \pi \left( \frac{\alpha \Lambda}{\lambda} \pm \frac{1}{2} \right) \frac{\lambda d}{\Lambda^2},$$

and

$\rho$  = specific gravity of the gas

$U$  = its sound velocity

$n_0$  = index of refraction of the gas in the absence of ultrasonic energy

$E$  = ultrasonic energy per  $\text{cm}^3$

$d$  = length of path through the sound field

$\lambda$  = light wavelength

$\Lambda$  = sound wavelength

$\alpha$  = the angle between impinging light rays and sound wave front.

Special emphasis is placed by Korff on two conditions with respect to the value of  $\alpha$ . One is the symmetrical condition,  $\alpha = 0$ , and is called symmetrical because with this value of  $\alpha$ , the intensity of the plus one and the minus orders should be the same. The second condition is called the Bragg condition and here  $\alpha$  takes on a value expressed by

$$\alpha = \pm \lambda / 2\Lambda .$$

In the latter situation, if  $\alpha$  takes on either of these values, the intensity of one of the first orders should be a maximum according to David's theory.

For the symmetrical case, the intensity of distribution of the plus one and minus one orders is given by

$$\frac{I_{\pm 1}}{I_0} = \frac{2\pi^2(n_0-1)^2}{\rho v^2} E \frac{d^2}{\lambda^2} \frac{\sin^2(\pi d \lambda / 2 \Lambda^2)}{(\pi d \lambda / 2 \Lambda^2)^2}$$

In the Bragg condition for which  $\alpha = \pm \lambda / 2 \Lambda$  and  $\beta = 0$ , the maximum intensity of one of the two orders is given by the expression

$$\left( \frac{I_1}{I_0} \right)_{\max} = \frac{2\pi^2(n_0-1)^2}{\rho v^2} E \frac{d^2}{\lambda^2} .$$

It is important to point out that this maximum in intensity, as seen earlier, will also be approached as the relation  $(\pi \lambda d / 2 \Lambda^2) \ll 1$  is better satisfied.

For velocity measurements it should be clear that the probability of attaining the best precision involves the measurement of a distance between two lines of similar intensity. For this reason attention must be concentrated on the intensity expression for the symmetrical condition. Regarding the expression concerned, it predicts a maximum in the intensity when the trigonometric



term has a value of unity since the factor  $d$  would cancel. This condition implies that

$$d\lambda/\Lambda^2 = (2q + 1), \quad q = 0, 1, 2, \dots$$

or

$$d = (2q + 1)\Lambda^2/\lambda = (2q + 1)U^2/f^2\lambda.$$

Thus, using  $\lambda = 5461 \text{ \AA}$ ,

$$d = [(2q + 1)U^2/f^2] 1.83 \times 10^{-4} \text{ cm}$$

or using  $\lambda = 4358 \text{ \AA}$ ,

$$d = [(2q + 1)U^2/f^2] 2.29 \times 10^{-4} \text{ cm}$$

provided the value of  $f$  is in megacycles and  $U$  in meters per second.

Application of these results to a case where  $U = 350$  meters second (velocity of ultrasound in air is about  $346 \text{ meters sec}^{-1}$  at room temperature and atmospheric pressure),  $\lambda = 5461 \text{ \AA}$  and a frequency of one megacycle,

$$d_{5461} = 22.42 (2q + 1) \text{ cm}$$

and if instead,  $\lambda = 4358 \text{ \AA}$ , then

$$d_{4358} = 28.05 (2q + 1) \text{ cm}.$$

Thus using a frequency of one megacycle and the green line, the theory predicts an impractical value in the crystal size for obtaining a maximum in the symmetrical intensity distribution under ordinary conditions.

Korff found that under similar conditions but using the 5461 A line and a frequency of  $4.28 \text{ mc sec}^{-1}$ , the theory predicted a minimum in the intensity using  $d = 2.30 \text{ cm}$  and two maxima, one at  $d = 1.15 \text{ cm}$  and the other at  $3.45 \text{ cm}$ . He found that the intensity increased linearly with a slope of slightly less than unity when plotted against  $d$  up to a value in  $d$  of  $2.0 \text{ cm}$ . Then the line becomes concave downwards to accomodate a point at  $d$  equal to  $3.2 \text{ cm}$ . In terms of the quantity  $(d\lambda/\Lambda^2)$ , the value of  $d = 2.0 \text{ cm}$  corresponds to  $(d\lambda/\Lambda^2) = 1.67$ , which is to be compared to the value unity predicted by theory for the first maximum.

Using light of wavelength 5461 A, Korff found that the intensity of the first orders was less than that obtained using the 4358 A line. This increase was found to be in the right direction but the values deviated about  $\pm 40\%$  from those predicted by David's theory.

The variation of the intensity due to pressure for the symmetrical condition -- assuming the velocity of ultrasound in the gas remains relatively constant -- is due to the factor involving the index of refraction

in the numerator and the density occurring in the denominator. For this evaluation reference is made to the Mosotti-Clausius equation (16, p. 536) which may be written as

$$n_o - 1 \cong 2\pi N \alpha_E \rho / M$$

where

$N$  = Avogadro's number

$\alpha_E$  = electron polarizability

$\rho$  = density of the gas under static conditions

$M$  = molecular weight of the gas.

Since the density is directly proportional to the pressure, other parameters being equal, the result is that in the absence of absorption of ultrasonic energy, the intensity of the first order intensity for the symmetrical condition should increase directly as the pressure. Korff did not study or propose this variation of intensity with pressure.

In regards to the absorption of ultrasound such as to affect the value of  $E$  in the intensity expression, Hayess and Winde (19, p. 196) point out that as the density increases the absorption decreases as indicated by the following relation

$$E = E_o \exp(-bz/\rho),$$

where  $E$  is the sound intensity at a distance  $z$  along the normal from the source of ultrasound,  $E_0$  is the value of  $E$  at  $z = 0$ ,  $b$  designates a constant and  $\rho$  has been defined.

The absorption referred to in the last paragraph is due to the classical, visco-thermal, absorption given as (21, p. 44)

$$a_c = \frac{8\pi^2}{3} \frac{f}{p} \frac{1}{\gamma} \left( \mu + \frac{3}{4} \frac{\gamma - 1}{c_p} \chi \right)$$

where

$\alpha_c$  = classical absorption due to viscosity and thermal conduction effects (per wavelength)

$\gamma$  = heat capacity ratio calculated in terms of the total heat capacities

$c_p$  = specific heat (joules/gram)

$\mu$  = coefficient of shear viscosity (poise)

$\chi$  = coefficient of thermal conductivity (joules/cm sec °C).

Thus summarizing the factors involving the intensity of the first order spectrum as derived by David for the symmetrical condition, it can be stated that:

- (1) The intensity should vary periodically with the length of path of the light,  $d$ , through the ultrasonic field by the factor  $\sin^2(\pi d \lambda / 2 \Lambda^2)$ . However, if



$(\pi \lambda d/2 \Lambda^2) \ll 1$ , then the intensity will depend directly on the square of the length of path of the light through the ultrasonic field.

- (2) The intensity should be 2.46 times greater using light of wavelength 4358 Å over that from 5461 Å since the intensity varies inversely as the fourth power of  $\lambda$ .
- (3) For a constant frequency the intensity should vary directly as the square of the ultrasonic velocity in the medium.
- (4) For a constant ultrasonic velocity and negligible ultrasonic energy absorption, the intensity varies inversely as the square of frequency.
- (5) The intensity varies directly as the pressure again in the absence of ultrasonic energy absorption.

## EXPERIMENTAL APPARATUS

The Optical System

The optical system employed is outlined in Figure 2. Here the light source is designated as H, a filter for producing monochromatic radiation as F, an adjustable aperture shutter as D, the slit as S and the photographic plate as P. The lens designated as  $L_1$  was a condenser type two and three-quarters inches in diameter with a focal length of three inches. It served to focus the light from the lamp onto the slit. The lens  $L_2$  was a Kodak Aero-Ektar and lens  $L_3$  was a Bausch and Lomb Aero-Tessar. Both had a focal length of 24 inches and were four inches in diameter.

Lens  $L_2$  was used as a collimating lens and  $L_3$  as a camera lens. Each of these two lenses,  $L_2$  and  $L_3$ , was housed in a 23 inch metal cone and was equipped with an adjustable diaphragm through which it was possible to use the full aperture or to reduce it to a diameter of approximately  $2\frac{1}{2}$  centimeters. The lenses  $L_2$  and  $L_3$  were coated in later stages of experimentation. The area enclosed with the broken line rectangle between  $L_2$  and  $L_3$  represents the location of the sample cell.

In the initial stages of this study, a 250 watt AH-2 General Electric mercury vapor lamp was used; as

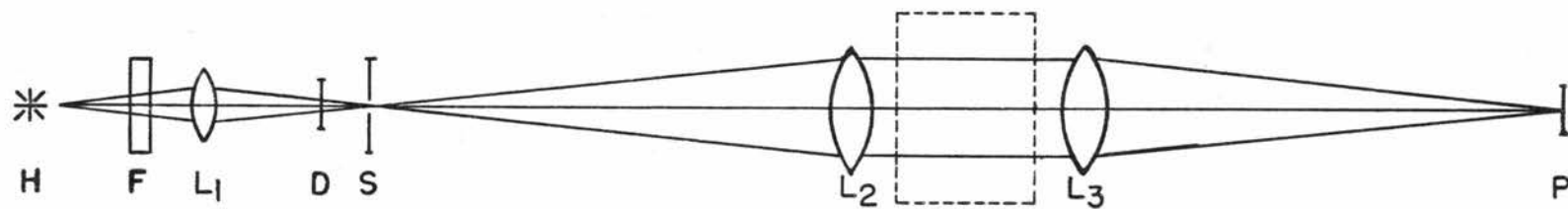


FIGURE 2 OUTLINE OF THE OPTICAL SYSTEM

the investigations progressed a more powerful lamp was used. This was a General Electric mercury lamp type H 400-ElT, having a wattage rating of 400.

As a filter for the 5461 Å Hg line, F consisted of a series of three separate solutions, viz., neodymium chloride, cupric nitrate and sodium chromate, made to comply with those specifications given by Stamm (55, p. 319-320). Transmission characteristics of these solutions were obtained with a Cary recording spectrophotometer using a one centimeter sample cell. The results are grouped together in Figure 3. An effective filter was obtained when each solution was contained in a 1x4x4 inch liquid tank and all three tanks were placed between the lamp H and the lens  $L_1$ .

The slit S was formed from two edges of a double edge razor blade. Its width was adjusted to be approximately 0.04 mm and the maximum height was about  $2\frac{1}{2}$  cm. As an innovation for varying the angle between the parallel beam of light and the ultrasonic wave fronts, the slit was placed on a mechanical stage movable in the vertical direction. This slit elevator consisted of a  $\frac{7}{8}$  inch diameter threaded shaft having ten threads per inch and threaded through the center of a flat gear in a 20:1 ratio. The shaft through the center of the worm gear extended on one end to a counter which read the



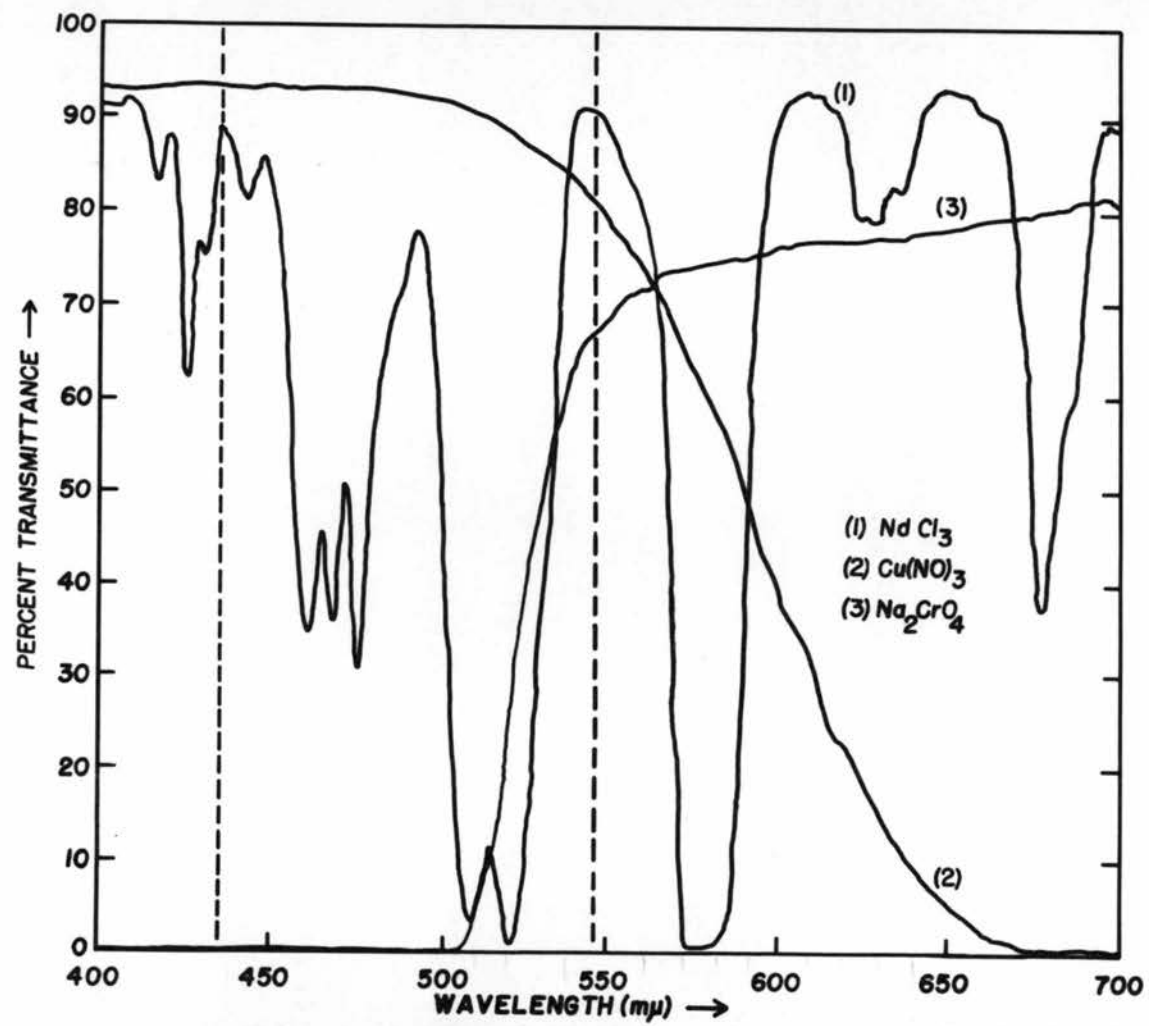


Figure 3. Transmission characteristics of the filter solutions.

tenths of revolution of the worm gear. On the other end of the shaft was a turning dial operated manually. With this arrangement, one complete turn of the worm gear moved the slit 0.005 inch vertically and it was possible to read directly to a tenth of this interval if necessary.

The camera, which used lens  $L_3$  as its objective, was made from a camera box originally made to accomodate a maximum size plate of 5x7 inches. A plate holder support was made such that a least five exposures could be obtained on one 4x5 inch plate, which was adopted as the standard size in this study after the intial investigations. For visual inspection of the image to be photographed, a ten power eyepiece was substituted to the plate.

### The Electrical System

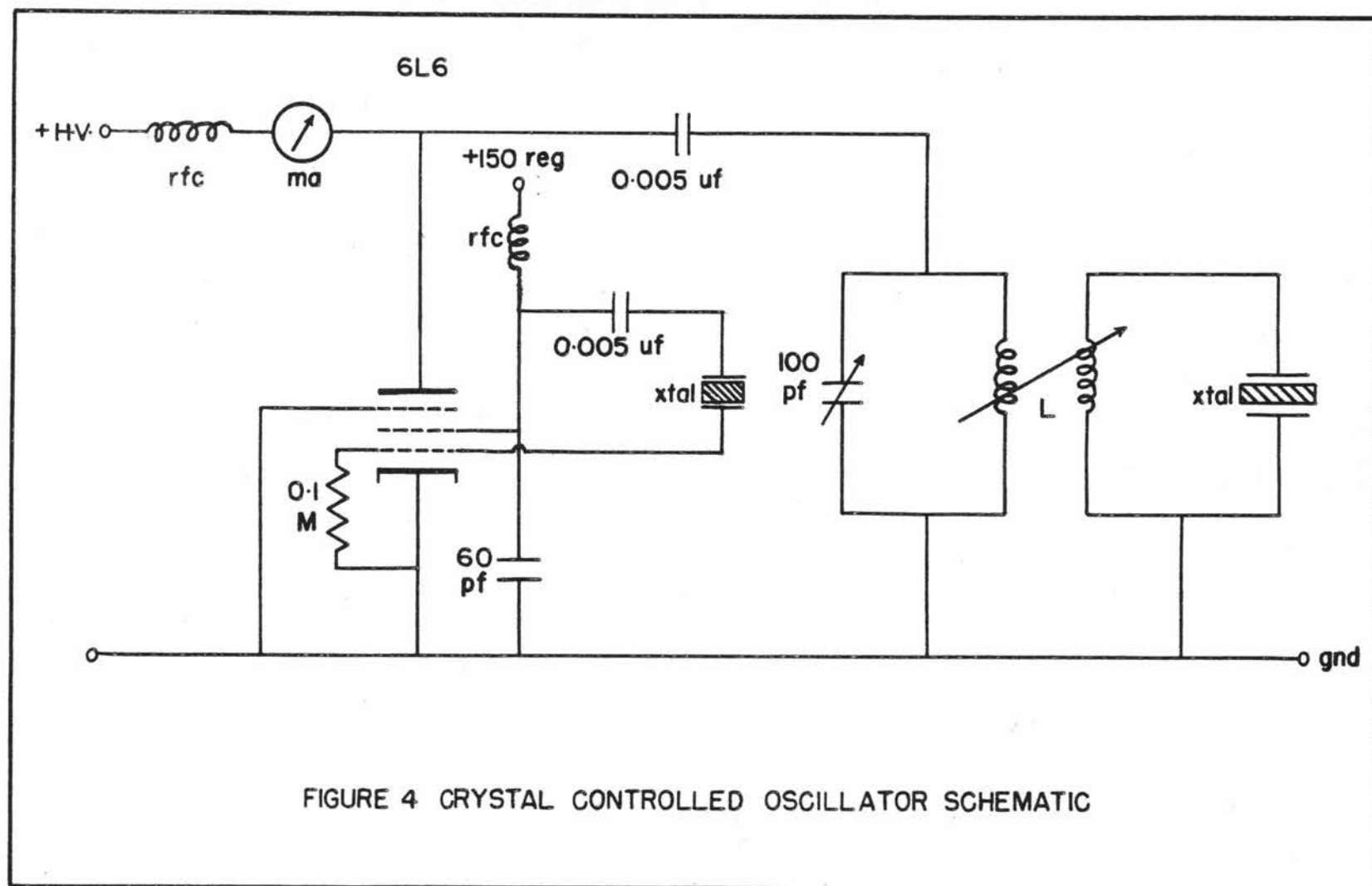
#### a. The transmitters.

Investigations for obtaining a suitable transmitter which led to the observation of diffraction in air at one atmosphere pressure necessitated the evaluation of two transmitters before the third and final one was selected.

Of the first two, one was a commercial transmitter, a Heathkit Model DX-40. This was used in

conjunction with a crystal having a fundamental frequency of seven megacycles and also, after a slight modification, with the third overtone of a one megacycle crystal. This transmitter used a 6L46 tube in the final stage and a pi-network antenna coupling which was to match a load of 50 to 1000 ohms. It was specified to have a peak power input of 75 watts on CW and 60 watts on phone. It could be either crystal or VFO controlled. After completing experimentation with a seven megacycle quartz crystal in its fundamental, second and third overtone, capacitance was added to the 80 meter tank circuit in order to activate the one megacycle crystal in its third overtone. The output of the transmitter was connected to the crystal in the low pressure cell through a length of RG 11/U coaxial cable.

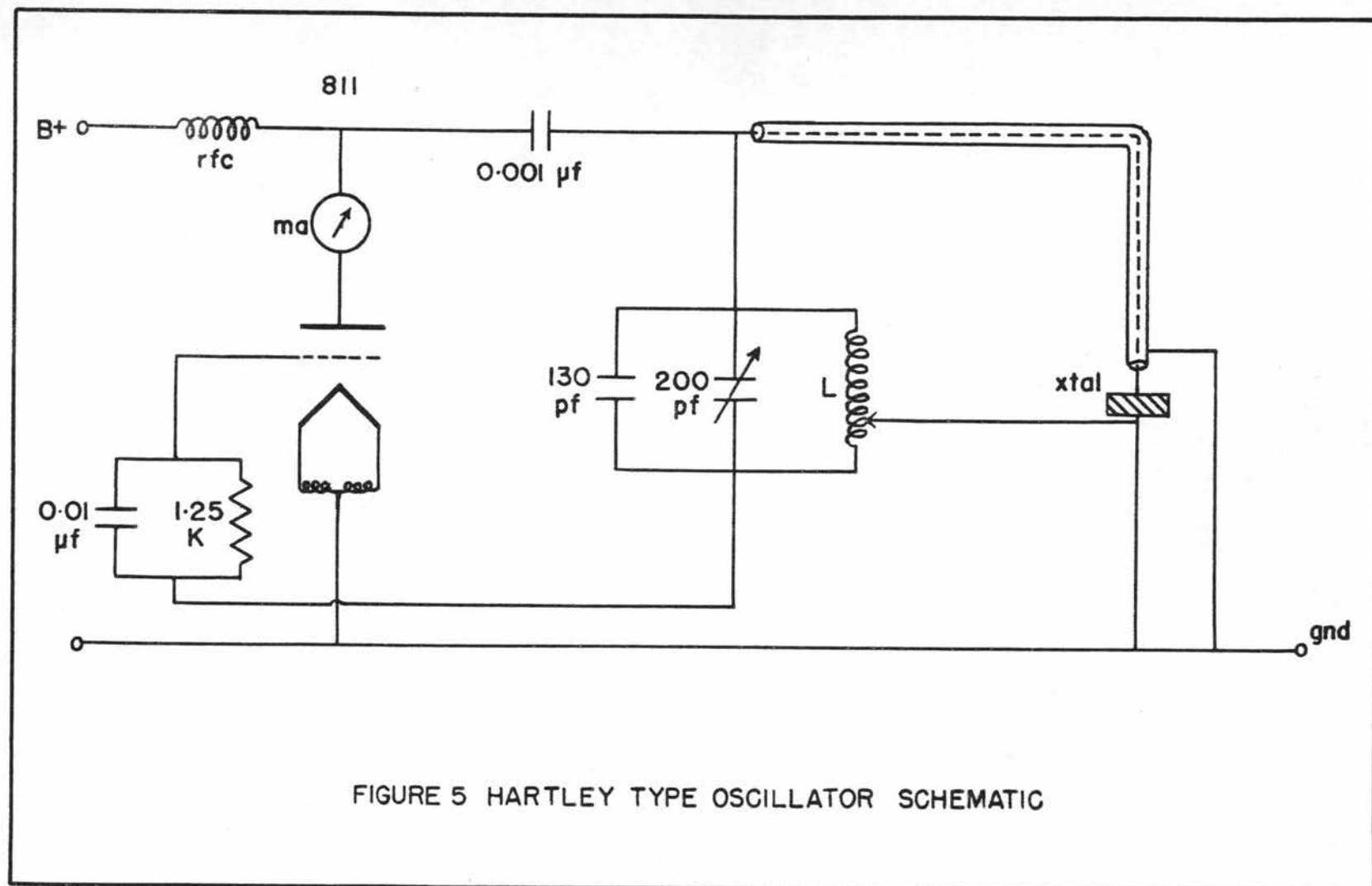
The second transmitter was also crystal controlled with a 999.5 kilocycle crystal and was built about a 6L6 vacuum tube. This was to activate a one megacycle crystal. The schematic diagram of the circuit is shown in Figure 4. The improvement of this circuit over that of the first transmitter lies in the coupling to the transducer crystal. The loose coupling shown was through a coil, L, whose specifications remained unknown. It was taken from a surplus aircraft transmitter type TA-12 made by Bendix Radio. It was with this oscillator that





diffraction in air was first seen when used to activate a one megacycle transducer crystal.

The third and final transmitter used was built basically as a Hartley oscillator. This oscillator was also built for one megacycle operation but had the added advantage that the frequency region covered could be changed by merely changing the LC combination. Moreover, it permitted a region of tuning over the proximity of the crystal's frequency of operation. The other feature which made this oscillator more desirable than the one built about the 6L6 vacuum tube, was the possibility of obtaining a considerably greater amount of power using the 811 tube. Figure 5 shows a schematic diagram of this circuit. This oscillator had a separately housed power supply which could deliver a maximum of 1600 volts  $B^+$  and 300 ma. The coil designated as L in Figure 4 was made by winding 54 turns of #18 enameled copper wire on a  $2\frac{1}{4}$  inch form. A tap was placed at  $12\frac{1}{2}$  turns from the grid leak connection. The variable condenser was a surplus element equipped with a gear arrangement for fine tuning. The variable portion of the condenser had a maximum capacitance of about  $200 \mu\mu\text{fd}$ . Thirty-one turns of a dial were required to cover the region between minimum and maximum capacitance.



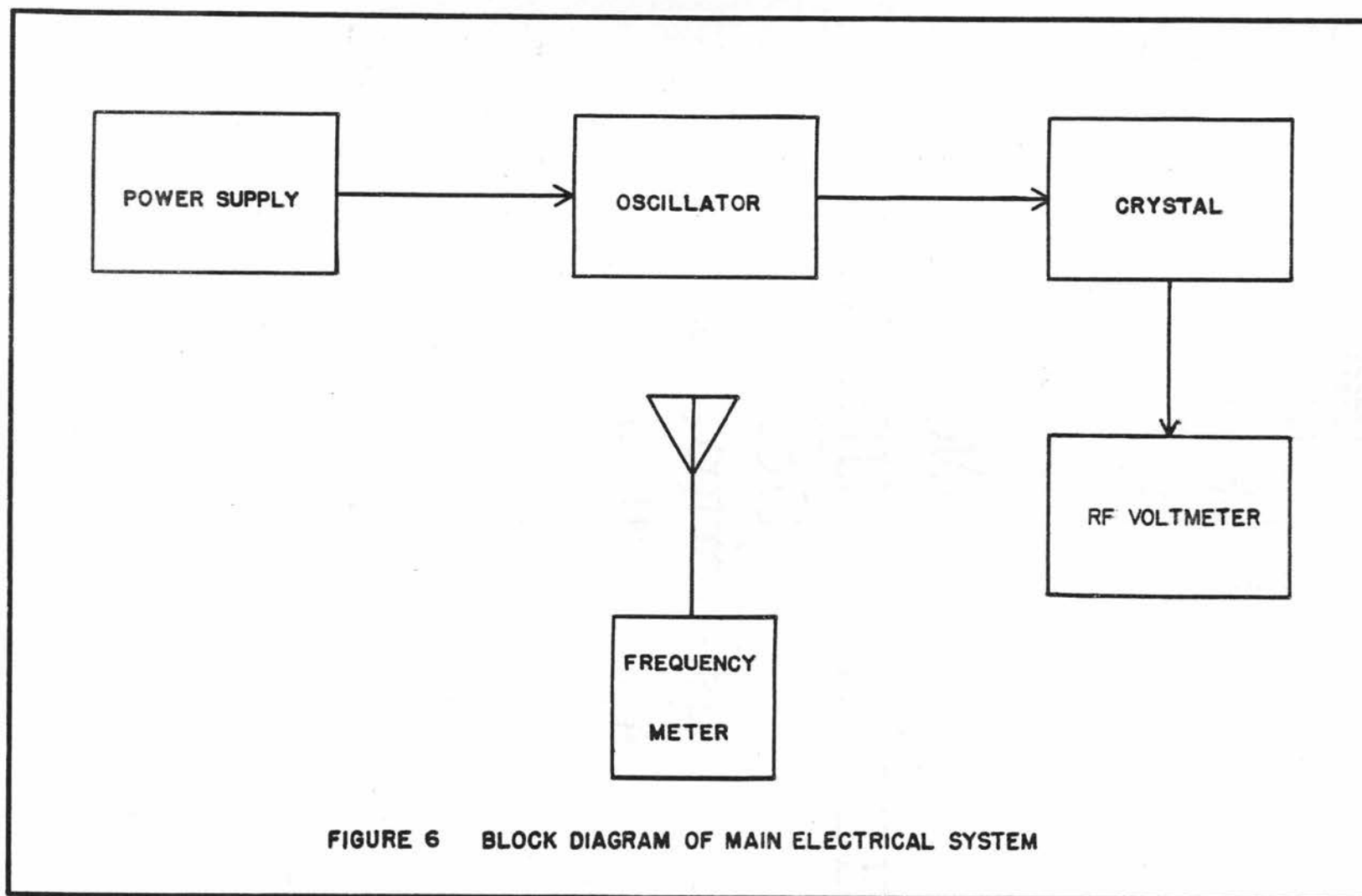
b. The frequency meter

The frequency of the crystal oscillation was monitored by using an LM Heterodyne Frequency Meter Model 15. The input signal was taken from an antenna passing over the gas cell. This incoming signal was mixed in the meter with a standard crystal frequency, fundamental or harmonic, and the beat picked up on a pair of headphones. The dial reading at which the beat became null was recorded as the corresponding ultrasonic frequency.

The meter, whose frequency range was listed as being from 125 to 20,000 kilocycles, was standardized during any exposure which involved the activation of the transducer crystal. The accuracy in frequency measurements with this particular meter was reported to be  $\pm 0.005$  kc. This was done by the usual check-point procedure. A block diagram of the foregoing described electrical system is shown in Figure 6.

c. Voltage measurements

The radio-frequency (rf) voltage measurements under 300 volts were made with a Hewlett-Packard Voltmeter Model 410B. For higher voltage measurements the B+ voltage on the plate of the 811 vacuum tube was used. The deviation between both values, rf and B+ voltages,





was small but increased as the voltage increased. Beyond 300 volts rf, the reading of B+ must be accepted only as an indication of the rf voltage on the transducer crystal.

### The Gas Cells

Two gas cells were employed in this investigation. One was a low pressure cell and the other a high pressure cell.

#### a. The low pressure cell

The low pressure gas cell was constructed from a two inch cross of Corning industrial glass made to be used in conjunction with pressures of about one atmosphere and below. The cell may be visualized as made by the symmetrical right angle intersection of two eight inch lengths of industrial glass pipe having an inner diameter of two inches. The cell is shown intact in Figure 7.

Two of the four openings of the cell were closed with two coated flat glass windows having a diameter of 65 mm and an 8 mm thickness. A rubber "O" ring was placed between each window and the cell aperture. The window was supported by a half-inch thick aluminum plate. The aluminum plate was recessed to accomodate the

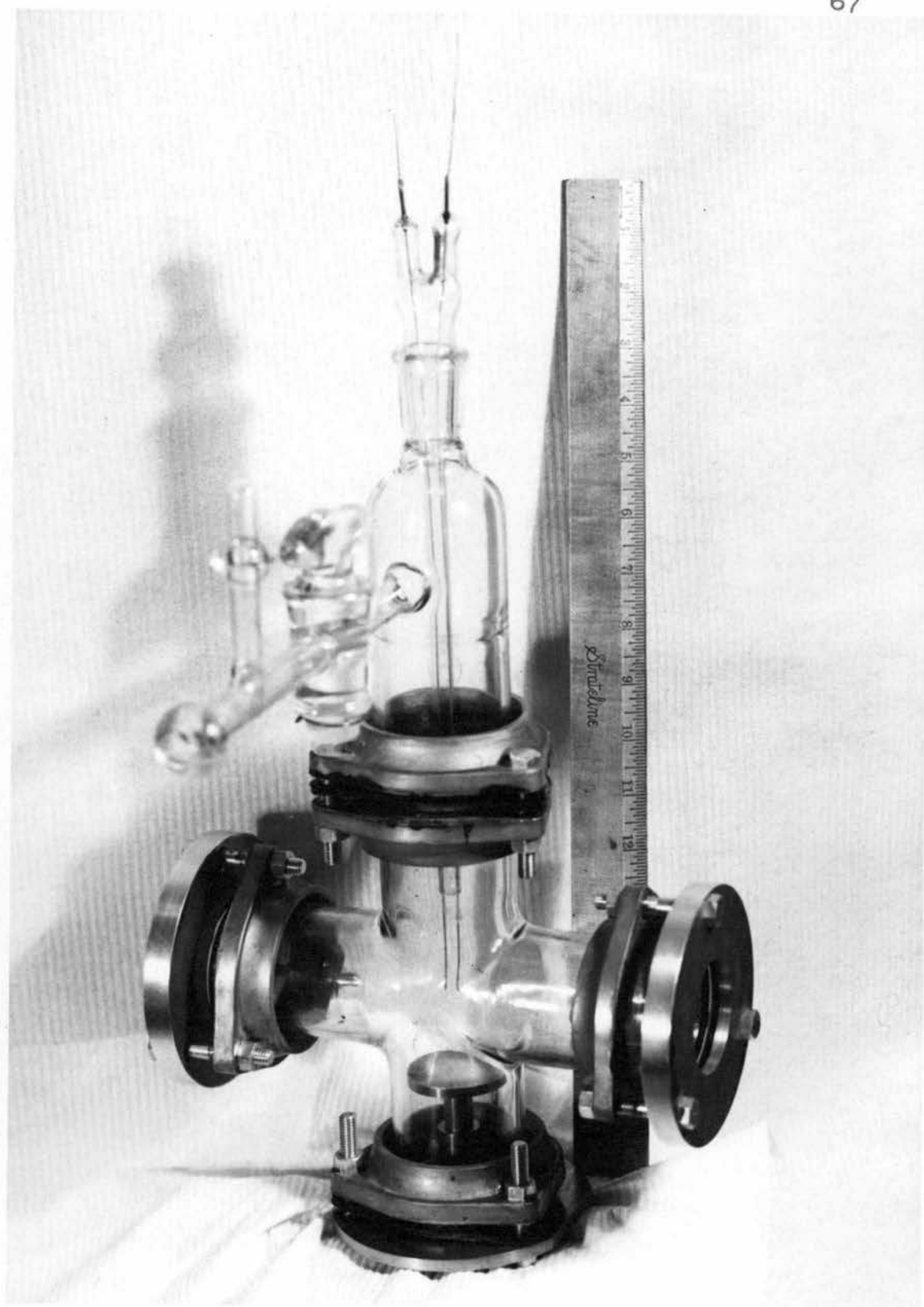


Figure 7. Photograph of low pressure gas cell.

window and another "O" ring was placed between them. The window was set in place by bolting the aluminum plate to an aluminum flange common to the cross.

On one of the remaining two apertures of the cross was placed a brass plate  $\frac{1}{4}$  inch thick and bolted in the same fashion. A neoprene gasket, also common to the cell, was placed between the brass plate and the glass cross. A brass cylinder having an inner diameter of half-inch and a wall thickness of  $\frac{1}{8}$  inch was silver soldered to the inside of the brass plate. The cylinder received a half-inch brass stem from a brass table which served as the support for the quartz crystals. This resulted in a telescopic joint between the brass plate and the brass table permitting the raising and lowering of the quartz transducer. A set screw held the quartz mount in place.

A Stupakoff seal placed in the brass plate served as the high voltage lead, the plate being the ground side. On the external side of the plate, a coaxial "T" connector was fixed to the lead.

The last of the cross openings, that opposite the brass plate, serving as support for the crystal mount, had a fine inch piece of industrial glass tubing similar to that from which the cross was made. It was also held in place with three bolts, a neoprene "O" ring and two

aluminum flanges. The outer end of this piece was brought to a  $\text{B } 24/40$  joint used as support for the inner joint holding the thermistor leads. This piece of glass also had a side arm and stopcock which could be connected to a vacuum line through a ball joint for evacuation and filling purposes.

The all glass vacuum line was equipped with an ordinary mercury manometer and meter stick such that the absolute pressure could be read to  $\pm 0.5$  mm with great ease.

b. The high pressure cell

The high pressure cell was built from a four inch cube of 2024 T-4 aluminum stock. Two cylindrical openings perpendicular to each other and each parallel to a cube surface normal were symmetrically worked in the aluminum. One such cylindrical opening was of a  $2\frac{1}{2}$  inch diameter and the other was 1 and  $\frac{3}{4}$  inches in diameter. The larger one accommodated the crystal mount and the smaller one was closed with the two coated glass windows previously used with the low pressure cell. These windows closed the ends of the 1 and  $\frac{3}{4}$  inch cylinder with a metal seal. An "O" ring,  $1/8 \times 2\frac{1}{4}$  inches was placed between the window and the aluminum block. A recessed aluminum plate held the window against the block



by the use of six bolts. The windows were cushioned against the aluminum plates with thin gasket material.

The larger openings were also closed with "O" rings and aluminum plates in metal seals. One of these plates supported the quartz crystal mount and also a Stupakoff seal for the high voltage lead, the body of the cell being used as ground. Again a "T" coaxial connector was employed to bring in the output from the transmitter.

The other plate closing the 2½ inch bore was equipped with Stupakoff seals for thermistor lead-ins. It also supported a brass nipple for connecting the cell to a gas line of copper tubing. In between the gas inlet from a gas cylinder and the high pressure cell were two taps. One was a Housekeeper seal which made it possible to connect the high pressure line to an all glass vacuum system. This permitted the rapid flushing of the cell when introducing a purified gas and also allowed the all glass system to be shut off from the high pressure line.

The second tap went to a high pressure gauge of the Bourdon type made by United States Gauge Company. The 4½ inch dial had a maximum reading of 200 psig.

All the high pressure line was made of ¼ inch copper tubing and ¼ inch Hoke valves. Two of the latter were used. One isolated the high pressure line from the

all glass vacuum line while the other isolated the gas cylinder from the rest of the system.

The construction of the more important functional elements of the high pressure cell was based on the low pressure cell as a model. This was true in particular with respect to the crystal mount support.

The high pressure cell was designed to safely withstand a working pressure of ten atmospheres. An exploded view of the high pressure cell was photographed and is shown in Figure 8.

#### Quartz Crystals and Their Mounts

The x-cut quartz crystals, purchased in a diameter of 1 and 3/4 inches, were silver plated in the laboratory according to the Brashear's silvering process (24, p. 2296-2997). In the cleaning procedure suggested previous to coating the crystal, it was found necessary to add to the procedure the rinsing of the crystal with stannous chloride just before the final washing. This step was taken from the cleaning procedure suggested by Strong (56, p. 154).

Very good plated surfaces resulted after subjecting the crystal to the silvering process three consecutive times. After the plated surfaces were dry, the perimeter of the plated crystal was cleaned with

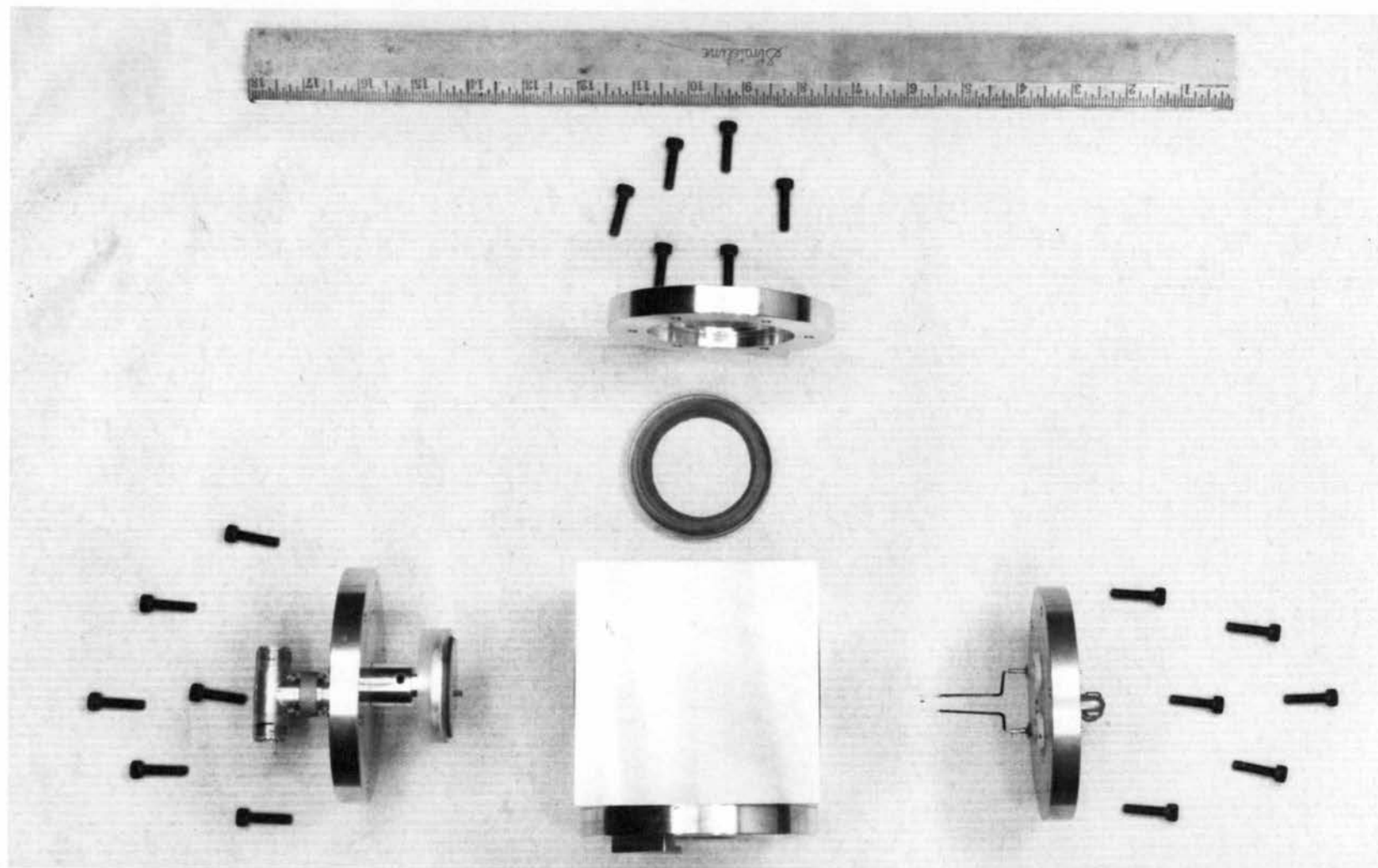


Figure 8. Photograph of disassembled high pressure cell.

concentrated nitric acid. The nitric acid was washed off immediately and the crystal allowed to dry. After drying the crystal's perimeter was cleaned with an organic solvent. Resistance measurements between the two crystal surfaces indicated a dc resistance of no less than 500 megohms.

Initially the quartz crystal mount called for a plastic ring, usually of Micarta or polystyrene, to hold the quartz transducer in place. The plastic ring was equipped with a 3/16 inch lip all about its perimeter such that a narrow brass shim stock rim electrode could be placed underneath the lip between the plated surface and the plastic. The electrode was made with a pigtail which protruded the plastic and was soldered to the high voltage Stupakoff lead.

To enhance the contact between the rim electrode and the crystal surface, the plastic ring was fitted with a thread and brass knurl nut such that when the nut was tightened the edge of it pressed against the underside of the brass table. Actually it was soon learned that tightening the nut produced too much damping on the crystal. Instead the ring was left loose and contact between the rim electrode and crystal surface depended entirely upon the tendency of the weight of the knurl nut to pull down the plastic ring. In this manner a



good electrical contact was made and the damping was lessened considerably.

The table upon which the plated crystal rested was a disc of  $\frac{1}{4}$  inch brass approximately the same diameter as the crystal.

During the preliminary stages of experimentation, the rim electrode was found to be deficient insofar that at higher voltages, about 250 volts ac, arcing occurred between the electrode and the crystal surface. The arcing caused oxidation and evaporation of the plated surface leading to very poor electrical contact and consequently inefficient electrical power transfer from oscillator to crystal. This objectionable feature was completely eliminated by removing the ring electrode and substituting a narrow strip of shim stock. The tip of the strip was adhered to the upper crystal surface with silver circuit paint. At worse, this connection was disturbed by what could be explained as flaking of the dry paint caused by the large amplitude of vibrations of the crystal at low pressures and high voltages. In addition to substituting for the rim electrode, a plastic ring was placed on the brass table such that it would prevent the crystal from falling off the table when the crystal was activated or the cell was moved. This ring did not necessarily come into contact with the crystal



and served to support the shim stock strip. Figure 9 is a photograph of the two crystal mounts described.

#### The Thermistor and Temperature Measurement

A bead type thermistor number GB32J2 obtained from Fenwal Electronics was used as the temperature sensing device. The specifications accompanying the thermistor listed a resistance of 2000 ohms at 25°C, a temperature coefficient of resistance equal to -3.9% per °C, and a time constant of two seconds. It was used as a variable resistance element in a Wheatstone bridge arrangement, resistance being continually monitored by a Leeds and Northrup Speedomax strip chart recording potentiometer type G. An outline of the bridge arrangement is shown in Figure 10.

The thermistor circuit was similar to that described by Zeffert and Witherspoon (60). A 1.5 volt telephone cell was used as the EMF source and was found to be satisfactory for an accuracy of 0.1°C between the temperature region of interest, 20 to 30°C. A resistance of 500 ohms was placed in series with the cell to maintain the thermistor current between 0.1 and 0.2 ma. With this current value, any heating due to the thermistor should have been negligible and the thermistor resistance variation was specified to be linear within this

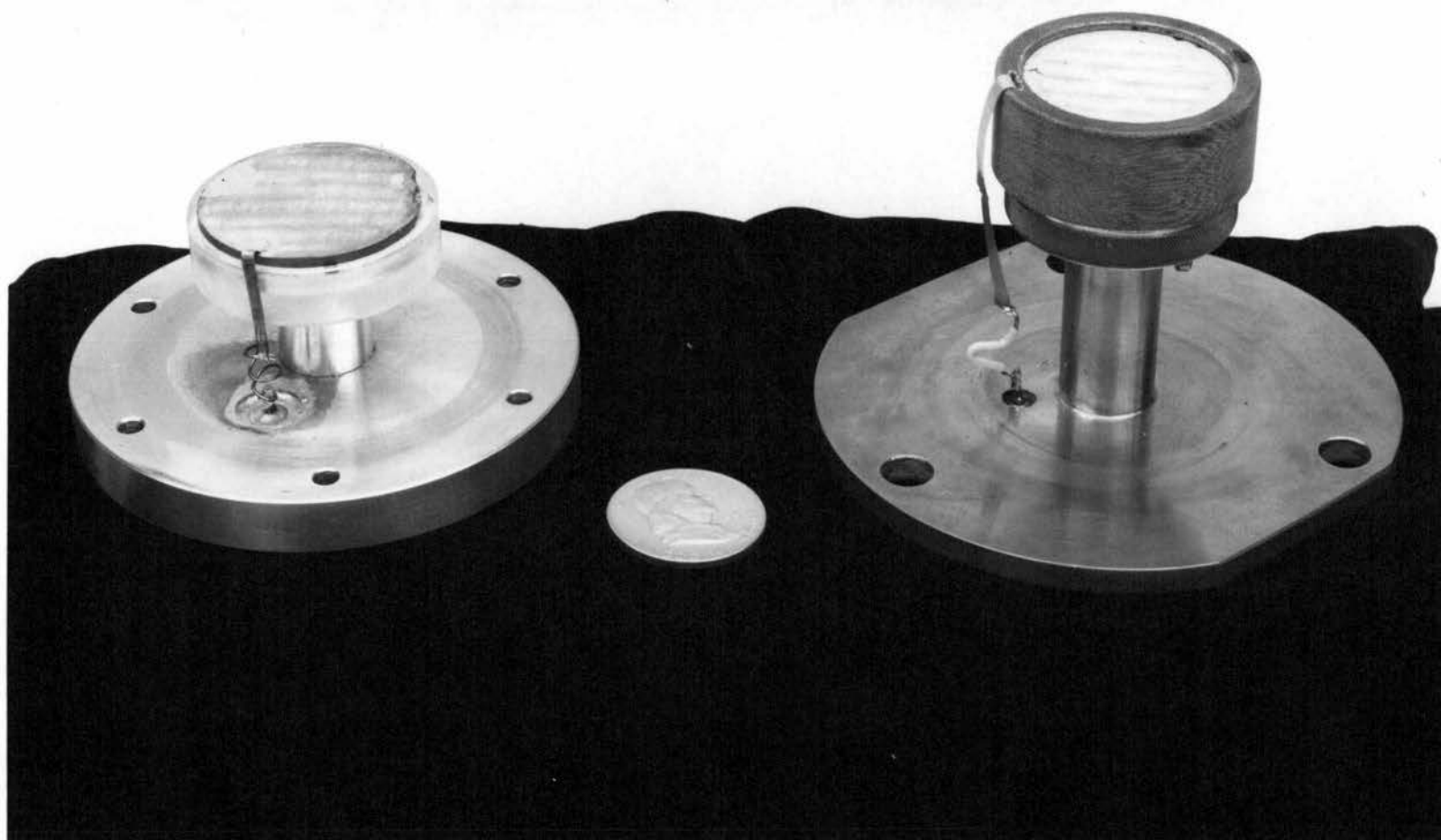


Figure 9. Photograph of the two crystal mounts used in this study.

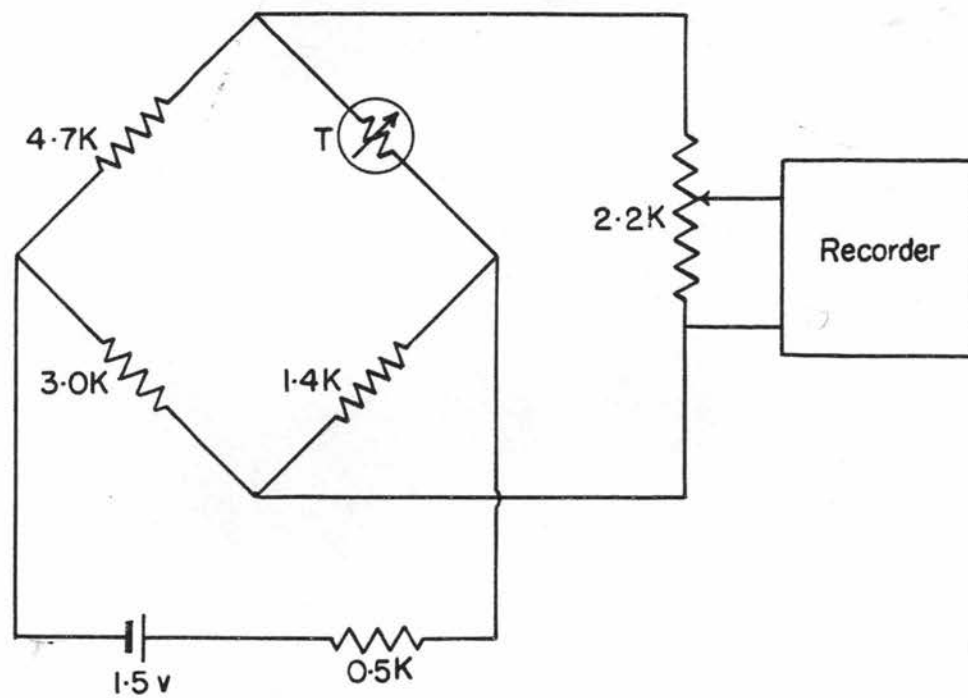


FIGURE 10 THERMISTOR MEASURING CIRCUIT SCHEMATIC

temperature range. The load on the Speedomax recorder, a variable 2000 ohm helipot, was set such that full scale deflection of the chart was equivalent to approximately a total temperature change of ten degrees. The chart was marked off in one hundred divisions, permitting the reading of the temperature to  $0.1^{\circ}\text{C}$  with sufficient accuracy.

The thermistor was calibrated in a water bath against a thermometer marked off in  $0.05^{\circ}\text{C}$  divisions. The thermometer had been previously calibrated by the Bureau of Standards. A typical calibration plot of temperature versus pen deflection could not be distinguished from a straight line with all the points falling within the line. Initially the calibration lines would be slightly displaced from each other. After a period of use of about three weeks this 'drift' disappeared. This variation seems to be characteristic of all new thermistors and has been associated with an aging process undergone by the thermistor. Nevertheless, even after the calibration remained essentially constant, to insure correct calibration, the thermistor was immediately calibrated after a series of exposures.

The thermistor was usually mounted so that it was in the center of the light beam and colinear with the parallel light beam directly above the crystal.

A photograph showing the high pressure cell in position in the optical path and the electronic instrumentation is shown in Figures 11 and 12.

#### The Comparator and Interval Measurement on the Plate

The distances between two points on the exposures were made with a traveling microscope having a magnification of ten. The movement of the eyepiece was controlled with a micrometer drive which was marked off to 0.01 mm. It had no provision for standardizing the direction of travel with the line joining the two points under question.



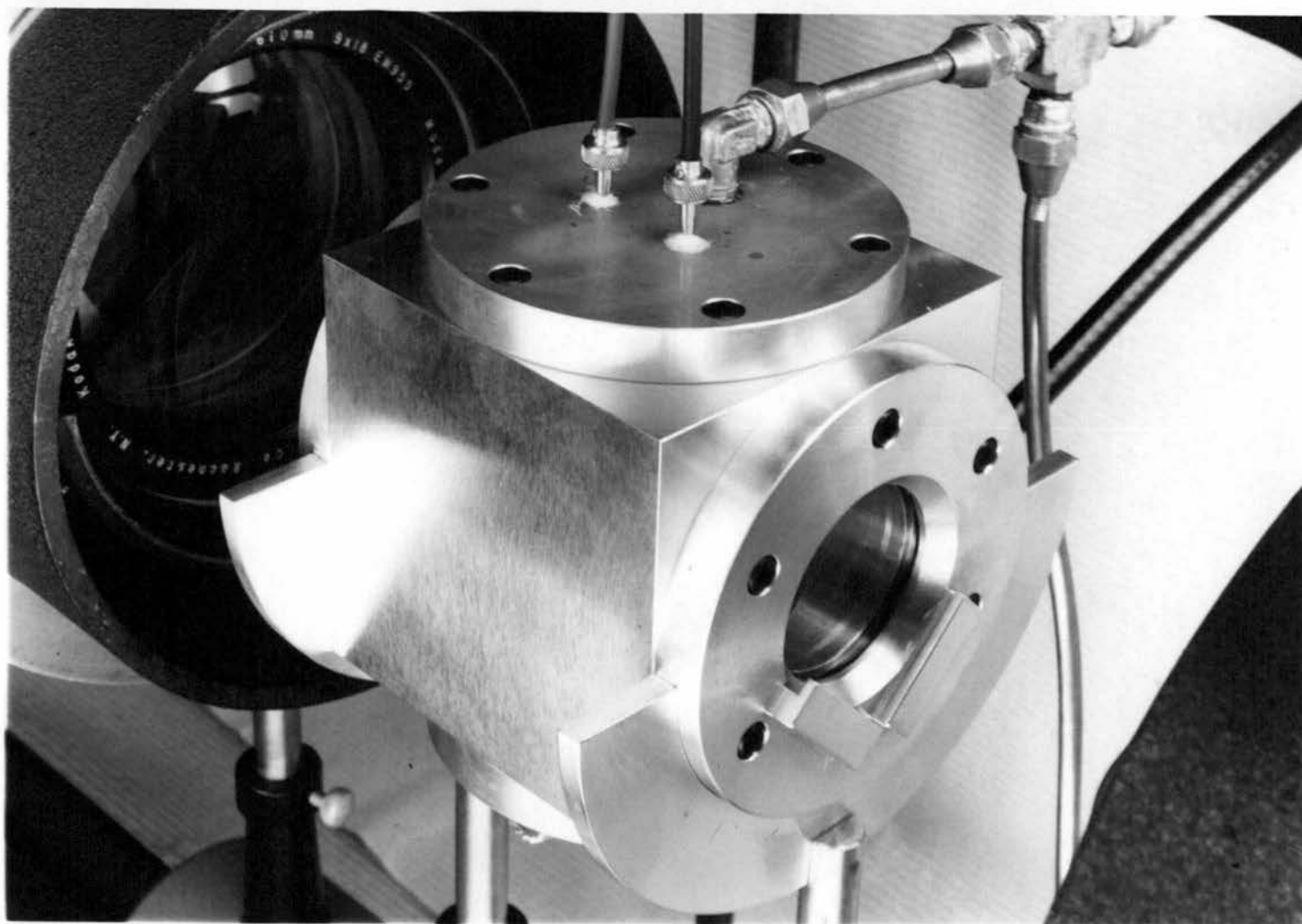


Figure 11. Enlargement of high pressure cell in position in optical path.

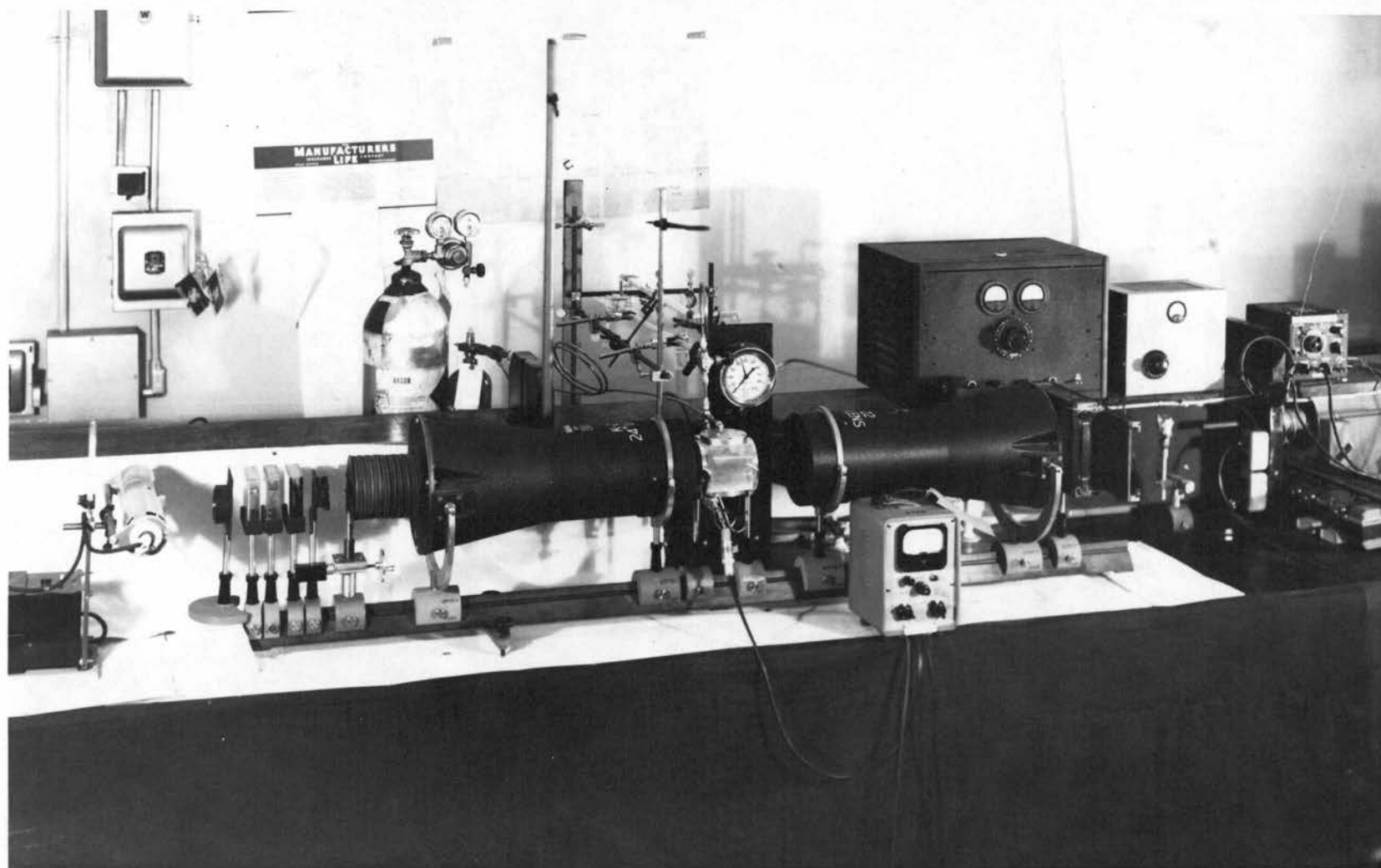


Figure 12. Photograph of whole system.

## EXPERIMENTAL RESULTS

In order to gain some familiarity with the effect of light diffraction by an ultrasonic field, it was felt worthwhile to initiate experimentation by observing the effect for a liquid. For this purpose it was found convenient to use the Heathkit transmitter in conjunction with a quartz crystal having a fundamental frequency of 7.1 megacycles per second. The liquid used was technical grade xylene containing all three isomers. One reason for selecting xylene lay in the fact that it has an index of refraction approximately equal to that of glass. The low pressure gas cell was used for this experiment.

Upon activation of the quartz crystal transducer, diffraction effects were easily seen and photographed. Using white light, several orders of the different wavelengths contained in mercury light could be readily distinguished. An approximate calculation of the velocity from the measured line spacings was in good agreement with the reported value. Visual inspection of the diffraction pattern from xylene showed that the image would lose definition and intensity as the time of activation of the quartz crystal increased. Although no cavitation appeared in the xylene, movement of the xylene surface was clearly evident. These observations could be

interpreted as a consequence of delivering too much power to the crystal. The power delivered to the crystal could be attenuated by reducing the input ac voltage to the Heathkit transmitter and also by tuning the transmitter to a lower plate current in the final output tube.

It seems important to point out that the frequency of the transmitted carrier wave could be controlled in the transmitter by the common control crystal method or by connecting a variable frequency oscillator (VFO) to the transmitter. Even though it was possible to see a diffraction pattern using either method of control, it was found that the  $7.1 \text{ mc sec}^{-1}$  transducer crystal could be activated by setting the VFO to any frequency. The notion to be conveyed here is the ease with which the crystal could be activated in a liquid to produce light diffraction.

Having gained this much experience, the next step was to remove the xylene from the low pressure gas cell and repeat the procedure in air at one atmosphere pressure using the  $7.1 \text{ mc sec}^{-1}$  crystal.

Such a venture was almost fruitless with the only positive result being that the activation of the quartz crystal could be measured in terms of a temperature measurement. The temperature measurement was carried out by placing a thermistor above the crystal and



monitoring the thermistor current. That such a temperature change indicated ultrasonic field intensity could be verified by noting that setting the VFO at a distant frequency from that of  $7.1 \text{ mc sec}^{-1}$ , no perceptible change in thermistor current could be seen whenever the transmitter was energized. This distant frequency was easily half a megacycle per second from that setting of the VFO which resulted in a maximum heating effect.

It was the latter observation which seemed to illustrate that the resonance peak of the crystal, i.e., the peak obtained by plotting the sound intensity produced by the crystal as a function of applied frequency, was extremely sharp in air at one atmosphere. Hayess and Winde (19, p. 201-202) have studied this effect as a function of pressure, and they have indicated the same conclusion.

Besides the fact that the transducer crystal possessed a very high selectivity for its fundamental frequency, the suspicion arose that using a  $7.1 \text{ mc sec}^{-1}$  frequency at one atmosphere the absorption of ultrasound in air was so high as to render more difficult any possibility of observing diffraction. For this reason it was considered advisable to work with a crystal having a fundamental frequency of  $1 \text{ mc sec}^{-1}$ .



For the evaluation of the relative probability with which a diffraction effect may occur at a particular frequency, reference is made to David's formulation. In his formula derived for the symmetrical case, it is easily shown that the diffracted light intensity varied inversely as the square of the ultrasonic frequency. In addition, the absorption of ultrasonic energy reduced the effective value of  $E$  occurring in his formula. The reduction is through the factor  $\exp(-\alpha z)$  which  $\alpha$  is the absorption coefficient and  $z$  is the perpendicular distance between a point in the ultrasonic field and the source of ultrasound. Thus the ratio of the diffracted intensities of two frequencies,  $f_1$  and  $f_2$ , is given by

$$(I_1)_{f_1} / (I_2)_{f_2} = (f_2 / f_1)^2 \times (\exp - [\alpha_{f_1} - \alpha_{f_2}] z).$$

In the case of air, Herzfeld and Litovitz (21, p. 240) give

$$\alpha = 16.8 \times 10^{-14} f^2 \text{ cm}^{-1}.$$

Assuming that the constant of proportionality between  $\alpha$  and  $f^2$  does not change appreciably within the frequencies concerned, viz., 1 mc and 7 mc, then

$$\exp [-(\alpha_{f_1} - \alpha_{f_2}) z] = \exp [-16.8 \times 10^{-14} (f_1^2 - f_2^2) z].$$

Therefore letting  $f_1 = 1$  mc,  $f_2 = 7$  mc and  $z = 1.5$  cm,

$$(I_1)_{1 \text{ mc}} / (I_1)_{7 \text{ mc}} = 2401 \exp(12.09)$$

Clearly, from the standpoint of available intensity of diffraction, there existed a decided advantage in experimenting with a one megacycle crystal.

The Heathkit was modified so as to be used to activate the third harmonic of the one megacycle crystal. The results with this combination were similar to those obtained with the 7.1 megacycle crystal. No diffraction could be seen in air but it was relatively easy to obtain diffraction using xylene.

These results of not being able to observe diffraction in air indicated that attention should be focused on the possibility of an impedance mismatch between transmitter and transducer crystal.

In order to consider this particular aspect, it became necessary to build a transmitter to be used for activation of the one megacycle crystal. One such transmitter is the crystal controlled Pierce oscillator outlined in Figure 4. Using the coupling system as described in the previous section and a control crystal having a labeled frequency of 999.5 kilocycles per second, it became possible to observe the minus and plus one orders in air at one atmosphere pressure.

Due to the restrictions on the Pierce type oscillator that (1) its frequency was limited to that of the control crystal and (2) that the voltage is restricted so as not to overactivate the control crystal, it became necessary to build the Hartley type oscillator described in the previous section and outlined in Figure 5. Nonetheless, the Pierce type transmitter showed that the carrier wave frequency could be adequately controlled with a crystal to the extent that any frequency drift of the transducer crystal due to temperature variation in being activated was not severe enough to prevent maintaining the ultrasonic field long enough to make an exposure. In addition, this result indicated that the plus and minus orders could be readily seen in air at one atmosphere pressure with at least 180 ac volts on the crystal with the indicated optical arrangement. This arrangement included the use of the lower power lamp, the AH-2 lamp.

The Hartley oscillator did not require any additional coupling network to match impedances. Instead it was found that having the crystal connected to this oscillator as shown in Figure 5, a very good match existed. With this arrangement, an ac voltage of approximately 200 was required to see the plus and minus first order in air using the 250 watt AH-2 lamp. Replacing

this lamp with the 400 watt H400-ElT, it was possible to observe the second order spectrum with ease.

### Procedure

In the process of obtaining results which were to serve as the ultimate criteria for evaluating the usefulness of the method, several details in the procedure required considerable attention. Most of these details were concerned with increasing the reproducibility of measurement. Some of these, however, also involved the accuracy of measurement.

There occurred three important items which affected the reproducibility of the measurement of the spacing,  $\delta$ , between lines in the diffraction spectrum. An obvious one was the selection of a suitable photographic emulsion. Of the five types of emulsions tested, Kodak's types I-G, III-G, 103-G, 103a-G and SA-1, type III-G emulsion afforded the best possibility for attaining good precision in measurement of the distance between lines. For visual reproduction the 103a-G emulsions gave the best results. It was also found that backed emulsions were to be preferred over the unbacked.

Another factor which affected the reproducibility of measurement was the positioning of the photographed image under the field of view of the comparator. For an



absolute measurement it was required that the measurement of the distance between lines be made along the perpendicular of these lines. Even if the edges of the plates had been parallel to the line of travel of the eyepiece, because of the homemade type of plate holder used, there remained no assurance that the lines in the photographed diffraction image would have been perpendicular to two edges of the plate. The elimination of this deficiency was accomplished by using the plus and minus first order diffraction produced by a Ronchi ruling. The diffraction lines from the ruling, which had a nominal value of 175 lines per inch, were placed on the plate by making an additional exposure of the diffraction produced by the ruling on each ultrasonic diffraction pattern; a requirement which was easily fulfilled. In this way, it was merely the ratio of the distances between ultrasonic diffraction lines and that of the Ronchi ruling which had to be considered. To obtain the sound wavelength,  $\lambda$ , it was necessary to multiply the inverse of this ratio with the Ronchi ruling constant. This constant was determined on the same comparator which was used to measure the distances between lines in the diffraction images.

The ruling constant is indicated as  $d$  in the data presented and the associated diffraction spacing



between the first orders is designated as  $\delta'$ . The value  $\delta'$  seen in the data may vary and is attributed to different comparators used in obtaining the data.

The preliminary procedure in obtaining a suitable image for determination of velocity required the removal of the gas cell from the optical system because (1) the evacuation and filling system was too remote and (2) the Ronchi ruling had to be placed in the optical path to obtain the second exposure. Such a procedure was found to affect the reproducibility of the results; consequently, a modification was made to each of the gas cells to accommodate the ruling in the optical path without having to change the position of the cell. This was accomplished by mounting a holder for the ruling on the cell. Although this required moving the ruling in and out, the manner of mount insured consistent orientation of the ruling. In addition a system for evacuation and filling purposes was constructed in the proximity of the cell so as not to require its removal from the optical system.

For a given wavelength of light, it was found that  $\delta'$ , the distance between the first orders of the Ronchi ruling diffraction pattern, took on a distinctly different value after the lenses were coated which happened to be the case after the preliminary data indicated that

having the lenses coated would be a decided improvement. The difference in focal length was not attributed to the coating as such but rather to the change in spacing between the elements of the lenses which was necessitated to prevent damage to the surfaces of the lenses.

In monitoring the vibration frequency of the quartz transducer, at least three distinct regions of frequencies were noted for the one megacycle per second crystals. The two different values found below  $1000 \text{ kc sec}^{-1}$  were attributed to the slightly higher damping on the crystal on two separate occasions. This difference in damping occurred as a consequence of touching up areas of the silver plated crystal surface with silver paint or by using the crystal in either of the two types of mounts described in the previous section. In general the freshly silver plated quartz crystal vibrated at a higher frequency and required less rf voltage for observation of diffraction in any of the gaseous media studied. Values of sound frequencies over  $1000 \text{ kc sec}^{-1}$  were possible through the ability of the quartz crystal to vibrate in a resonance or anti-resonance frequency (7, p. 349, 389). It was found that when the crystal vibrated in the lower of the two frequencies, the resonance frequency, a higher intensity in the diffraction pattern was apparent.

An interesting observation made when using the

high pressure cell filled with nitrogen under one atmosphere was that as the tuning was changed to produce a more intense first order diffraction, the plus and minus first orders increased in intensity as usually observed. At a particular point in the tuning the intensity of the first orders abruptly decreased but the second order diffraction appeared and both orders, first and second, seemed to have equal intensity, but lower intensity than that of the first orders by themselves.

Other qualitative observations made suggested that the intensity of the ultrasonic diffraction lines was greater for those associated with the 4358 Å Hg line over those associated with the 5461 Å line.

It was also observed that the intensity of the diffraction pattern formed by ultrasound in ammonia was the greatest of any of the gases investigated. The least intense pattern was, without doubt, that associated with Freon-12. Otherwise the magnitude of this property decreased in the order of nitrogen, air, argon, nitrous oxide and sulfur dioxide, with the definite break occurring between argon and nitrous oxide.

In measuring the distances between the two sets of plus and minus first orders, one set due to the ultrasonic diffracted light and the other to the Ronchi ruling, indicated an asymmetry in the different spacings.



In general the spacing between both minus orders and the spacing between both plus orders were not equal. In the final stages of this work, the difference in these spacings were measured and found to be as large as 0.25 mm for nitrous oxide and no greater than 0.18 mm for nitrogen at the same elevation of the slit. No correlation between the spacings difference and accuracy or precision of velocity measurements could be ascertained. However, it appeared that as the symmetry in spacing improved, so did the intensity distribution between the plus and minus first orders of the diffraction pattern produced by the ultrasonic field.

In analyzing the recordings of the temperature variation during the time involved in tuning the transmitter to yield an optimum diffraction pattern and the photographing of the pattern, it was noted that as the tuning of the transmitter approached that frequency resulting in the optimum image from the standpoint of intensity, the temperature would slowly rise, accelerating as the optimum condition was reached. The time required for this process of tuning and photographing was about 100 sec, the exposure time rarely amounting to 10% of this value.

The temperature of the gas during an exposure was taken at a point in the recording corresponding to the

moment the shutter was snapped. The temperature changes were more severe with gases under low pressures than with gases at higher pressures. Typical temperature changes are tabulated in Table 1.

---

Table 1  
Observed Typical Temperature  
Variations

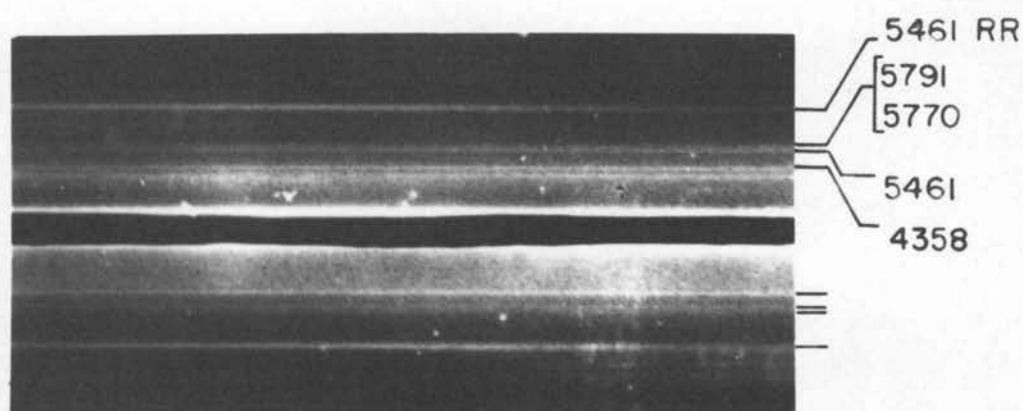
Gas	Pressure	Voltage	$T_f - T_i = \Delta T(^{\circ}\text{C})$
$\text{N}_2\text{O}$	10 atm	180 rf	$26.4 - 25.9 = 0.5$
	1 atm	260 rf	$26.9 - 24.6 = 2.3$
	1 atm	350 B+	$24.5 - 21.6 = 2.9$
	.4 atm	400 B+	$29.7 - 23.1 = 6.6$
$\text{N}_2$	10 atm	9.8 rf	no change
	1 atm	125 rf	$24.6 - 23.9 = 0.7$
Ar	1 atm	110 B+	$25.4 - 24.6 = 0.8$
	.4 atm	300 B+	$28.4 - 25.3 = 3.1$

---

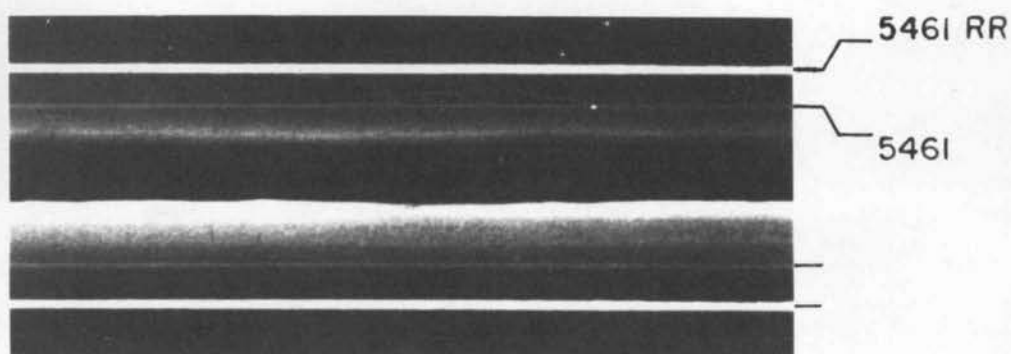
In Table 1,  $T_f$  and  $T_i$  indicate final and initial temperatures, respectively, while  $\Delta T$  is the temperature change. The temperature change during the period of exposure may safely be assumed to have been less than 1/10 of the  $\Delta T$ 's reported above.

Photographs of diffraction spectra produced by an ultrasonic field in those gases studied in this work are shown in Figures 13, 14 and 15. The photographs are approximately ten-fold enlargements of the





P = 798.0 mm      t = 1/2 sec  
f = 976.5 kc/sec      I-G plate  
E = 400 volts B+



P = 618.5 mm      t = 1 sec  
f = 1001.2 kc/sec      I-G plate  
E = 500 volts B+

Figure 13. Light diffraction by an ultrasonic field in sulfur dioxide.

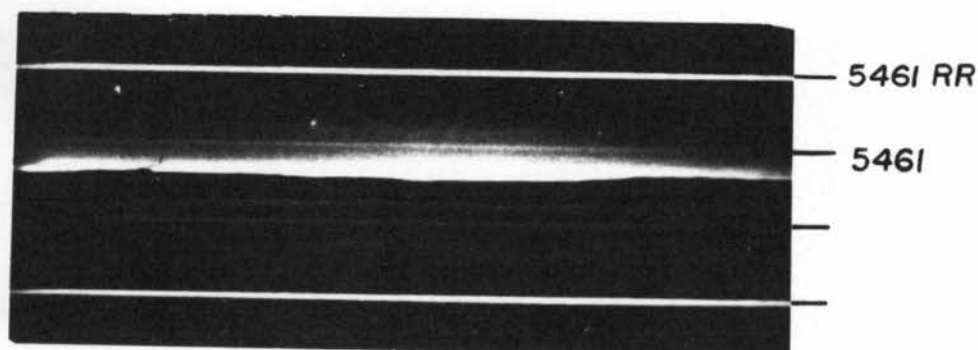
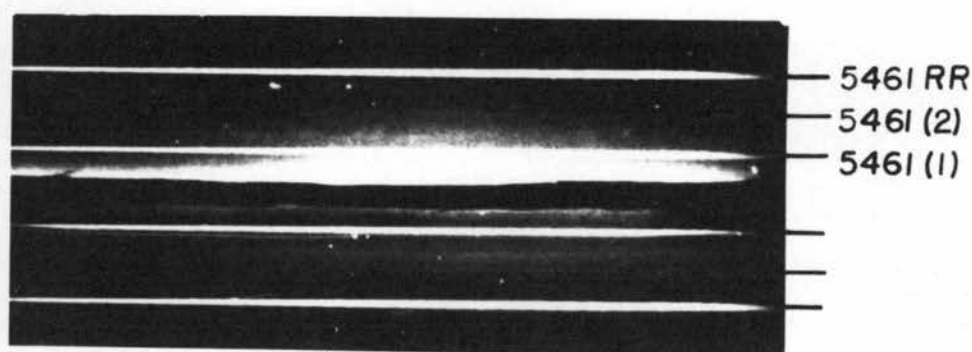
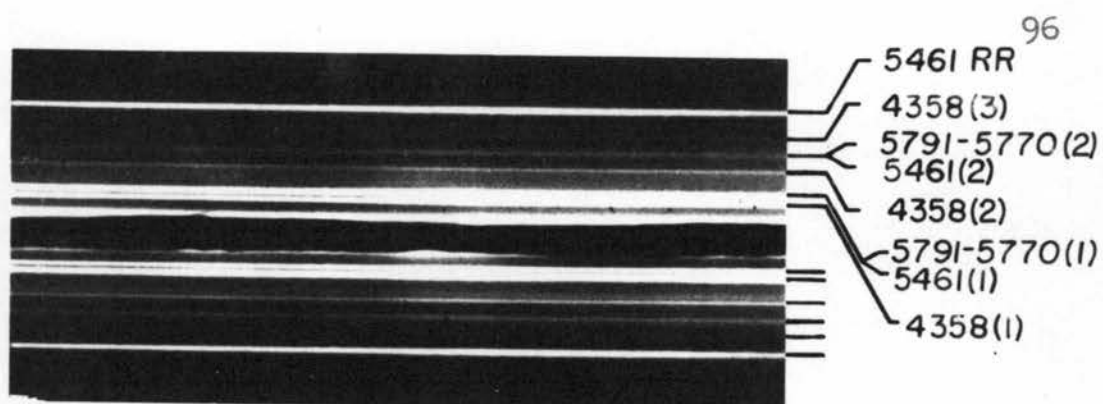
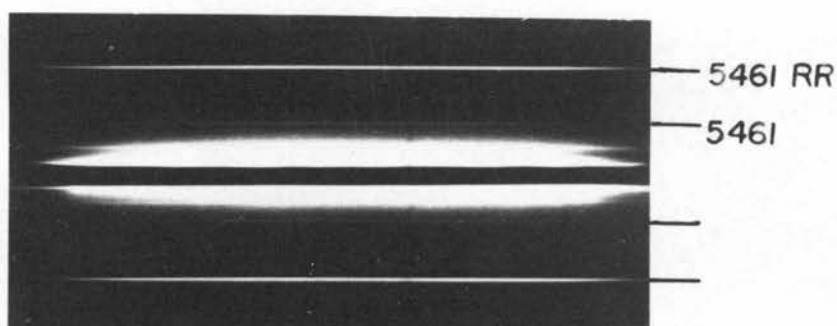


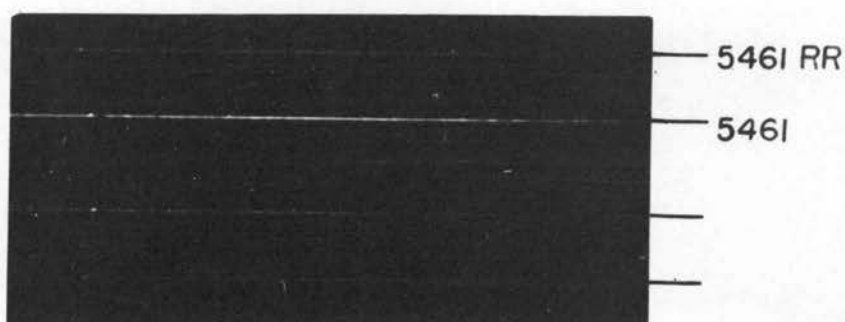
Figure 14. Light diffraction by an ultrasonic field in ammonia.

## ARGON



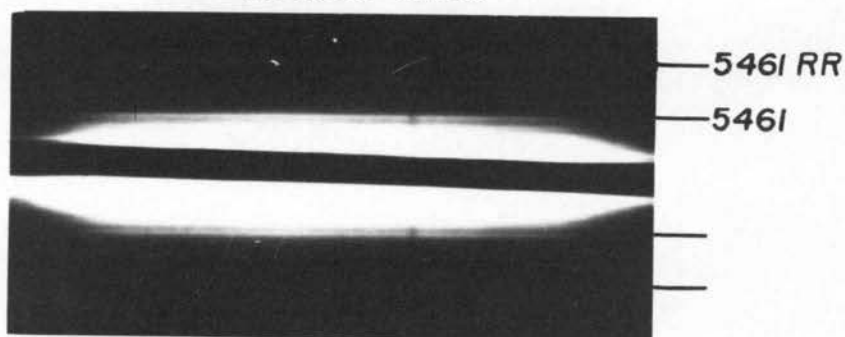
$P = 792.0 \text{ mm}$        $t = 1 \text{ sec}$   
 $f = 996.2 \text{ kc/sec}$       III-G plate  
 $E = 110 \text{ volts B}^+$

## NITROGEN



$P = 777.0 \text{ mm}$        $t = 1/2 \text{ sec}$   
 $f = 994.4 \text{ kc/sec}$       III-G plate  
 $E = 600 \text{ volts B}^+$

## NITROUS OXIDE



$P = 609.5 \text{ mm}$        $t = 3 \text{ sec}$   
 $f = 995.1 \text{ kc/sec}$       III-G plate  
 $E = 400 \text{ volts B}^+$

Figure 15. Light diffraction by an ultrasonic field in three different gases.

originally photographed diffraction spectra.

In all the exposures shown, the outermost lines from the center on each side are from diffraction by the Ronchi ruling and are so indicated by labeling the line with letters RR. These photographs are only representative of the results obtained in this work since the quality desired in the exposure for display purposes was not the same quality needed for the optimum precision in measuring distance intervals. The reason for this lay in the larger line breath necessary for visualization of the diffraction image without a microscope. For example, the breath of the Ronchi ruling line in the lower photograph of Figure 13 was already too great to determine its center with good precision.

The large voltages indicated on the figures are not to be considered as necessary for attaining good precision in the distance interval measurements.

Figure 13 shows the diffraction spectra obtained using sulfur dioxide. The zero order has been partially blocked out with a crude mask, the purpose being to enhance the appearance of the diffraction lines and to prevent halation of the film by the more intense zero order. In this figure the top photograph was obtained using white light while the bottom photograph made use of the green line only. In the photograph associated



with white light, the double line due to green and yellow light was easily resolved under the comparator and is barely resolvable with the unaided eye.

Figure 14 are images of the diffraction associated with ammonia. The top photograph illustrates the greater intensity of the diffraction spectra associated with the 4358 Å line; whereas two orders of the green line can be seen on each side of the zero order, three orders of the 4358 Å line can be seen. Reference to the top photograph in Figure 13 of sulfur dioxide also shows a similar result with respect to the intensities.

The photograph in the center of Figure 14 serves to show the greater magnitude of the intensity of diffraction due to ammonia and is to be compared with the lower photograph of Figure 13. The lower photograph in Figure 14 shows the relative intensity of the diffraction produced by ammonia at 0.2 atmosphere pressure, a pressure at which even in the case of nitrogen difficulty was encountered.

Figure 15 shows results obtained for those gases used in obtaining the final results. The two calibration gases were argon and nitrogen while the gas under study was nitrous oxide. In general, diffraction using nitrogen was slightly easier to photograph than argon, but of the three diffraction spectra shown in this figure,

diffraction by nitrous oxide was the most difficult. When mentioning difficulty in reference to photographing diffraction spectra, it is meant that a higher voltage was required to obtain a diffraction image of sufficient intensity to be visually discernible.

Structure unassigned in the photographs of Figures 13, 14 and 15 are attributed to reflection effects and to Fraunhofer diffraction.

Asymmetry in the line intensities is present in these photographs and is attributed to those reasons given by Korff (33, p. 708-720). This asymmetry is best shown by the nitrogen diffraction spectra shown in Figure 15. Attention is called to the broader appearance of the lines associated with the heavier gases,  $\text{SO}_2$  and  $\text{N}_2\text{O}$ . The diffraction lines associated with argon or ammonia were definitely sharper than those with nitrous oxide.

### Preliminary Results

1. For sulfur dioxide,  $\text{SO}_2$ . The source of this gas was Charg-a-Cans available from the American Potash and Chemical Company. The purity indicated on the can was very close to 99.97%. Observation of the diffraction pattern produced by this gas was difficult below pressures of 600 mm without possibly using a voltage which

could harm the transducer crystal. The diffraction pattern by sulfur dioxide was studied using only the less efficient transducer mount. The exposures which were obtained for this gas were with a B+ voltage of 400 to 500. The values obtained in the neighborhood of a frequency of one megacycle per second and a pressure of one atmosphere, ranged from 218.2 to 221.0 m sec<sup>-1</sup>, and are to be compared to a value obtained from the investigations of Petralia (43) of 220.5 m sec<sup>-1</sup>. The values obtained in this work were corrected to 25°C without any correction for non-ideality. The average distance between the first order diffraction for the green line was 3.00 mm and 2.38 mm for the blue line. The values of SO<sub>2</sub> were obtained before the cell position had been made permanent.

2. Freon-12, dichlorodifluoromethane, CCl<sub>2</sub>F<sub>2</sub>. This substance was also obtained in the Charg-a-Cans. It was appreciably more difficult to observe diffraction by this gas than by SO<sub>2</sub>. Although the plus and minus first orders were seen convincingly with a B+ voltage of 700 and at one atmosphere pressure, no attempt to photograph a diffraction pattern was made because of the high voltage required.

3. Ammonia, NH<sub>3</sub>. This gas was obtained from a cylinder secured from Pennsalt Corporation in 1954 and

whose purity remained unknown. Observation of diffraction by this gas showed it to produce the most intense diffraction pattern for a given voltage than any other gas studied. Using one atmosphere pressure, once the diffraction pattern was obtained with approximately 125 volts rf on the crystal, it was possible to retain a good image down to 23 volts rf. In this case the second order diffraction spectrum could be observed with 60 volts rf and the third order with 110 volts rf. It became possible to photograph the first order diffraction using ammonia under a pressure of 0.2 atmosphere employing 200 volts rf.

The results of a series of exposures using the low pressure cell and ammonia pressures of one to 0.4 atmosphere gave an average result for the sound velocity of  $430.4 \text{ m sec}^{-1}$ . Here again no correction was made for non-ideality and the observed velocities were corrected to  $300^\circ\text{K}$ . The theoretical values for the limiting velocities give:  $U_0 = 439.2$  and  $U_\infty = 441.9 \text{ m sec}^{-1}$ . These calculated values are for  $300^\circ\text{K}$ .

The green line was predominantly employed with ammonia since using the blue line resulted in having diffraction lines too close to the zero order. The measured spacing between the first order spectrum due to the green line was about 1.45 mm, nearly half that



found for sulfur dioxide.

4. Nitrogen,  $N_2$ . This gas was investigated principally for calibration purposes. Results obtained with nitrogen showed several interesting features.

One of these features indicated that the spacings between the second orders and that between the first orders were not simply related by an integer as the grating equation predicts. In general, conclusions derived from this and similar experiments indicated that the spacing associated with the second order was slightly smaller than that associated with the first order. With a 900 volt B+ only orders up to and including the third were photographed. Actually in the best alignment possible five and perhaps six orders could be seen with this voltage using green light.

Another interesting result was obtained by investigating the sound velocity of nitrogen as a function of rf voltage on the crystal while the pressure remained constant. The results are shown in Table 2 and plotted in Figure 16. Only the first orders were analyzed for this correlation.

In Table 2, the first column is the exposure number and is so designated by e.n., the second column is the ratio of the distance between the first order diffraction of the Ronchi ruling,  $\delta'$ , and the diffraction

Table 2

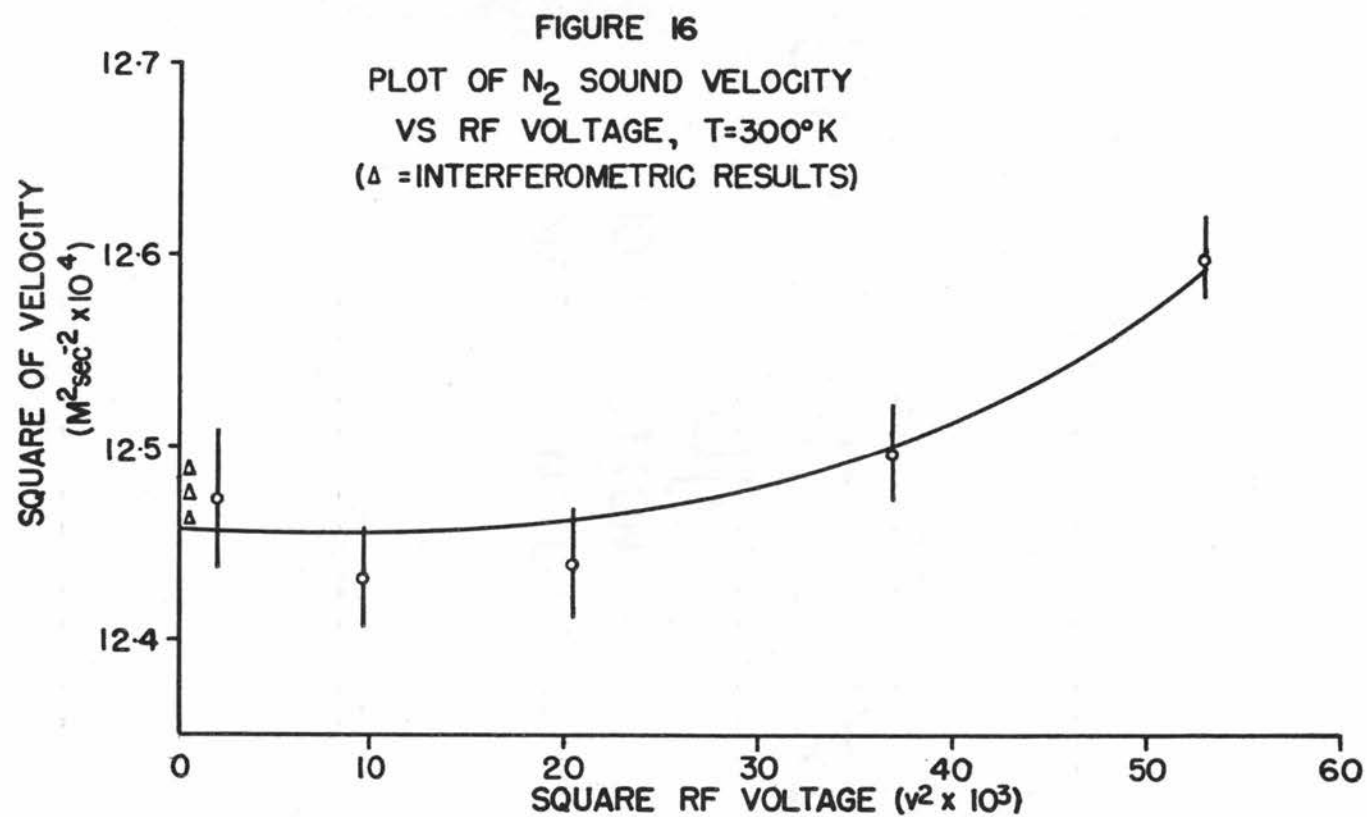
Idealized Sound Velocity Values of Nitrogen  
at Constant Pressure and Variable rf Voltage

e.n.	$\delta'/\delta$	$\Lambda$ (mm x $10^{-3}$ )	f (kc/sec)	$U_T$ (m/sec)	T °K	$U_{1300^\circ K}^2$ (m <sup>2</sup> /sec <sup>2</sup> x $10^4$ )	$V^2$ (volts <sup>2</sup> )
1	2.3946 $\pm$ 0.0036	354.26 $\pm$ 0.67	996.9	353.17 $\pm$ 0.67	299.16	12.4731 $\pm$ 0.0374	2,116
2	2.3916 $\pm$ 0.0022	353.81 $\pm$ 0.53	996.5	352.58 $\pm$ 0.53	298.86	12.4309 $\pm$ 0.0261	9,604
3	2.3920 $\pm$ 0.0029	353.87 $\pm$ 0.60	996.7	352.70 $\pm$ 0.60	298.80	12.4398 $\pm$ 0.0299	20,449
4	2.3978 $\pm$ 0.0019	354.73 $\pm$ 0.50	996.6	353.51 $\pm$ 0.50	298.86	12.4966 $\pm$ 0.0250	36,864
5	2.4074 $\pm$ 0.0010	356.15 $\pm$ 0.46	996.7	354.96 $\pm$ 0.46	298.91	12.5995 $\pm$ 0.0227	52,900
						theory 12.4616	

P = 1.019 atm

series 2151n

d = 0.14794  $\pm$  0.00018 mm



due to the ultrasonic field,  $\delta$ ; the third column is the ultrasonic wavelength,  $\Lambda$ , found by multiplying the corresponding values of column 2 by the ruling constant,  $d$ ; column 4 lists the frequency; the observed velocity at the temperature assigned to the experiment is listed in column 5 as  $U_T$ ; column 6 lists the temperature of the experiment; column 7 lists the square of the velocity corrected for non-ideality and temperature to 300°K and in the last column is listed the square of the rf voltage. The maximum error in precision for this series is 0.19%. The deviations listed in this table are standard deviations.

The curve in Figure 16 has been extrapolated to zero voltage and has incorporated the theoretical value of the sound velocity for nitrogen at this point. The points plotted include the standard deviation values. In absence of any voltage reference, the values reported by Boyer (5), Deshpande (11) and Lewis (39, p. 75), all obtained by the interferometric method, are shown close to zero voltage for convenience. The values assigned for each author's work were corrected for the temperature but not for gas non-ideality.

The set of data used to obtain the curve of Figure 16 was obtained by keeping fixed the position of the cell within the optical system. This condition was found



necessary since the data obtained by removing the cell after each exposure gave a random behavior when correlated to obtain a similar curve.

Another experiment performed with nitrogen involved observing the effect on the velocity of ultrasound in the gas as the pressure was decreased and the rf voltage on the transducer crystal remained relatively constant.

Three exposures were made each at a different pressure using voltages which centered about 64 volts rf and which were all within 6 volts of each other. The fourth exposure using a pressure of approximately 0.6 atmosphere required using 115 volts rf on the crystal which according to Figure 13 would not produce too high a deviation at one atmosphere pressure; however, this fact is to be applied with caution when dealing with a different pressure.

The results of this experiment are shown in Table 3, and illustrate that as the initial pressure is decreased the velocity is decreased. The identity of the columns is as before; however, in this table the last column indicates the pressure, P. The results shown here were obtained concurrently with those previously reported for ammonia. The comparison of these sets of results afford a good illustration of the optical method at low

Table 3

Observed Sound Velocity of Nitrogen  
at Constant rf Voltage and Variable Pressure

e.n.	$\delta'/\delta$	$\Lambda$ (mm x 10 <sup>-3</sup> )	f (kc/sec)	U <sub>T</sub> (m/sec)	T °K	U <sub>i</sub> <sup>2</sup> <sub>300°K</sub> (m <sup>2</sup> /sec <sup>2</sup> x 10 <sup>4</sup> )	P (atm)
1	2.3644 ± 0.0026	349.08 ± 0.42	1002.0	349.78 ± 0.46	296.36	12.3848 ± 0.0210	1.032
3	2.3643 ± 0.0014	349.07 ± 0.28	1000.2	349.14 ± 0.28	296.81	12.3218 ± 0.0136	0.855
4	2.3653 ± 0.0024	349.21 ± 0.38	1000.0	349.21 ± 0.38		12.3244 ± 0.0197	0.709
5	2.3665 ± 0.0021	349.39 ± 0.35	996.9	348.31 ± 0.35	297.01	12.2548 ± 0.0184	0.589

d = 0.14764 ± 0.00007 mm

series 2231n

V: e.n. 1, 3 and 4; 64 ± 6 volts

e.n. 5; 115 volts

pressures. The nitrogen result is lower than the theoretical value by about 0.5% while that of ammonia was found to be lower by 2.5%.

### Final Results

Analysis of the preliminary results indicated that the precision of velocity measurements was at worst 0.20% using the standard deviation, the average standard deviation error being approximately 0.15%. This result plus the fact that the available range of frequency-pressure ratios in this work were in the neighborhood of one served to choose the nitrous oxide system as one for which velocity dispersion effects could be determined employing this optical method. Two works (58, p. 1-24; 25) indicated that the maximum in the velocity dispersion occurred in the  $f/p$  values accessible with the experimental conditions employed here; in addition, they confirmed the fact that the velocity dispersion amounts to 13.1 m/sec at 300°K or about 4.9% of the lower velocity, a value of 25 times greater than the maximum precision error found in the preliminary results with nitrogen.

The reported purity of the nitrous oxide obtained for this work, obtained from the Ohio Chemical Pacific Company, was 99.3%.

The first results obtained with this gas were similar to those of sulfur dioxide insofar that compared to ammonia and nitrogen a higher voltage was required to observe diffraction using  $N_2O$  and  $SO_2$ . The high pressure cell was used to complete the known dispersive region of  $f/p$  values. The low pressure cell was employed to obtain velocity data for the higher values of  $f/p$  although the entire region covered with both cells could have been covered by the high pressure cell.

Diffraction patterns of some known non-dispersive gas were analyzed concurrently with nitrous oxide for calibration purposes. In the low pressure cell, argon was used; in the high pressure cell, nitrogen. Both gases were obtained from Matheson. The pre-purified nitrogen was reported to have a minimum purity of 99.996% and argon 99.998%. Only the first order spectra were evaluated for determining precise values of velocity but second order spectra obtained only with nitrogen was also evaluated. The latter was done to point out the revelant feature that in the usual case the interval between second orders was not equal to the first order interval.

The values obtained for argon and nitrous oxide are shown in Tables 4 and 5, respectively. The exposure



Table 4

## Experimentally Determined Velocity of Argon

e.n.	$2\delta$ (mm)	$2\delta'$ (mm)	$\Delta$ (mm) $\times 10^3$	$f$ kc sec <sup>-1</sup>	P atm	T °K	$U_T$ m sec <sup>-1</sup>	$U_R$ 300°K m sec <sup>-1</sup>	V B+ volts
5	1.944 $\pm .0007$	4.240 $\pm .002$	323.55	996.2	1.042	298.66	322.32	323.03 $\pm .19$	110
4	1.949 $\pm .001$	4.247 $\pm .003$	323.26	996.6	0.808	299.04	322.16	322.68 $\pm .29$	200
3	1.942 $\pm .001$	4.244 $\pm .001$	324.14	996.2	0.600	299.87	322.91	322.98 $\pm .16$	250
2	1.932 $\pm .001$	4.247 $\pm .001$	326.07	996.7	0.400	301.42	324.99	324.28 <sup>1</sup> $\pm .16$	300
							theory	322.61	

series 36ln  
d = 0.14835 mm

Table 5

Observed Velocity of  $N_2O$   
using Low Pressure Cell

e.n.	$\delta$ (mm)	$\delta'$ (mm)	$f$ kc sec <sup>-1</sup>	P atm	$\Lambda \times 10^3$ (mm)	T °K	$U_T$ m sec <sup>-1</sup>	V B+ volts	$f/p$ mc atm <sup>-1</sup>
5	1.1192 ± .0008	2.1107 ± .0008	996.2	1.033	278.43	297.58	277.38	350	0.9644
4	1.1193 ± .0016	2.1104 ± .0006	996.0	1.034	278.38	298.58	277.26	400	0.9632
3	1.1185 ± .0004	2.1142 ± .0008	995.1	0.802	279.07	298.88	277.70	400	1.241
2	1.1202 ± .0004	2.1099 ± .0009	994.9	0.599	278.08	299.35	276.66	400	1.661
1	1.1036 ± .0008	2.1046 ± .0016	996.2	0.395	281.55	301.51	280.48	400	2.522

series 351n  
d = 0.14764 mm

times used to photograph the diffraction patterns with argon were all one second. In the case of nitrous oxide, all exposure times were three seconds except for one which was four seconds. All the final results were obtained by using type III-G plates, and the green Hg line.

An experiment similar to the one made with argon and nitrous oxide in the low pressure cell was performed with nitrogen and nitrous oxide using the high pressure cell. For each gas, the pressure region covered was from one to ten atmospheres. The data for nitrogen are shown in Table 6 and that for nitrous oxide in Table 7.

For nitrogen all exposure times were  $\frac{1}{2}$  second. Exposures 41511 and 41512 were singled out for observing the larger velocity values obtained from the second order spectrum. Exposure times used with nitrous oxide were one second for five of the lowest pressure values, exposures 41524 to 41529. One-half second exposures were used for the other three pressures.

With regard to corrections for non-ideality of the gases, it is pointed out in Appendix 1 that the corrections for argon at the pressures used are within experimental error. However, the gas non-ideality corrections for nitrogen above pressures of two atmospheres and for nitrous oxide at all pressures used were considered.

Table 6

Observed Velocity of Nitrogen using the High Pressure Cell

e.n.	$2\delta$ (mm)	$2\delta'$ (mm)	$\Lambda \times 10^3$ mm	$f$ kc sec <sup>-1</sup>	$P$ atm	$T$ °K	$U_T$ m sec <sup>-1</sup>	$V$ ac volts	$f/p$ mc atm <sup>-1</sup>
3	1.795 ± 0.001	4.228 ± 0.002	349.27	1001.4	10.3 <sup>2</sup>	297.65	349.76 .12%	9.8	0.0972
4	1.786 ± 0.003	4.232 ± 0.002	351.50	997.0	7.6 <sup>3</sup>	297.55	350.45 .19%	14	0.1312
5	1.788 ± 0.001	4.229 ± 0.001	350.75	996.9	5.2 <sup>8</sup>	297.45	349.66 .11%	27	0.1881
6	Ratio: 2.367 ± 0.004 = $\delta'/\delta$		351.05	996.8	4.2 <sup>0</sup>	297.34	349.93 .19%	40	0.2373
7	1.785 ± 0.003	4.230 ± 0.001	351.50	996.8	2.6 <sup>3</sup>	297.37	350.38 .19%	56	0.3834
8	1.786 ± 0.001	4.231 ± 0.001	351.35	996.7	1.7 <sup>5</sup>	297.41	350.19 .11%	87	0.5695
9	1.791 ± 0.003	4.229 ± 0.003	350.16	996.7	1	297.52	349.00 .20%	125	0.9967
1a*	3.526 ± 0.002	4.229 ± 0.001	355.80	996.4	9.7 <sup>4</sup>	298.16	354.52 .11%	105	0.1027



Table 6 - Cont.

e.n.	$2\delta$ (mm)	$2\delta'$ (mm)	$\Delta \times 10^3$ mm	f kc sec <sup>-1</sup>	P atm	T °K	$U_T$ m sec <sup>-1</sup>	V ac volts	f/p mc atm <sup>-1</sup>
1b**	5.285 ± 0.004	4.229 ± 0.001	356.09	996.4	9.7 <sup>4</sup>	298.16	354.81 .12%	105	0.1027
2 <sup>+</sup>	3.525 ± 0.003	4.235 ± 0.002	356.39	996.7	9.8 <sup>4</sup>	297.87	355.21 .13%	63	0.1017

series 4151n

 $d = 0.14831 \text{ mm} \pm 0.00014; 0.09\%$ \*  $2\delta_{+2,-2}$ \*\*  $2\delta_{+3,-3}$ +  $2\delta_{+2,-2}$

Table 7

Observed Velocity of Nitrous Oxide; 1 to 10 atmospheres

e.n.	$2\delta$ (mm)	$2\delta'$ (mm)	$\Delta \times 10^3$ mm	f kc sec <sup>-1</sup>	P atm	T °K	$U_T$ m sec <sup>-1</sup>	V ac volts	f/p mc atm <sup>-1</sup>
1	2.408 ± 0.001	4.228 ± 0.002	260.43	996.8	10.28	299.52	+ .29 259.60 .11%	58	0.0974
2	2.429 ± 0.003	4.234 ± 0.002	258.50	1002.0	10.28	300.03	+ .41 259.02 .16%	180	0.0980
3	2.363 ± 0.003	4.226 ± 0.005	265.18	995.8	7.62	299.98	+ .53 264.07 .20%	187	0.1307
4	2.353 ± 0.002	4.231 ± 0.003	266.66	996.5	5.31	300.07	+ .37 265.73 .14%	187	0.1877
5	2.371 ± 0.004	4.230 ± 0.002	264.58	996.6	4.42	300.38	+ .53 263.68 .20%	180	0.2255
7	2.281 ± 0.002	4.236 ± 0.003	275.41	996.6	1.77	300.41	+ .41 274.47 .15%	180	0.5630

Table 7 - Cont.

e.n.	$2\delta$ (mm)	$2\delta'$ (mm)	$\Delta \times 10^3$ mm	$f$ kc sec <sup>-1</sup>	$P$ atm	$T$ °K	$U_T$ m sec <sup>-1</sup>	$V$ ac volts	$f/p$ mc atm <sup>-1</sup>
8	2.263 $\pm 0.001$	4.230 $\pm 0.002$	277.19	996.5	1	300.87	$\begin{matrix} +.30 \\ 276.22 \\ .11\% \end{matrix}$	260	0.9965

series 4152n

 $d = 0.14831 \text{ mm} \pm 0.00014, .09\%$

The effect of these corrections on the observed velocities for nitrogen and nitrous oxide is illustrated in Tables 8 and 9. The correction factors are discussed in Appendix 1.

In Tables 8 and 9, the values under the column  $U_r$  are the average values of the observed velocities and are indicated for comparison. In Table 9 the values associated with  $U_i'$  are those values still uncorrected for the calibration factor. Velocity values associated with  $U_i$  are the final corrected idealized values.

Whereas the calibration of the low pressure cell indicated no necessity for a correction factor as evidenced by the values obtained for argon, using the high pressure cell necessitated a correction factor of 1.0066 in order to raise the observed idealized velocity value to that predicted by theory for nitrogen. As has been stated earlier, the three velocity values not used in the averaging process in the nitrogen velocity have been excluded for a particular reason. The values for the velocity of nitrous oxide in the last column of Table 9 have been multiplied by the correction factor 1.0066.

The theoretically calculated limiting velocity values for nitrous oxide at 300°K are:  $U_0 = 268.57$  and  $U_\infty = 281.65 \text{ m sec}^{-1}$ . The necessary information for their calculation has been presented in Appendix 1.



Table 8

## Idealized Nitrogen Velocities

e.n.	$U_r$ (m/sec)	$U_i$ 300°K (m/sec)	f/p (Mc/atm)
41519	349.00	$350.28 \pm 0.70$	0.997
41518	350.19	$351.43 \pm 0.39$	0.570
41517	350.38	$351.53 \pm 0.67$	0.383
41516	349.93	$350.78 \pm 0.67$	0.237
41515	349.66	$350.38 \pm 0.39$	0.188
41514	350.45	$350.75 \pm 0.67$	0.131
41513	349.76	$349.60 \pm 0.42$	0.097
average; $350.68 \pm 0.67$			
theory; 353.01			
$353.01/350.68 = 1.0066$			
41512	355.21	$355.78 \pm 0.46$	0.102
41511a	354.52	$354.91 \pm 0.39$	0.102
41511b	354.81	$355.20 \pm 0.43$	0.101

Table 9

Corrected Sound Velocities of Nitrous Oxide.  $T = 300^\circ\text{K}$ 

e.n.	$U_r$ (m/sec)	$U_i$ (m/sec)	$U_i^2$ (m/sec) <sup>2</sup>	f/p (Mc/atm)	$U_1$ (m/sec)	$U_1^2$ (m/sec) <sup>2</sup>
3511	280.48			2.522	$280.76 \pm 0.31$	$7.8826 \pm 0.0126$
3512	276.66			1.661	$277.21 \pm 0.17$	$7.6845 \pm 0.0062$
3513	277.70			1.241	$278.26 \pm 0.17$	$7.7429 \pm 0.0062$
3514	277.26			0.963	$278.09 \pm 0.42$	$7.7334 \pm 0.0162$
3515	277.38			0.964	$278.21 \pm 0.22$	$7.7401 \pm 0.0085$
41528	276.22	$277.05 \pm 0.30$	$7.6757 \pm 0.0123$	0.997	$278.88 \pm 0.31$	$7.7774 \pm 0.0124$
41527	274.47	$275.84 \pm 0.41$	$7.6088 \pm 0.0160$	0.563	$277.66 \pm 0.42$	$7.7095 \pm 0.0162$
41525	263.68	$267.11 \pm 0.53$	$7.1348 \pm 0.0200$	0.225	$268.87 \pm 0.54$	$7.2291 \pm 0.0202$
41524	265.73	$270.25 \pm 0.38$	$7.3035 \pm 0.0146$	0.188	$272.03 \pm 0.38$	$7.4000 \pm 0.0148$
41523	264.07	$270.41 \pm 0.54$	$7.3122 \pm 0.0200$	0.130	$272.20 \pm 0.54$	$7.4093 \pm 0.0208$
41522	259.02	$267.57 \pm 0.43$	$7.1594 \pm 0.0165$	0.098	$269.34 \pm 0.43$	$7.2544 \pm 0.0167$
41521	259.60	$268.17 \pm 0.30$	$7.1915 \pm 0.0115$	0.097	$269.94 \pm 0.30$	$7.2868 \pm 0.0117$

Theory;  $U_0^2 = 7.2130 \times 10^4 \text{ m}^2/\text{sec}^2$

$U^2 = 7.9327 \times 10^4 \text{ m}^2/\text{sec}^2$

The experimental results obtained in this work are presented in Table 10 in a form useful for determining the value for a single vibrational relaxation time as determined by equation (71) of Chapter 2.

Tables 11 and 12 summarize those results obtained by Walker and coworkers and Holmes and coworkers. The values given here for Walker's work have been determined by applying only the non-ideality correction factor to his data. The work by Walker and coworkers indicates that they applied a correction factor to accomodate the error introduced into the velocity measurements by the phenomenon of absorption. No such correction is included in the values given here.

The data attributed here to Holmes and coworkers were interpolated from a curve given in their work. The curve was obtained from plotting the square of the idealized velocity values against the log of  $f/p$ . The work of Holmes and coworkers is given for 25°C and has been corrected to 300°K.

The single vibrational relaxation time reported by Walker and coworkers for 27°C and a value of  $f/p$  of  $1 \text{ mc atm}^{-1}$  was  $0.92 \mu\text{s}$  (microseconds). That reported by Holmes and his group was  $0.97 \mu\text{s}$  at 25°C.

The optical data obtained in this work and the data of the two other references are plotted in Figure 17

Table 10

Values of  $h(U_i)$  for Nitrous Oxide from Optical Data

$(f/p)$ (mc/atm)	$(f/p)^2$ (mc/amt x $10^{-1}$ ) <sup>2</sup>	$U_i^2$ (m/sec x $10^2$ ) <sup>2</sup>	$U_i^2 - U_o^2$ (m/sec x $10^2$ ) <sup>2</sup>	$U_\infty^2 - U_i^2$ (m/sec x $10^2$ ) <sup>2</sup>	$h(U_i)$
.097	.941	7.2868	.0738	.6459	.114
.098	.96	7.2544	.0414	.6783	.061
.13	1.69	7.4093	.1963	.5234	.375
.19	3.61	7.4000	.1870	.5327	.351
.225	5.06	7.2291	.0161	.7036	.023
.56	31.4	7.7095	.4965	.2232	2.224
1.00	100.	7.7774	.5644	.1553	3.634
.96	92.2	7.7401	.5271	.1926	2.737
.96	92.2	7.7334	.5204	.1993	2.611
1.24	153.8	7.7429	.5299	.1898	2.792
1.66	275.6	7.6845	.4715	.2482	1.900
2.52	635.0	7.8826	.6696	.0501	13.37



Table 11

Values of  $h(U_i)$  for nitrous oxide (Walker, et al.)

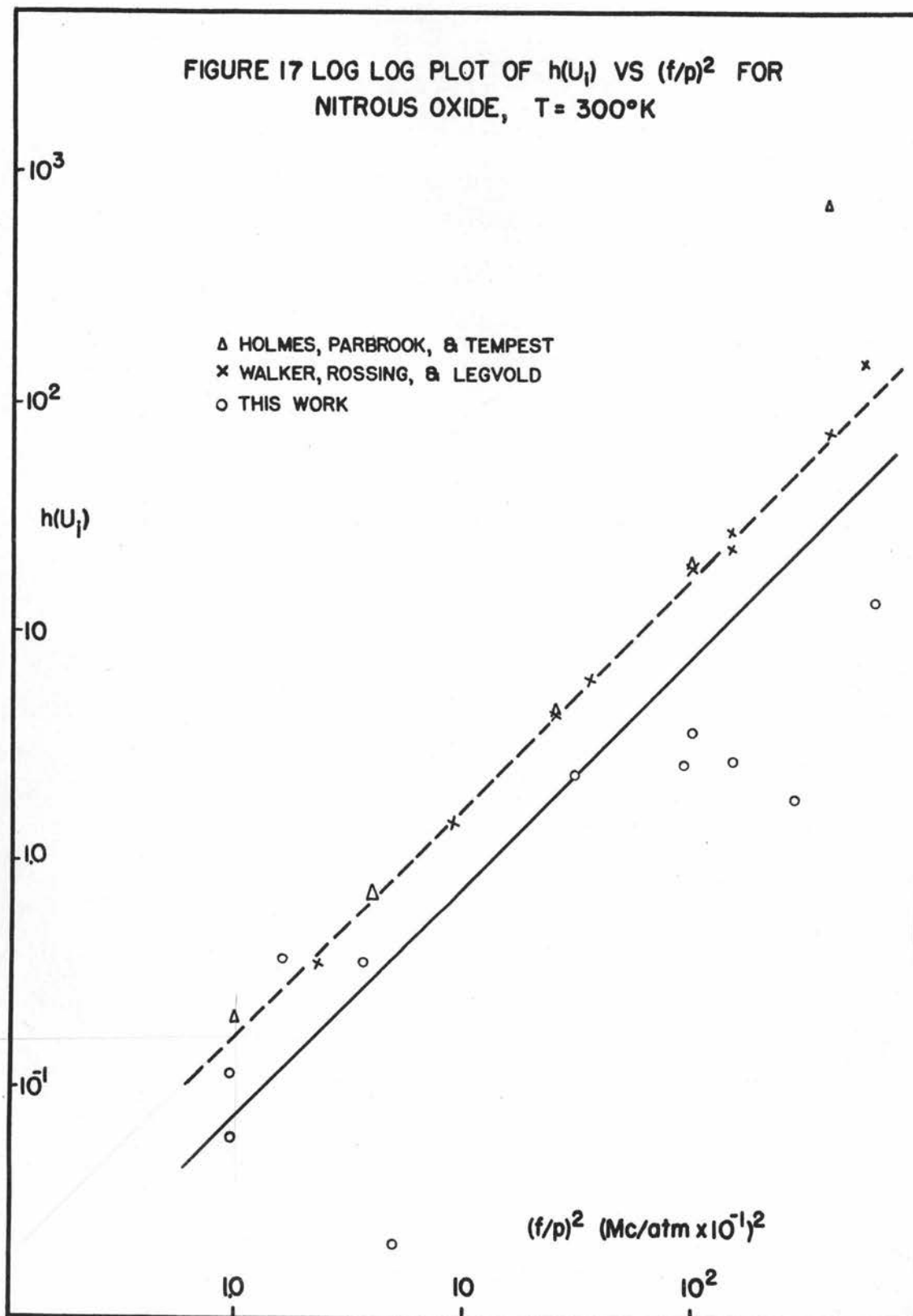
$(f/p)$ (mc/atm)	$(f/p)^2$ (mc/atm $\times 10^{-1}$ ) <sup>2</sup>	$U_i^2$ (m/sec $\times 10^2$ ) <sup>2</sup>	$U_i^2 - U_o^2$ (m/sec $\times 10^2$ ) <sup>2</sup>	$U_\infty^2 - U_i^2$ (m/sec $\times 10^2$ ) <sup>2</sup>	$h(U_i)$
.15	2.25	7.4038	.1908	.5289	.3607
.30	9.	7.6439	.4309	.2888	1.492
.30	9.	7.6549	.4419	.2778	1.591
.50	25.	7.7976	.5846	.1351	4.327
.60	36.	7.8325	.6195	.1002	6.183
.60	36.	7.8340	.6210	.0987	6.292
1.00	100.	7.8984	.6854	.0343	19.98
1.20	144.	7.9077	.6947	.0250	27.79
1.20	144.	7.9031	.6901	.0296	23.31
2.00	400.	7.9228	.7098	.0099	71.70
2.40	576.	7.9281	.7151	.0046	155.5
4.00	1600.	7.9311	.7181	.0016	448.8

Table 12

Values of  $h(U_i)$  for Nitrous Oxide (Holmes et al.)

$f/p$ (Mc/atm)	$(f/p)^2$ (Mc/atm $\times 10^{-1}$ ) <sup>2</sup>	$U_i^2$ (m/sec $\times 10^2$ ) <sup>2</sup>	$U_i^2 - U_o^2$ (m/sec $\times 10^2$ ) <sup>2</sup>	$U_\infty^2 - U_i^2$ (m/sec $\times 10^2$ ) <sup>2</sup>	$h(U_i)$
0.1	1	7.334	0.121	0.599	0.202
0.2	4	7.513	0.300	0.420	0.714
0.5	25	7.803	0.590	0.130	4.54
1.0	100	7.899	0.686	0.034	20.2
2.0	400	7.932	0.719	0.001	719
5.0	2500	7.938	0.725	-	-

FIGURE 17 LOG LOG PLOT OF  $h(U_1)$  VS  $(f/p)^2$  FOR  
NITROUS OXIDE,  $T = 300^\circ\text{K}$



in conformance with equation (70). Using the value of  $C_V^\infty$  and  $C_V^0$  calculated in Appendix 1, viz.,  $C_V^0/C_V^\infty = 1.436$ , and expressions (68) and (71), the optical data yield a vibrational relaxation time,  $\tau_0$ , of  $0.63 \mu s$  using the value of  $h(U_1)$  corresponding to an  $f/p$  value of  $1 \text{ mc atm}^{-1}$ . Similar computations for the plots obtained from the data of Walker and coworkers gives  $\tau_0 = 0.96 \mu s$  and Holmes and coworkers data yield a value of  $0.99 \mu s$  for  $\tau_0$ .



## DISCUSSION OF RESULTS

Correlation of the physical properties of the several gases investigated with the ease with which it was possible to observe a diffraction image, gives qualitative agreement with the formula as developed by David (9) and discussed by Korff (33, p. 708-720) for the light intensity distribution in the plus and minus first orders. The test involved the recording of the voltage required on the crystal in order to produce a progressive ultrasonic field of sufficient intensity which would result in a reasonably good image of the diffraction spectrum. A semi-quantitative correlation is possible assuming an effective path length,  $d$ , for the circular crystal which was used in this study. As will be recalled, Korff's form of David's equation for the symmetrical condition is given by

$$\frac{I_{+1}}{I_0} = \frac{2\pi^2(n_0-1)^2}{\rho v^2} \cdot \frac{d^2 \sin^2(\pi d \lambda / 2 \Lambda^2)}{\lambda^2 (\pi d \lambda / 2 \Lambda^2)^2}$$

where  $n_0$  is the index of refraction and other quantities having previously defined. This equation may be reduced by the relation

$$v^2 = \gamma(P/\rho)$$

to yield

$$\frac{I_1}{I_0} \propto (n_0 - 1)^2 \frac{U^2}{\rho} \frac{E}{f^2 \lambda^4} \sin^2(\pi d \lambda / 2 \Lambda^2)$$

Assuming constant sound intensity,  $E$ , and constant sound and light frequency, it is seen that the amplitude of the intensity expression depends only on the ratio of the square of the sound velocity to the density multiplied by  $(n_0 - 1)^2$ . It is not necessary to consider the actual density but for purposes of illustration, it is sufficient to use the molecular weights,  $M$ , and the approximate sound velocities,  $U$ , of the gases involved. Approximate values of  $(n_0 - 1)$  were obtained from the critical tables (14, p. 1-12). These tables do not give a value of  $(n_0 - 1)$  for Freon-12. The evaluation is shown in Table 13 where only approximate values for the quantities involved have been used. The value of  $d$  was taken as 3.14 cm and corresponds to the largest square which may be constructed in a circle of 4.45 cm diameter.

Table 13 indicates that of the gases studied, sulfur dioxide should yield the most intense spectra which was found not to be the case. A discrepancy also exists for the value associated with nitrous oxide. However, it should be pointed out that Table 13 and the experimental results are in relative agreement with respect

Table 13

Correlation of First Order Diffraction  
as Predicted by David's Theory

	NH <sub>3</sub>	N <sub>2</sub>	Ar	N <sub>2</sub> O	SO <sub>2</sub>
a. U(m/sec)	440	350	320	270	220
b. U <sup>2</sup> (10 <sup>4</sup> m <sup>2</sup> /sec <sup>2</sup> )	19.4	12.2	10.2	7.29	4.84
c. M(g/mole)	17	28	40	44	64
d. U <sup>2</sup> /M	1.1	0.44	0.26	0.17	0.08
e. n <sub>0</sub> -1(10 <sup>-6</sup> )	379	298	282	510	664
f. (n <sub>0</sub> -1) <sup>2</sup> U <sup>2</sup> /M	15.8	3.92	2.08	4.42	3.53
g. sin <sup>2</sup> ( $\pi d \lambda / 2 \Lambda^2$ )	0.019	0.048	0.068	0.130	0.283
h. f x g	0.316	0.188	0.141	0.575	0.999

to ammonia, nitrogen and argon. No explanation can be given for the disagreement between the intensities predicted by the theory for nitrous oxide and sulfur dioxide. However, it may be that absorption effects, which are predominant in these gases, may play a dominant role in reaching a suitable explanation.

Diffacted light distribution in the pattern as observed for nitrogen where the diffracted intensity of the first order decreased only to result in having both the first and second orders appear may be explained on the basis of the theory developed by Raman and Nath (46, 47, 48, 49). The point involved here is better discussed by them than by David and has reference to the fact that the intensities of all orders, including the zero order, are interrelated.

In securing a useful photograph of the diffraction pattern, consideration is necessary as to the possibility of the zero order image darkening the emulsion where the diffraction lines appear. According to the intensity formula as interpreted here, if a gas is selected which possesses a low sound velocity such as to result in a larger spacing between the first orders in the diffraction spectrum, the intensity of the diffracted light will be less.

However, the formula also indicates that the



intensity depends inversely as the fourth power of the light wavelength. This means that using the 4358 Å Hg line, the intensity gain over the use of the green line is about 2.5. This statement is qualitatively consistent with the observed fact. The brilliance of the lamp with respect to the blue and green line need be evaluated to reach a definite conclusion as to the validity of the fourth power. According to the literature available describing the sensitivity of the emulsion G to these two wavelengths (12, p. 22), it appears that the sensitivity is the same.

The question of using a more intense ultrasonic field requires much consideration. The indication that the velocity of nitrogen varies so strongly with the crystal voltage as indicated in Figure 13 may suggest a limit in useable voltage. The velocity value found from the separation between the second order lines with nitrogen at ten atmospheres indicates that using voltages high enough to observe the second order is already too high. This suggestion is not consistent with the observation made by Hayess and Winde (19, p. 201), namely, that the velocity of sound in nitrogen at ten atmospheres did not vary when the rf voltage was varied from 30 to 400 volts. In this present work, using ten atmospheres of nitrogen, velocity discrepancies are found



between 10 and 63 volts rf. Using the first of these voltage values shows only the first order spectrum while the second order appears as well as the first with 63 volts rf. Hayess and Winde indicate a value for nitrogen at ten atmospheres of about  $359 \text{ m sec}^{-1}$  while the values obtained in the present work at 10 and 63 volts rf are about 352 and  $357 \text{ m sec}^{-1}$ , respectively. For these values the correction factor of 1.0066 has been invoked. With respect to the observation of Hayess and Winde that the velocity does not vary with voltage up to 400 volts, it may be that the effect which is responsible for the high velocity value is already present at 30 volts rf.

Using the optical method at high gas pressures, Noury (41, p. 217-259) found that the velocity of nitrogen for a pressure of 12.4 atmospheres is about  $354.8 \text{ m sec}^{-1}$ . In the description of the apparatus used, it appears that the voltage used was rather high.

The effect which seems to give large values of velocity for nitrogen at high rf voltages relative to the pressures used may have its origin in a wave distortion caused by the large intensity magnitude of the pressure wave induced by the crystal vibrations. This effect has been discussed by Hubbard (27) and coworkers and further analyzed by Fox and Wallace (13).

Hubbard and coworkers obtained a shadow photograph

of a progressive ultrasonic field produced in air at 27°C by activating a quartz crystal having a fundamental frequency of  $407 \text{ kc sec}^{-1}$  with 325 volts. The microphotometer scan of the resulting photograph indicates the progressive distortion of the ultrasonic waves as they recede from the source. The wave changes into one having steep fronts and according to Hubbard and coworkers, an increasing content of second and third harmonic components.

Hubbard and his group also used the negative of the shadow photograph as a diffraction grating and found that for that region associated with the early stages of the ultrasonic wave which comprised the region occupied by the first eleven wavelengths, only the two first order diffraction lines were observed. Using the negative at its midpoint so as to obtain diffraction from the region with more distortion, the first and second diffraction orders could be seen clearly while the third order was faintly visible according to Hubbard. Using the remainder of the negative corresponding to the most distortion region in the field and the least ultrasonic intensity, only the first and second orders were visible.

The analysis of this photograph by Fox and Wallace with their interpretation of the nature of progressive sound waves of finite amplitude indicates clearly the

manner in which the wave changes form. They find that the distortion referred to gives rise to an increase in the wave velocity by an additive term dependent on the particle velocity. These authors have analyzed the microphotometer scan obtained by Hubbard and coworkers even to the extent of determining the relative percentage content of the fundamental and second and third harmonic frequency components in the wave as it proceeds from the source as well as their phase relationship.

The results of the present work seem to indicate that the second order already appears when distortion, and therefore an increase in phase velocity, of the wave has appeared regardless of the gas pressure. This suggestion that the distortion is independent of the pressure is not supported by the ideas of Fox and Wallace if the initial pressure wave remains constant and independent of pressure. However, since the initial pressure wave depends on the acoustic impedance matching between quartz transducer and medium, the formulas of Fox and Wallace cannot be applied until the relationship of this matching is investigated.

The analysis of velocities obtained from an ultrasonic field comprised of waves of finite amplitudes is not consistent with the theory of vibrational relaxation times as presented earlier. The theory is built on the

assumption that the analysis is with reference to waves of infinitesimal amplitudes since the linearization of the mass-flow equation is dependent upon this property.

It is tempting to analyze the deviation of the predicted integer ratio of the measured distance of the first order spectrum to that of the second order spectrum by considering a one to one correspondence between the intervals in the distorted wave and those of the diffraction pattern. The proposition here is that since the interval between pressure maxima is not constant as the wave recedes from the source, there shall appear a greater deviation between two pressure maxima separated by two "wavelengths" than two pressure maxima separated by one "wavelength". The deviation mentioned is that visualized when one compares a wavelength of a wave of infinitesimal amplitude with a "wavelength" of a wave of finite amplitude. Thus, it is only a matter of stating that since a one-to-one correspondence has been assigned, the velocity calculated from the second order spectrum should be larger than the velocity calculated from the first order spectrum. The one-to-one correspondence seems a flaw in this argument, but is presented for the lack of any better explanation.

The effect of the sound intensity on the velocity has also been considered by Schreuer (53, p. 215-230)



with regard to liquids to the extent that he has suggested that reported velocity values should be accompanied by a statement regarding the magnitude of the sound intensity.

The result obtained with nitrogen that the sound velocity depends on the rf voltage on the crystal need not necessarily invalidate that information obtained for other gases in which higher voltages were used. This may seem paradoxical but it is difficult to accept that too much distortion would appear before at least the first order diffraction would appear. This statement is supported by the good agreement between the theoretical values and the experimental values found for sulfur dioxide and argon where such voltages were employed that would have given a high value for nitrogen had it been used.

The unusually high velocities found in using low pressures and comparatively higher voltages must be accepted on the basis of wave distortion effects.

The asymmetry found between the first order diffraction spectrum of the Ronchi ruling and that of the diffraction spectrum by the ultrasonic field is consistent with the notion that the parallel beam of light was not perpendicular to the normal of the sound wave front. This is indicated that the observation that the



symmetry in intensity distribution became better the more symmetrical the diffraction line pattern became. If such is the case, this type of measurement provides a means by which the setting corresponding to  $\alpha = 0$  in David's theory may be ascertained. Korff found that the symmetrical position as indicated by that setting of  $\alpha$  which gave rise to a symmetry in intensity distribution was not equal to  $\alpha = 0$  as measured; he attributed this slight deviation to the non-ideality of the sound wave field. The results obtained in this work, particularly with respect to the increase in difficulty in obtaining a symmetrical pattern when studying argon and then nitrous oxide, lends to Korff's conclusion. The non-ideality suggested here is not associated with wave distortion due to waves of finite amplitude but rather to the effect which the phenomenon of absorption would have on the wave train.

It is to be recalled that measurements with respect to some standard gas have been made on the basis that whatever may be the deviation from an ideal planar sound field, the deviation remains constant irrespective of the gas under study. Such deviation was Bömmel's (3, p. 3-20) main reason for trying to detect dispersion in a gas using two simultaneous frequencies and making a relative measurement in this way instead of relating the

measurement to a previous studied non-dispersive gas.

The effect of absorption of ultrasound energy on the diffracting ability of the ultrasonic field bears some consideration. In interferometry the absorption coefficient has a direct effect on the velocity measurements but according to Herzfeld and Litovitz (21, p. 64), the error arising from this effect is outside present experimental error. Even then, it appears feasible to make corrections for this effect as has been done by Walker and coworkers (58, p. 1-24). In the optical method described here, any effect by the absorption phenomenon is indirect since it would effect the diffracting properties of the ultrasonic waves. A thorough analysis of diffraction by gaseous media would require introduction of this effect into the relation expressing the periodic variation of the refractive index.

The solutions of the wave equation regarding diffraction of light by ultrasonic waves are based on the variation of the index of refraction as

$$n = n_0 + n_1 \cos(2\pi z/\Lambda)$$

where

$n$  = the instantaneous index of refraction  
 $n_0$  = the index of refraction in the undisturbed medium

$n_1$  = the amplitude of the change in the index of refraction due to the pressure wave

$\Lambda$  = the sound wavelength

$z$  = the distance of the observation point along the normal from the ultrasound source.

A more appropriate description of the variation in the index of refraction would be

$$n = n_0 + n_1 (\cos 2\pi z/\Lambda)(\exp -\alpha z)$$

where  $\alpha$  is the sound absorption coefficient and  $\exp -\alpha z$  is a decay factor for the amplitude which arises as a consequence of the dissipation of the energy of the pressure wave as it travels away from the source. Such a substitution into the wave equation for  $n$  may not permit a solution to be had readily but the proper solution would be a more realistic one.

Because of the unknown and indirect relation of the absorption coefficient on the property of the sound field to serve as a diffracting medium, a correction to the measured velocity values to allow for this effect is not yet possible in general. However, for the case in which the path length,  $d$ , through the ultrasonic field is short, and when further  $2\pi n_1 d/\lambda < 1$ , it can easily be shown that ultrasonic absorption will introduce a further factor of the form  $[(1 - \exp -\alpha a)^2/\alpha^2 a^2]$  into the

expression for the ratio of the first to the zeroth order. Here  $\alpha$  is the ultrasonic absorption coefficient and  $a$  is the aperture in the direction of propagation of the ultrasound.

In examining the accuracy of the velocity values, it must be remembered they were based entirely on the measurement of the Ronchi ruling constant with an uncalibrated comparator. Although some of the results indicated good accuracy, such as those obtained with argon, this was only an indication of good optical alignment. The absence of accuracy was also dependent on the fact that there occurred no guarantee that the manner in which the Ronchi ruling constant was measured was correct. A correct measurement has to insure that the measurement is made along a line perpendicular to the grating lines. A deviation of approximately three degrees from this arrangement would suffice to cause an error in the accuracy by 0.1%. Any deviation from perpendicularity in the measurement -- therefore any deviation at all -- would give only a larger ruling constant than the true value and thus, would tend to increase the measured velocity values with respect to the known accurate values. The measured values reported in this work tend to be low instead of high.

An important factor influencing the accuracy of



the velocity measurement was the alignment of the slit to the plane wave fronts of the ultrasonic waves. The effect of alignment is analogous to the alignment between a slit and the lines of a grating. As Sawyer (51, p. 174-178) points out, any misalignment involving a rotation of the slit or grating with respect to each other in a plane perpendicular to the axis joining the two elements would tend to decrease the spacing in the diffracted orders again leading to a higher velocity. This also is true of a misalignment involving the rotation of the grating about an axis parallel to the slit and perpendicular to the line joining the two elements. Considerations regarding the same type of misalignment between slit and Ronchi ruling and Ronchi ruling and ultrasonic field results in similar effects. However, because of the possible alignment combinations of the three optical elements, i.e., the slit, ultrasonic field and Ronchi ruling, the measured velocity values could result in being either high or low. Nonetheless, this alignment may be calibrated and indeed corrected by experimenting with a nondispersive gas. This explanation serves to account for the fact that the results of the sound velocity measurements for argon obtained using the low pressure cell did not necessitate using a calibration factor, while the average sound velocity of nitrogen

obtained using the high pressure cell indicated a factor of 1.0066 was required to convert the observed values to agree with the theoretical value.

Other possible sources of error would be impurities or improper temperature measurements or a combination of both. An error in the reading of the temperature of one degree would already cause 0.15% error. Particular attention to any temperature error in this experiment seems warranted in view of the inquiry as to whether the temperature denoted by the thermistor is the temperature which should be assigned to the system at the time of exposure. This notion indicates that the measurements associated with the least temperature change should be the more reliable ones. The best evidence to evaluate this notion should perhaps be drawn from the results obtained with argon. In reference to these data, the exposure associated with the velocity value of  $323.0 \text{ m sec}^{-1}$  and which is slightly higher than the others, except for the exposure made at 0.4 atm pressure, had a temperature change of  $0.8^{\circ}\text{C}$ , while exposures associated with pressures of 0.8 and 0.6 atm had a temperature change of  $1.1^{\circ}$  and  $2.0^{\circ}\text{C}$ . The velocity of the last exposure at 0.4 atm had the greatest temperature change of  $3.1^{\circ}\text{C}$  but it is also true that any distortion giving higher velocity values should be predominant at

lower pressures. Separation of both effects seems necessary for a convincing argument that the temperature as indicated by the thermistor is not the temperature which should be taken for the system under study. On the basis of the comparison of the velocity values found for argon and the temperature variation, the view presented here is that such temperature measurements should be accepted with a degree of caution.

In regards to errors arising from impurities these are always likely possibilities particularly when no special precautions are taken as was true of this work. However, the purities given for the various gases, except for nitrous oxide, can be considered as very high. Argon has the best purity followed very closely by nitrogen; yet nitrogen gave the low value referred to. It would be indeed surprising if after evacuating the cell overnight and flushing with the gas at atmospheric pressure three times, as was the case, enough impurities remained to reduce the purity of nitrogen to yield a low velocity value. The purity of ammonia was questionable since its history was unknown except that the gas cylinder was four years old and nearly empty from intermittent use. With regards to nitrous oxide which had a stated purity of 99.3%, Walker has indicated that the main impurity is nitrogen and his studies show that the velocity is

increased when nitrogen is added as the impurity.

On the other hand, according to an investigation by Wight (59) concerning the effect of small amounts of water on the relaxation time of nitrous oxide implies that the relaxation time of nitrous oxide and 0.2% water vapor mixture would be  $0.63 \mu\text{s}$ . The stated purity of the nitrous oxide used could certainly accomodate this much water vapor.

The slope of the line drawn in Figure 14 was made equal to one as is demanded by the theory for a single vibrational relaxation time. The position of the line was determined by weighing those points obtained at the lower  $f/p$  values slightly more. Such a procedure may be justified on the basis that (1) the temperature change at higher pressure is less, (2) any external impurity taken on by the gas would have a more severe effect at the low pressures than at high pressures, (3) distortion at lower pressures is more prevalent and reproducibility less (an observation consistent with the conclusion of Petersen (42)) and (4) better photographs of the diffraction image were obtained at the higher pressures.

The value of the single relaxation time from the curve representing the optical data of  $0.63 \mu\text{s}$  brackets the vibrational relaxation time value between 0.1 and  $1.3 \mu\text{s}$ . As such the value of  $0.63 \mu\text{s}$  indicates that



at 300°K, about 5,500 collisions are required to reduce the energy departure from thermal equilibrium to  $1/e$  of its value. The number of collisions was determined by using the formula (28, p. 835)

$$Z = \tau_o / \tau_c$$

where  $\tau_c$ , the time between collisions, is given as  $1/15 \times 10^{-10}$  sec at 300°K by Herzfeld and Litovitz (21, p. 252).

The value of  $0.63 \mu s$  is to be compared with that value best representative of the interferometric method as given by Walker and his group (58, p. 19) as  $0.92 \mu s$  and that derived from the data of Holmes and coworkers (25) of  $0.99 \mu s$  at 300°K. The value obtained by Jacox and Bauer (28, p. 844) using the spectrophone was  $0.8 \mu s$ .

Thus, the value for the vibrational relaxation time of nitrous oxide obtained by this work using the optical method gives quantitative agreement within a factor of two with those values reported using two different experimental techniques.

On the average, the lower limit of precision in sound velocity measurements for the gases studied was 0.15% based on the standard deviation. The accuracy for the sound velocity measurement of nitrous oxide was approximately 0.75%, a value obtained by comparing the

sound velocity value with that reported by Walker and co-workers for an  $f/p$  value of 1 Mc/atm. A statement of this accuracy must include the usual assumptions characteristic of such comparisons, the important one being that the two systems studied were identical.

The accuracy of the results do not permit the suggesting of any other collision mechanism other than that due to double collisions. Moreover, it prevents suggesting that more than one relaxation time is involved.

The fact that this work remains the first to report detection of a dispersion in sound velocity associated with a vibrational relaxation time, should serve as encouragement that if the optical method receives the attention given other methods to obtain the same results it may become a very reliable method.

Those items which should receive notable attention in improving the optical method must include the temperature measurement and temperature control. It seems that using higher temperatures may tend to make any temperature change due to formation of an ultrasonic field less significant. Whatever the temperature control may be, activation of the quartz crystal with pulses of rf energy will increase the reliability of measurement. Noury (41, p. 217-259) has managed to make this feat possible

along side exposing the plate only during the time the ultrasonic field is on. His work, however, involved a minimum pressure of 12 atmospheres.

Use of off-axis parabolic mirrors as the important elements in the optical system should remove the objectionable scattered light present in a lens system and caused by the reflection from the several glass-air interfaces. The use of a long focal length objective element, say 300 cm, will cause a separation of diffracted orders to be sufficiently large that the limiting value in the precision should occur in the accuracy with which the focal length is known. Such an arrangement should allow a precision of at least 0.1%.

The findings of Gollmick (17, p. 1-47) as to the necessity for using a mounting of the crystal transducer to eliminate excessive damping is emphasized. The determination of the impedance of such an element should hold a high priority in order to adequately match an oscillator to the transducer and resulting in minimizing the heating effect and increasing the efficiency of the transducer. The use of a standing sound field may be preferable to minimize any contribution the phenomenon of absorption may give to the non-ideality of the sound field.

Korff was able to photograph diffraction of light

by ultrasonic waves in air having a frequency of  $4.28 \text{ mc sec}^{-1}$ . In view of this and of the results attained in this work, it seems that for a gas as efficient as ammonia in regard to the ability of producing a diffraction pattern, photographing of diffraction to values of  $f/p$  in the neighborhood of  $10 \text{ mc atm}^{-1}$  should be possible.



## BIBLIOGRAPHY

1. Bär, R. Über die Lichtbeugung der Ultraschallen in Luft. *Helvetica Physica Acta* 9:367-371. 1936.
2. Bergmann, Ludwig. Der Ultraschall und seine Anwendung in Wissenschaft und Technik. 6d ed. Stuttgart, S. Hirzel Verlag, 1954. 1114 p.
3. Bömmel, Hans. Die Messung der Geschwindigkeit und der Absorption von Ultraschall in Gasen vermittelst der optischen Methode. *Helvetica Physica Acta* 18: 3-20. 1945.
4. Born, Max and Emil Wolf. Principles of optics. New York, Pergamon Press, 1959. 803 p.
5. Boyer, Robert A. Ultrasonic velocities in gases at low pressures. *Journal of the Acoustical Society of America* 23:176-178. 1951.
6. Brillouin, Léon. Diffusion de la lumière et les rayons x par uns corps transparent homogène influence de l'agitation thermique. *Annales de Physique* 17: 88-122. 1922.
7. Cady, Walter Guyton. Piezoelectricity. New York, McGraw-Hill, 1946. 806 p.
8. Cajori, Florian. Newton's Mathematical principles. Berkeley, University of California Press, 1934. 680 p.
9. David, Erwin. Intensitätsformeln zur Lichtbeugung an schwachen Ultraschallwellen. *Physikalische Zeitschrift* 38:587-591. 1937.
10. Debye, P. and R. W. Sears. On the scattering of light by supersonic waves. *Proceedings of the National Academy of Sciences* 18:409-414. 1932.
11. Deshpande, D. D. Ultrasonic velocity and absorption in gases. *Journal of the University of Poona, Science Section* 14:55-61. 1958.
12. Eastman Kodak Company. Kodak photographic films and plates for scientific and technical use. Rochester, 1960. 40 p.

13. Fox, F. E. and W. A. Wallace. Absorption of finite amplitude sound waves. *The Journal of the Acoustical Society of America* 26:994-1006. 1954.
14. Fox, J. J. and F. G. H. Tate. Refractivity of all gases and vapors and of elementary substances in the isotropic solid and liquid states. In: *International critical tables*, vol. 7. New York, McGraw-Hill, 1930. p. 1-12.
15. Germann, A. F. O. and S. F. Dickering. Critical-point data. In: *International critical tables*, vol. 3. New York, McGraw-Hill, 1928. p. 248-249.
16. Glasstone, Samuel. *Textbook of physical chemistry*. 2d ed. Princeton, D. Van Nostrand, 1956. 1320 p.
17. Gollmick, Hans Joachim. *Untersuchungen über die Lichtbeugung an Ultraschallwellen in Gasen*. Ph. D. thesis. Berlin, Berlin University, 1940. 47 numb. leaves. (Microfilm)
18. Hayess, E. *Untersuchungen über den Mechanismus der Ultraschallausbreitung in Stickstoff unter hohem Druck*. *Zeitschrift für Physikalische Chemie* 206: 210-220. 1957.
19. Hayess, E. und B. Winde. *Untersuchungen über die Anwendbarkeit der Schallgittermethode in Gasen*. *Zeitschrift für Physikalische Chemie* 206:194-209. 1957.
20. Herzberg, Gerhard. *Molecular spectra and molecular structure. II. Infrared and Raman spectra of polyatomic molecules*. New York, D. Van Nostrand, 1954. 632 p.
21. Herzfeld, Karl F. and Theodore A. Litovitz. *Absorption and dispersion of ultrasonic waves*. New York, Academic Press, 1959. 535 p.
22. Herzfeld, K. F. and F. O. Rice. Dispersion and absorption of high frequency sound waves. *The Physical Review* 31:691-695. 1928.
23. Hirschfelder, Joseph O., Charles F. Curtiss and R. Byron Bird. *Molecular theory of gases and liquids*. New York, John Wiley and Sons, 1954. 1219 p.

24. Hodgman, Charles D. (ed). Handbook of chemistry and physics. 36th ed. Cleveland, Chemical Rubber Publishing Co., 1954. 3173 p.
25. Holmes, R., H. D. Parbrook and W. Tempest. The propagation of sound in nitrous oxide. *Acustica* 10:155-159. 1960.
26. Hubbard, J. C. The acoustic resonator interferometer: II. Ultrasonic velocity and absorption in gases. *The Physical Review* 41:523-535. 1931.
27. Hubbard, J. C., J. A. Fitzpatrick, B. T. Kankovsky and William J. Thaler. Distortion of progressive ultrasonic waves. *The Physical Review* 74:107-108. 1948.
28. Jacox, Marilyn E. and S. H. Bauer. Collision energy exchange in gases. Use of the spectrophone for studying relaxation processes in carbon dioxide. *The Journal of Physical Chemistry* 61:833-844. 1957.
29. Jahnke, Eugene and Fritz Emde. Tables of functions with formulae and curves. 4th ed. New York, Dover Publications, 1945. 306 p., addenda, 76 p.
30. Johnston, Herrick L., Lydia Savedoff and Jack Belzer. Contributions to the thermodynamic functions by a Planck-Einstein oscillator in one degree of freedom. Washington, Office of Naval Research, 1949. 159 p.
31. Keller, Hans H. Ultraschallabsorption in Gasen. *Physikalische Zeitschrift* 41:386-393. 1940.
32. Klose, Jules Z. Ultrasonic dispersion and absorption in n-hexane vapor. *The Journal of the Acoustical Society of America* 30:605-609. 1958.
33. Korff, Wilhelm. Photometrische Untersuchungen der Lichtbeugung und Ultraschallwellen in Flüssigkeiten und Gasen. *Physikalische Zeitschrift* 37:708-720. 1936.
34. Lacam, André. Vitesse des ultrasons dans l'azote jusqu'à des pressions atteignant 1150 atm. *Le Journal de Physique et le Radium* 14:351-352. 1953.



35. Lacam, André and Jack Noury. Vitesse des ultrasons dans l'argon jusqu'à des pressions atteignant 950 atm. Comptes Rendus Hebdomadaires des Séances de l'Académie des Sciences (Paris) 236:362-364. 1953.
36.                     . Sur le rapport  $\gamma$  des chaleurs spécifiques de l'argon sous pression. Comptes Rendus Hebdomadaires des Séances de l'Académie des Sciences (Paris) 236:589-590. 1953.
37. Landau, L. and E. Teller. Zur Theorie der Schall-dispersion. Physikalische Zeitschrift der Sowjetunion 10:34-43. 1936.
38. Laplace, Pierre Simon. Oeuvres completes. Vol. 14. Paris, Gauthier-Villars, 1912. 465 p.
39. Lewis, Donald Richard. Heat capacities of hydrocarbon gases measured with the ultrasonic interferometer. Ph.D. thesis. Madison, University of Wisconsin, 1948. 100 numb. leaves.
40. Lucas, R. and P. Biquard. Nouvelles propriétés optiques des liquides soumis à des ondes ultrasonores. Comptes Rendus Hebdomadaires des Séances de l'Académie des Sciences (Paris) 194:2132-2134. 1932.
41. Noury, Jack. Étude expérimentale de la celerité des ultrasons dans la région critique des fluides. Journal des Recherches du Centre National de la Recherche Scientifique, Laboratoires de Bellevue 36:217-259. 1956.
42. Petersen, Otto. Entwicklung einer optischen Methode zur Messung von Ultraschallabsorptionen in Gasen und Flüssigkeiten. Physikalische Zeitschrift 41: 29-36. 1940.
43. Petralia, S. Interferometria ultrasonora nei gas (III). Velocità e assorbimento di ultrasuoni nell'anidride solforosa. Il Nuovo Cimento 9:818-824. 1952.
44. Pierce, George W. Piezoelectric crystal oscillators applied to the precision measurement of the velocity of sound in air and CO<sub>2</sub> at high frequencies. Proceedings of the American Academy of Arts and Sciences 60:271-302. 1925.



45. Pohlmann, R. Sichtbarmachung von Ultraschall in Gasen und seine Intensitätsmessung. Die Naturwissenschaften 23:511. 1935.
46. Raman, C. V. and N. S. Nagendra Nath. The diffraction of light by high frequency sound waves: Part I. Proceedings of the Indian Academy of Sciences 2:406-412. 1935.
47. \_\_\_\_\_. The diffraction of light by high frequency sound waves: Part II. Proceedings of the Indian Academy of Sciences 2:413-420. 1935.
48. \_\_\_\_\_. The diffraction of light by high frequency sound waves: Part III. Proceedings of the Indian Academy of Sciences 3:75-84. 1936.
49. \_\_\_\_\_. The diffraction of light by high frequency sound waves: Part IV. Generalised theory. Proceedings of the Indian Academy of Sciences 3: 119-125. 1936.
50. Rushbrooke, G. S. Introduction to statistical mechanics. London, Oxford University Press, 1955. 334 p.
51. Sawyer, Ralph A. Experimental spectroscopy. 2d ed. New York, Prentice Hall, 1951. 358 p.
52. Schaafs, Werner. Schallgeschwindigkeit und Molekülstruktur in Flüssigkeiten. Ergebnisse der Exakten Naturwissenschaften 25:109-192. 1951.
53. Schreuer, E. Präzisionsmessungen der Ultraschallgeschwindigkeit in verschiedenen Flüssigkeiten und ihre Bedeutung für die Frage der Schalldispersion, sowie für die Methodik der Ultraschallgeschwindigkeitsmessungen. Akustische Zeitschrift 4:215-230. 1939.
54. Sette, D., A. Busala and J. C. Hubbard. Energy transfer by collisions in vapors of chlorinated methanes. Journal of Chemical Physics 23:787-793. 1955.
55. Stamm, Robert F. A fast grating spectrograph. Industrial and Engineering Chemistry, Analytical edition 17:318-331. 1945.

56. Strong, John. Procedures in experimental physics. New York, Prentice-Hall, 1938. 642 p.
57. Tawil, Edgar-Pierre. Les ondes stationnaires ultrasonores rendues visibles dans les gas par la methode des stries. Comptes Rendus Hebdomadaires des Seances de l'Academie des Sciences (Paris) 191:92-95. 1930.
58. Walker, Richard A., Thomas D. Rossing and Sam Legvold. The role of triple collisions in excitation of molecular vibrations in nitrous oxide. Washington, 1954. 24 p. (U. S. National Advisory Committee for Aeronautics. Technical note 3210)
59. Wight, Howard M. Vibrational relaxation in  $N_2O-H_2O$  and  $N_2O-D_2O$  mixtures. The Journal of the Acoustical Society of America 28:459-461. 1956.
60. Zeffert, B. M. and R. R. Witherspoon. A thermistor temperature recorder. Analytical Chemistry 28: 1701-1705. 1956.

## APPENDIX 1

VELOCITY CORRECTIONS DUE TO  
GAS NON-IDEALITY

In this work two methods were used to correct experimental velocities to correspond to velocities for the ideal gas. Both methods make use of the second virial coefficient,  $B$ .

The first method relies on using the virial coefficient as a function of temperature obtained from the Beattie-Bridgman equation of state. The work of Hirschfelder, Curtiss and Bird (23, p. 253) shows that in this case

$$B(T) = B_0 - (A_0/RT) - (c/T^3) \quad 1a$$

for which they have given values of the constants  $B_0$ ,  $A_0$  and  $c$  for several gases.

The above expression was then used in conjunction with the equation relating observed sound velocity,  $U_r$ , and the velocity of the ideal gas,  $U_i$ , given by Herzfeld and Litovitz (21, p. 191). They write the relation as

$$U_r^2 = U_i^2 \left( 1 + 2P \left[ B' + \frac{R}{C_p^0} \frac{\partial (TB')}{\partial T} + \frac{1}{2} \frac{R^2}{C_p^0 C_v^0} T \frac{\partial^2 (TB')}{\partial T^2} \right] \right), \quad 2a$$

where  $B' = B/RT$ .

Substitution of the following three equations,

$$B' = B/RT = (B_0/RT) - (A_0/[RT]^2) - (c/RT^4) \quad 3a$$

$$\partial(TB')/\partial T = A_0/(RT)^2 + 3c/RT^4 \quad 4a$$

and

$$\frac{\partial^2(TB')}{\partial T^2} = -2A_0/R^2T^3 - 12c/RT^5, \quad 5a$$

into equation 2a, it is possible to arrive at

$$U_r^2 = U_i^2 \left( 1 + 2P \left[ \frac{B_0}{RT} - \frac{A_0}{(RT)^2} \frac{1}{\gamma_0} - \frac{c}{RT^4} \left( 3\gamma_0 - 8 + \frac{6}{\gamma_0} \right) \right] \right) \\ = U_i^2 (1 + 2PF). \quad 6a$$

In this equation P is in atmospheres, T in degrees Kelvin and R is 0.08205 liter atm deg<sup>-1</sup> mole<sup>-1</sup>.

In the case of three of the gases studied in this work,

$A_0 = 1.2907$ ,  $B_0 = 0.03931$  and  $c = 5.99 \times 10^4$  for argon,

$A_0 = 1.3445$ ,  $B_0 = 0.05046$  and  $c = 4.20 \times 10^4$  for nitrogen and

$A_0 = 2.3930$ ,  $B_0 = 0.03415$  and  $c = 476.87 \times 10^4$  for ammonia.

For ammonia where  $\gamma_0 = 1.307$ , F has a value of



$-5.391 \times 10^{-3}$  at  $300^\circ\text{K}$ . Therefore the non-ideal correction to the observed velocity  $U_r$  for ammonia at one atmosphere would be such as to increase it by 0.54%.

For nitrogen under the same conditions,  $F$  has a value of  $+4.12 \times 10^{-4}$  and indicates that the ideal sound velocity is lower by about 0.04% than the observed velocity.

In argon the deviation between ideal and real sound velocities is less than 0.01% under the same conditions.

In the case of nitrogen, the correction factor was applied for pressures above two atmospheres.

The method for correcting the observed velocity of nitrous oxide to ideal velocity values is essentially that given by Sette and coworkers (54). The relation involving the real gas velocity,  $U_r$ , and the ideal gas velocity,  $U_i$ , in terms of the second virial coefficient,  $B$ , is given by the expression

$$U_r/U_i = 1 + P \left( B/RT + \frac{1}{C_v^0} \left[ \frac{dB}{dT} + \frac{RT}{2C_p^0} \frac{d^2B}{dT^2} \right] \right) = 1 - GP. \quad 7a$$

Here  $P$  is the pressure in atmospheres and the heat capacities  $C_v^0$  and  $C_p^0$  have been defined. These may be calculated a priori and in the case of nitrous oxide were calculated and found to be  $3.659R$  and  $4.659R$ , respectively, at  $300^\circ\text{K}$ . These values were obtained from the vibrational frequencies listed in Herzberg (20, p. 278).

$\nu \text{ cm}^{-1}$	u	C/R	d	$(C/R)_t$
588.8	2.824	0.536	2	1.072
1285.0	6.163	0.084	1	.084
223.5	10.664	0.003	1	.003

total = 1.159

In this tabulation,  $\nu$  is the vibrational frequency at a particular normal mode,  $u = 1.439 \nu / T$ , and the associated value of the vibrational heat capacity was obtained from tables of Einstein oscillator functions (30, p. 1-159). More precisely the evaluation of  $u$  should be at the temperature of the experimental observed velocity,  $U_r$ . However since the velocities observed for  $\text{N}_2\text{O}$  were so close to 300°K that the effective vibrational contribution to the heat capacities would not be changed within the experimental error if the actual temperature of the experiment were used, this procedure seemed justified. The column denoted by  $d$  represents the degeneracy of the mode; the column denoted by  $(C/R)_t$  is values of the total vibrational heat capacity contribution by each mode.

For calculating the second virial coefficient, Sette and coworkers give the well known expression derived from the Berthelot equation involving the critical temperature,  $T_c$ , and the critical pressure,  $P_c$ . Thus,

$$B = \frac{9}{128} \frac{RT_c}{P_c} \left( 1 - \frac{6T_c^2}{T^2} \right). \quad 8a$$

Substitution of this expression into the relation involving the real gas and ideal gas velocities yields,

$$-G = 0.0703 \frac{T_c}{P_c T^3} \left\{ T^2 + 6T_c^2 \left( 3 \left[ \frac{\gamma_o - 1}{\gamma_o} \right] - \gamma_o \right) \right\} \quad 9a$$

where  $\gamma_o$  is the ratio of the heat capacities,  $C_p^o/C_v^o$ .

In the case of  $N_2O$ ,  $\gamma_o = 1.273$  and  $P_c = 71.7$  atm while  $T_c = 309.7^\circ K$ . The latter two values were obtained from the International Critical Tables (15, p. 2418-249).

Substitution of  $\gamma_o$  for  $300^\circ K$  yields,

$$-G_{N_2O} = \frac{0.3036}{T^3} (T^2 - 36.25 \times 10^4). \quad 10a$$

For the exposures used in obtaining the vibrational relaxation time for nitrous oxide, the necessary data for obtaining the idealized sound velocities are tabulated in Table 14.

In the case of ammonia where  $\gamma_o = 1.307$  at  $300^\circ K$  and for which  $T_c = 405.6^\circ K$ , and  $P_c = 111.5$  atm, formula 9a becomes

$$-G_{NH_3} = \frac{0.2558}{T^3} (T^2 - 59.421 \times 10^4)$$

which for  $300^\circ K$  yields

Table 14

Summary of G Values for N<sub>2</sub>O

e.n.*	T(°K)	G	P(atm)	GP	1-GP	1/(1-GP)
3515	297.58	.0032	1.04	.0033	0.9967	1.003
3514	298.58	.0031	1.04	.0032	.9968	1.003
3513	298.88	.0031	0.80	.0025	.9975	1.002
3512	299.35	.0031	0.60	.0018	.9982	1.002
3511	301.51	.0030	0.40	.0012	.9988	1.001
41521	299.52	.0031	10.28	.0318	.9682	1.033
41522	300.03	.0031	10.28	.0318	.9682	1.033
41523	299.98	.0031	7.62	.0236	.9764	1.024
41524	300.07	.0031	5.31	.0164	.9836	1.017
41525	300.38	.0030	4.42	.0132	.9868	1.013
41527	300.41	.0030	1.77	.0053	.9947	1.005
41528	300.87	.0030	1.00	.0030	.9970	1.003

\*Exposure number



$$(-G_{\text{NH}_3})_{300^\circ\text{K}} = -4.775 \times 10^{-3}$$

and is to be compared with the value previously mentioned and obtained from a different method.

## APPENDIX 2

CONSIDERATIONS OF CORRECTIONS  
FOR FOCAL LENGTH

In the grating-type of formula used to determine the sound wavelength, the sine of the diffraction angle was approximated in that the true relation

$$\sin \theta = n\lambda$$

became

$$\Lambda \frac{\delta_n}{F} \cong n\lambda$$

where  $\Lambda$  designates the sound wavelength,  $\delta_n$  the distance between the  $n^{\text{th}}$  order diffraction line from the zero order,  $F$  the focal length of the objective lens, and the wavelength of light used.

Actually the sine of the diffraction angle,  $\theta$ , should be

$$\frac{\delta_n}{(\delta_n^2 + F^2)^{1/2}} \quad \cdot \quad 1b$$

An analysis of the error inherent in the focal length using the approximation mentioned above is given in percent as

$$50(\delta_n/F)^2,$$

where the binomial expansion for the square root term has been invoked to the second term. For an error of 0.05% in the focal length, it must be that the value of  $\delta_n$  is as least as large as given by

$$\delta_n = 0.032 F$$

which, using a focal length of 61 cm, yields  $\delta_n = 19.5$  mm, a value which is about 20 times larger than most values obtained in this work.

Another possible source of error in the effective focal length of the objective concerns the corrections of the velocities due to refraction. This effect has its origin in light impinging on a boundary formed by two media having different indices of refraction. The phenomena of reflection accompanying refraction need not be considered as having an effect on the focal distance but is of great importance in determining an efficient optical system for studying gases at low ultrasonic frequencies or gases such as ammonia which have a relatively high velocity.

Since the diffracted light by the ultrasound field does take on a direction different than the parallel light, the main concern is in the immediate vicinity where the diffracted light passes through the cell window and into the outer atmosphere. A consideration of the

problem in this particular region shows that the evaluation of the effect on the diffracted light involves only the index of refraction of the gas in the cell and outside the cell.

The treatment has been presented by Schaafs (54, p. 121-122) and outlined by Hayess and Winde (19, p. 203) and is reiterated here.

Schaafs considers  $\sin \theta$  as expressed by

$$\frac{s_n}{\left( s_n^2 + \left[ A - k \left( 1 - \frac{1}{M} \right) \right]^2 \right)^{1/2}} \quad 2b$$

under the hypothesis that  $s_n$  would be the distance between the zero order and the  $n^{\text{th}}$  order if the effective focal distance would be  $A$  as measured along the optical axis from a point on a plane perpendicular to the axis and bisecting the ultrasonic field.

A similar form of this equation may be derived involving the consideration of Figure 18.

The attention is centered about the shortening of  $A$  by  $\Delta$  yielding an effective focal distance,  $A_{\text{eff}}$ , for which  $A_{\text{eff}} = A - \Delta$ . The distance  $A_{\text{eff}}$  would then be the apparent focal length due to the refraction of the diffracted ray. A consideration of the geometry involved yields that



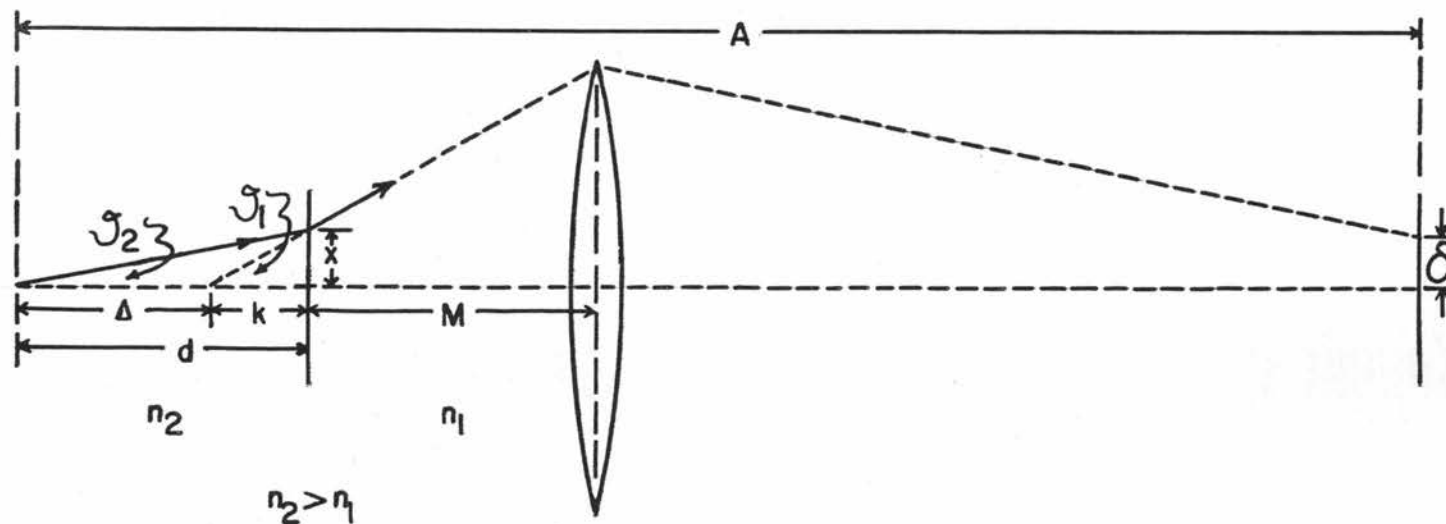


FIGURE 18 ILLUSTRATION OF REFRACTION EFFECT ON FOCAL LENGTH

$$\frac{x}{d} \cong \sin \mathcal{Y}_2 \quad \text{and} \quad \frac{x}{k} \cong \sin \mathcal{Y}_1$$

where  $k + \Delta = d$  and  $x$  is the height from the optical axis to a point common to the two rays which intersect on the boundary. Thus,

$$\frac{k}{d} \cong \frac{\sin \mathcal{Y}_2}{\sin \mathcal{Y}_1} = \frac{n_1}{n_2}$$

or

$$k = \frac{n_1}{n_2} d,$$

where  $n_1$  designates the index of refraction.

From the last relation and the relation

$\Delta = d - k$ , it follows that

$$\Delta = d \left(1 - \frac{n_1}{n_2}\right).$$

Now  $A - \Delta = A_{\text{eff}}$ , thus

$$\begin{aligned} \sin \theta &= \frac{s_n}{(s_n^2 + A_{\text{eff}}^2)^{1/2}} = \left\{ 1 + \left( \frac{A_{\text{eff}}}{s_n} \right)^2 \right\}^{-1/2} \\ &= \left\{ 1 + \left( \frac{A - d \left(1 - \frac{n_1}{n_2}\right)}{s_n} \right)^2 \right\}^{-1/2} \quad . \quad 4b \end{aligned}$$

which is the form of equation 2b given by Schaafs.

Consequently,

$$\Lambda = n\lambda \left\{ 1 + \left( \frac{A - d \left( 1 - \frac{n_1}{n_2} \right)}{s_n} \right)^2 \right\}^{\frac{1}{2}} \quad 4b$$

In the approximation involving a thin lens, Schaafs states that  $A$  is replaced by the focal length  $F$  and  $s_n$  by  $\delta_n$  which yields

$$\Lambda = n\lambda \left\{ 1 + \left( \frac{F - d \left( 1 - \frac{n_1}{n_2} \right)}{\delta_n} \right)^2 \right\}^{\frac{1}{2}} \quad 5b$$

In the present work, the conditions under which such a focal length correction would be most appropriate would be the experiment involving 10 atm pressure of  $N_2O$ . In this situation, setting  $k = 50$  mm and  $n_2 = 1.0050$ , the correction amounts to less than 0.04%.